Recent Advances on Anthracene-based Photoinitiators of Polymerization

Frédéric Dumur

HAL Id: hal-03615922
https://hal.science/hal-03615922

Submitted on 22 Mar 2022

Recent Advances on Anthracene-based Photoinitiators of Polymerization

Frédéric Dumur[a]*

[a] Aix Marseille Univ, CNRS, ICR, UMR 7273, F-13397 Marseille, France

frederic.dumur@univ-amu.fr

Abstract

Photopolymerization is an active research field, and this intense research activity is supported by the numerous and emerging applications related to this polymerization technique. Especially, the historical UV approach is more and more discarded in favour of visible light photopolymerization making use of cheap, lightweight, compact, low intensity and energy-saving light sources that are light-emitting diodes (LEDs). With aim at developing photoinitiators fitting with these light sources, anthracene has been identified as a promising scaffold for the design of photoinitiators of polymerization. In this review, an overview of the recent advances concerning anthracene-based photoinitiators is provided. To evidence the interest of these structures, comparisons with benchmark photoinitiators will be provided.

Keywords

Photoinitiator; anthracene; photopolymerization; LED; low light intensity

1. Introduction

During the past decade, photopolymerization has been the focus of intense research efforts, resulting from the transition currently existing between the traditional UV photopolymerization in favour to the next generation of photoinitiating systems activable under low light intensity and in the visible range.[1–19] Nowadays, photopolymerization is used in a wide range of applications ranging from coatings, adhesives, 3D and 4D printing and microelectronics.[20–29] Emergence of visible light photopolymerization is supported by the recent safety concerns raised by the traditional UV photopolymerization.[30] Indeed, UV light can be at the origin of eye damages and skin cancers.[30–32] Ozone is also produced during UV photopolymerization what constitutes a serious drawback for the manipulator.[33] To end, UV photopolymerization also entails high running costs related to the use of expensive irradiation setups but also to the high energy consumption of these devices. Face to these considerations, a great deal of efforts has been devoted to develop cheaper and more environmentally friendly polymerization processes. In this field, visible light photopolymerization exhibit several advantages compared to UV photopolymerization. Notably, cheap light sources such as Light-Emitting Diodes (LEDs) can be used. Interest of LEDs also relies in the low heat release, enabling to carry out polymerizations at room temperature.[34] A higher light penetration of the incident light can also be obtained in the

visible range. Notably, if the light penetration is limited to 600 μm at the best at 320 nm, this latter can range between a few millimetres until 5 cm by irradiating between 400 and 800 nm (See Figure 1).[12,35]
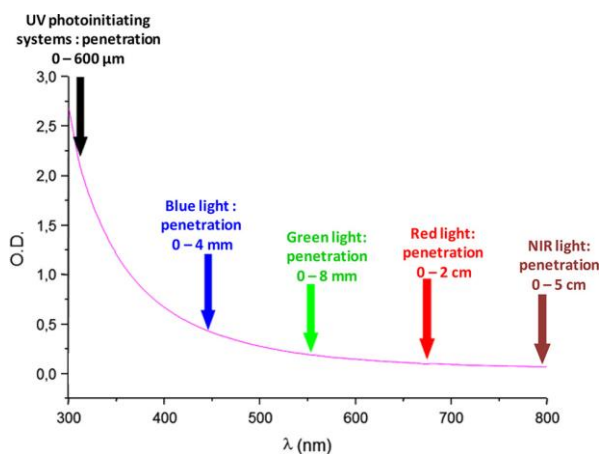

Figure 1. Light penetration in a polystyrene latex with an average diameter of 112 nm. Reprinted with permission from Bonardi et al.[35]

Photopolymerization can also be carried out in solvent-free conditions, avoiding the release of volatile organic compounds (VOCs).[33] To end, a spatial and a temporal control can also be obtained what constitute serious advantages compared to the solution-phase polymerization. However, if visible light photopolymerization seems to be an appealing approach, several drawbacks still exist. Notably, a lower reactivity of visible light photoinitiators compared to that of UV photoinitiators is often mentioned.[10,11,36–47] This is directly related to the use of less energetic irradiation wavelengths. Visible light photoinitiators also often impose a residual colour to the final coatings, these molecules being strongly coloured molecules. At present, visible light photoinitiating systems capable to bleach are still scarce in the literature, even if a few examples based on chalcones, diketopyrropyrroles and other structures have recently been reported. In order to develop highly efficient photoinitiating systems, a wide range of structures have been examined over the years, ranging from copper complexes,[47–62] to dithienophospholes,[63] iron complexes,[38,40,64–69] polyoxometalates,[70,71] iridium complexes,[72–79] naphthalimides,[46,80–95] dihydroanthraquinones,[96] perovskites,[97,98] chalcones,[28,44,45,99–109] diketopyrrolopyrroles,[110–112] camphorquinones,[113,114] iodonium salts,[80,115–121] push-pull dyes,[65,122–135] helicenes,[136,137] Schiff bases,[138] chromones and flavones,[139–141] benzophenones,[142–149] metal organic framework (MOFs),[64,150,151] squaraines,[43,152–154] carbazoles,[36,155–162] triphenylamines,[163] acridones,[164,165] zinc complexes,[166] coumarins,[42,167–177] phenazines,[178] phenothiazines,[179] 2,3-diphenylquinoxaline derivatives,[180,181] porphyrins,[182,183] curcumin,[184–187] cyclohexanones[188–191] perylenes,[41,192–194] thioxanthones,[195–206] pyrenes,[37,207–213] acridine-1,8-diones,[214–216] and cyanines. [217–219,219–221] Thanks to the different structures examined, photoinitiating systems activable from the near UV/visible range until the near-infrared region have been proposed. With aim at investigating new structures, anthracene has been identified as a promising scaffold, this dye being successfully used as a

UV photoinitiator. Anthracene is a polyaromatic structure extensively used in Organic Electronics for the design of dyes for solar cells,[222] singlet emitters for organic light-emitting diodes[223] or fluorescent probes.[224,225] Interest for this structure was notably motivated by its low oxidation potential facilitating its incorporation in multi-layered devices.[226] However, the scope of application of anthracene also includes photopolymerization. To illustrate this, anthracene was notably used as the dye for the sensitization of cationic initiators such as onium salts,[227–236], as an oxygen scavenger or as a photosensitizer for free radical polymerizations.[237,238] By mean of light-induced controlled radical polymerization of methacrylates, light responsive metal–organic framework (MOF) were also prepared.[239] However, use of anthracene was not limited to sensitization and anthracene has also been investigated as a photo and thermal stabilizer for monomers.[240] Recently, anthracene was also examined as an annihilator in combination with various photosensitizers for triplet-triplet annihilation-based up-conversion polymerizations.[220] Using this approach, near-infrared light could be used as safe irradiation sources. By the unique ability of anthracene to photodimerize under UV light, anthracene when conveniently substituted was also used as a monomer for various applications. Notably, surface patterning using a photomask,[241] on-surface synthesis of two-dimensional polymers,[242] hierarchical patterning of self-wrinkling[243] can be cited as relevant examples. By using anthracene as the monomer, synthesis of microporous ladder polymers by photodimerization was beneficial for the design of porous structures usable for advanced separation and catalysis.[244] If anthracene was used in the past as a monomer and as a UV photosensitizer for cationic and free radical polymerizations, dyes absorbing in the visible range were also elaborated with this scaffold, enabling to develop approximately ten different families of visible light photoinitiators. In this review, an overview of the recent advances concerning the design of visible light photoinitiators of polymerization is provided. By mean of chemical engineering, highly efficient photoinitiators could be prepared. To evidence the interest of these structures, comparisons with benchmark photoinitiators and structures previously reported in the literature is established.

2. Anthracene-based photoinitiators of polymerization

2.1. Anthracene-based chalcones

Chalcones are natural dyes that can be found in numerous fruits, vegetables and flowers.[245–248] Chalcones are also well-known to dimerize upon photoexcitation, resulting in the formation of cyclobutane rings by a [2+2]cycloaddition and this strategy was notably applied to the crosslinking of polymer chains.[45,249] However, chalcones can also be used as dyes for the sensitization of iodonium salts. In 2014, a series of chalcones was investigated for the first time as photoinitiators of polymerization for the free radical polymerization of acrylates.[107] In this series of four chalcones, photoinitiating ability of the anthracene-based dye was compared to that of four other chalcones varying by the structure of the electron-donating groups (See Figure 2). Examination of their UV-visible absorption properties in acetonitrile revealed the absorption maxima of chalcones to redshift from CPD-1 (λ_{max} = 315

nm) to CPD-2 (λ_{max} = 329 nm), CPD-3 (λ_{max} = 361 nm), CPD-4 (λ_{max} = 401 nm) and CPD-5 (λ_{max} = 435 nm), attributable to an improvement of the electron-donating ability from a benzene ring (CPD-1) to dimethylaminobenzene in CPD-5 (See Figure 3). Notably, due to the presence of weak electron donors in CPD-1-CPD-3, absorption spectra of the different chalcones remained strongly UV-centrered. Conversely, for CPD-4 and CPD-5 bearing stronger electron donating groups, a significant push-pull effect could occur within these structures, red-shifting their absorption spectra compared to CPD-1-CPD-3 and extending their absorption range. Thus, absorption spectra extending from 300 until 500 nm could be determined. In this series of chalcones, anthracene was identified as the best electron-donating group after dimethylaminobenzene, by the position of the intramolecular charge transfer (ICT) band. Considering the absorption spectra of CPD-4 and CPD-5, polymerization tests were caried out with a laser diode at 457 nm (100 mW/cm²) and a LED at 462 nm (10 mW/cm²).
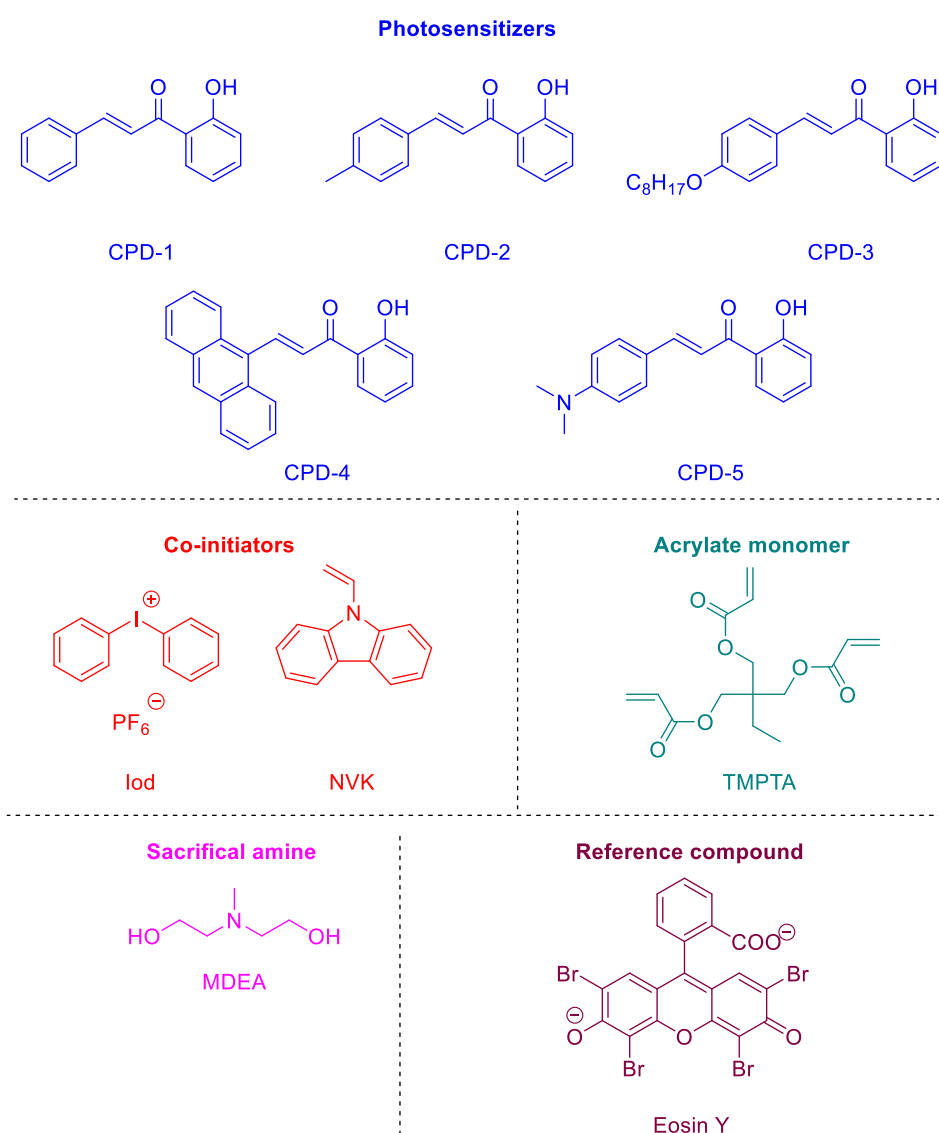

Figure 2. Chemical structures of CPD-1-CPD-5, the acrylate monomer and different additives.
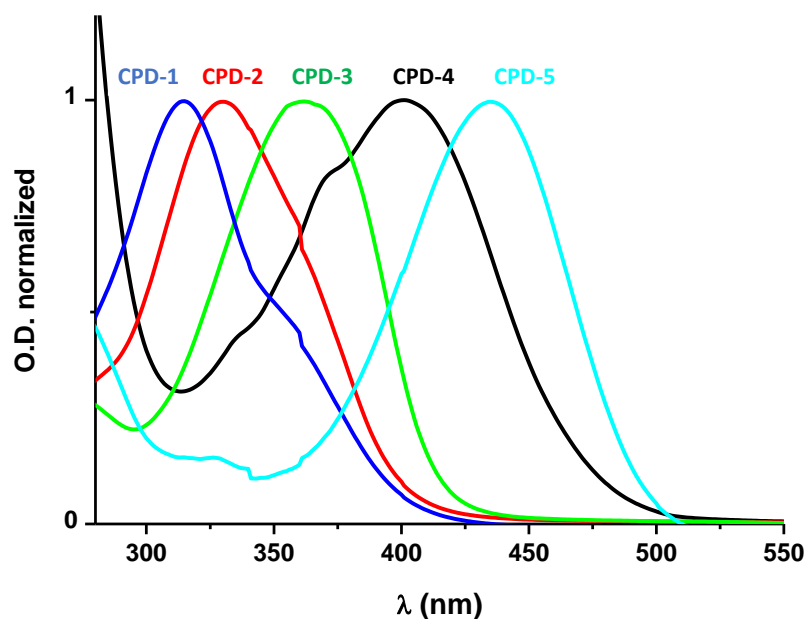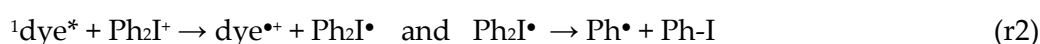
Figure 3. UV-visible absorption spectra of CPD-1-CPD-5 in acetonitrile. Reprinted with permission of Tefhe et al. [107].

Examination of the photoinitiating ability of CPD-4 during the free radical polymerization (FRP) of trimethylolpropane triacrylate (TMPTA) upon irradiation with a laser diode emitting at 457 nm revealed the three-component CPD-4/Iod/NVK (0.5%/3%/3% w/w/w) photoinitiating system to furnish a monomer conversion of 25% after 400 s, lower than that obtained with CPD-5 (55%). Due to the lack of absorption at 457 nm, no polymerization was detected for the other dyes (CPD-1-CPD-3). Comparison with the reference system Eosin-Y/methyldiethanolamine (MDEA) (0.1%/3% w/w) revealed the CPD-4-based three-component system to exhibit lower photoinitiating ability than the reference system which could led to a TMPTA conversion of 30% in the same irradiation conditions. To support the polymerization process of TMPTA, a mechanism reported numerous times for various three-component dye/Iod/NVK photoinitiating systems was proposed by the authors.[1,250–252] Thus, upon photoexcitation of the dye (r1), a photoinduced electron transfer towards the electrodeficient iodonium salt can occur, generating Ph• upon decomposition of $Ph_2I•$ (see r2). If Ph• radicals are inherently initiating species capable to initiate the FRP of TMPTA, Ph• radicals can also react with *N*-vinylcarbazole (NVK), furnishing new radicals Ph-NVK• (r3) exhibiting a higher reactivity than Ph• radicals.

$$dye \rightarrow {}^1dye* \ (h\nu) \tag{r1}$$

$${}^1dye* + Ph_2I^+ \rightarrow dye^{•+} + Ph_2I• \quad and \quad Ph_2I• \rightarrow Ph• + Ph\text{-}I \tag{r2}$$

$$Ph• + NVK \rightarrow Ph\text{-}NVK• \tag{r3}$$

In 2020, the combination of anthracene and ferrocene (CPD-10 and CPD-11) was examined for the FRP of polyethylene glycol (600) diacrylate (PEG-diacrylate) (See Figure 4).[99] For comparison, a series of chalcones bearing iodo or methoxy-substituents (CPD-6-CPD-9) was prepared.
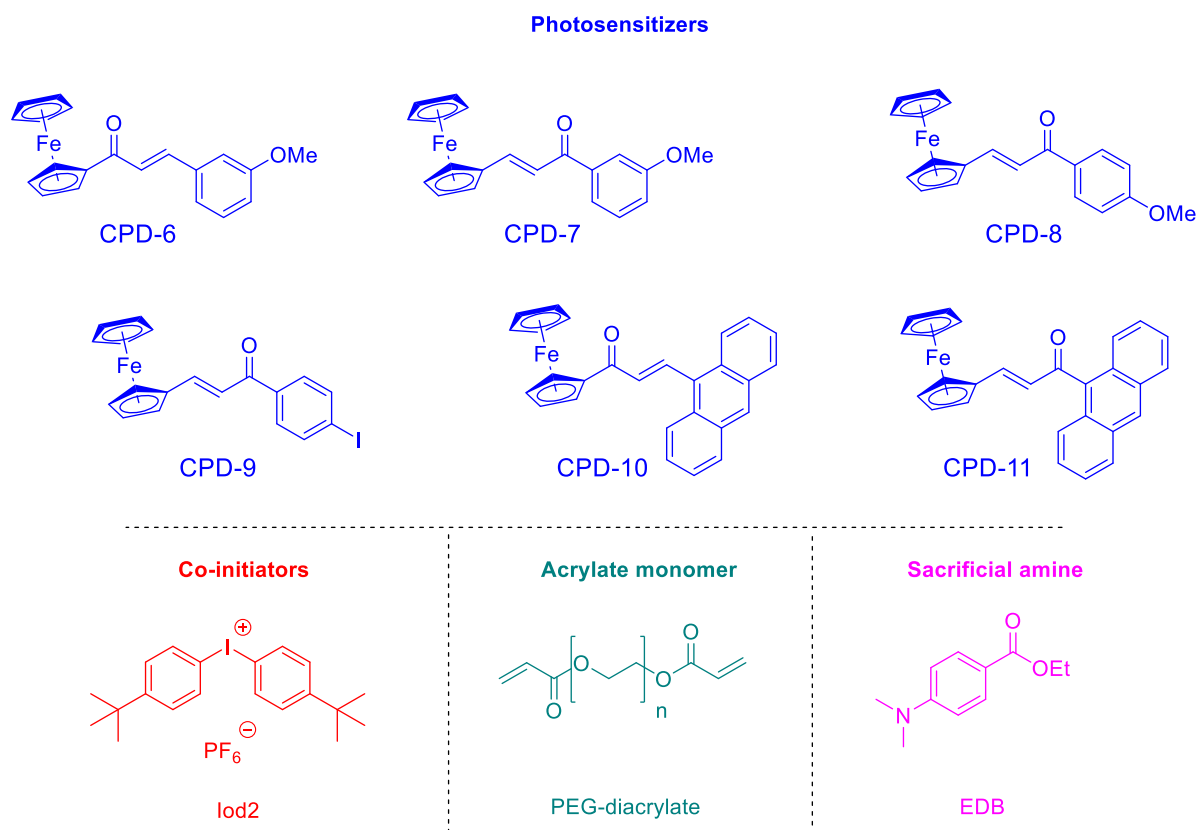
Figure 4. Chemical structures of chalcones CPD-6-CPD11, different additives and monomer.

Compared to the reference system (blank control) only composed of the two-component Iod2/EDB (1.5%/1.5%, w/w) system that furnished a final monomer conversion of 49% in thin films in laminates after 200 s of irradiation, significant differences in terms of final monomer conversions could be found between CPD-10 and CPD-11, differing by the position of the anthracene moiety. Indeed, when anthracene was used as an electron donor, a final monomer conversion of only 31% could be obtained with the three-component CPD-10/Iod2/EDB (1.5%/1.5%/1.5% w/w/w) system whereas the conversion could be increased up to 80% with the three-component CPD-11/Iod2/EDB (1.5%/1.5%/1.5% w/w/w) system. In this case, anthracene is included in the acetophenone moiety. In these different systems, higher final monomer conversions were obtained when ferrocene was used as an electron donor, as exemplified with CPD-7, CPD-9 or CPD-11. Only CPD-8 furnished a lower monomer conversion (40%), resulting from the adverse electron donating effect of the methoxy group on acetophenone.
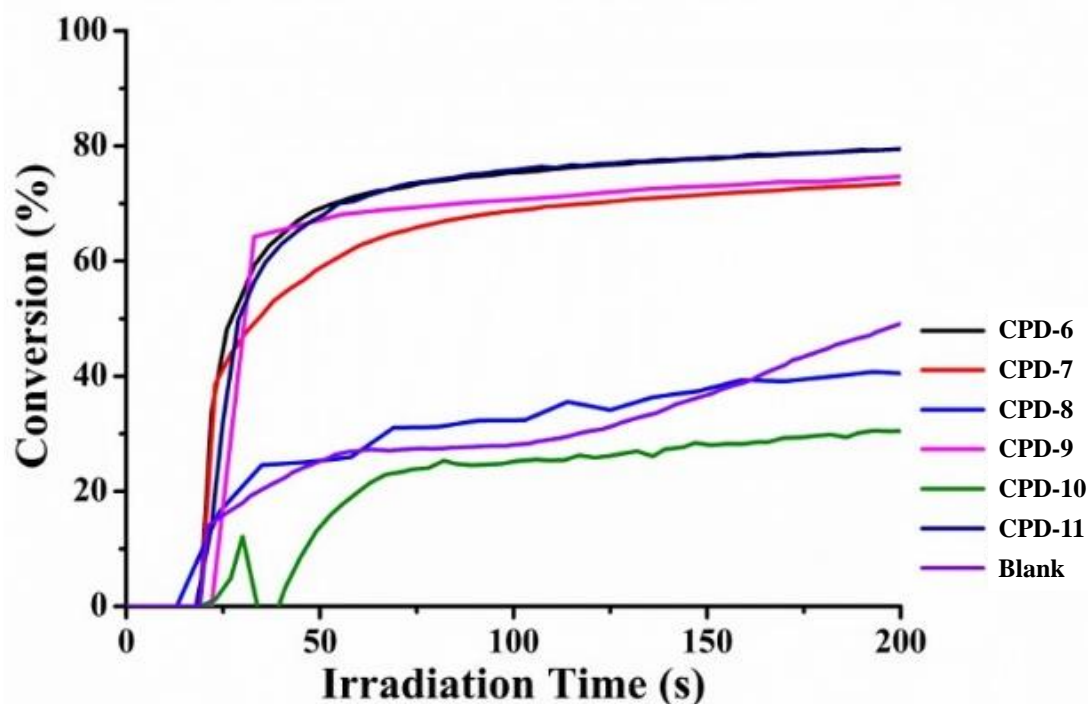
Figure 5. Photopolymerization profiles of PEG-diacrylate using the three-component dye/Iod2/EDB (1.5%/1.5%/1.5% w/w/w) system upon irradiation at 405 nm with a LED. Reprinted with permission of Chen et al. [99]

Table 1. Final monomer conversion obtained at 405 nm forPEG-diacrylate using three-component photoinitiating systems chalcone/Iod2/EDB (1.5%/1.5%/1.5% w/w/w) in thin films.

Chalcone initiating systems in PEG-diacrylate						
Chalcone	CPD-6	CPD-7	CPD-8	CPD-9	CPD-10	CPD-11	Blank
FCs	79.5%	73.5%	40.3%	74.7%	30.5%	79.5%	49%

Photolysis experiments carried out to investigate the high efficiency of the three-component systems revealed the chalcone/EDB interaction to be faster than that observed for the chalcone/Iod2 combination. Therefore, occurrence of a polymerization process resulting from the concomitant existence of an oxidative and a reductive cycle was proposed (See Figure 6). Upon photoexcitation of the chalcone, a photoinduced electron transfer towards the iodonium salt can occur, inducing its decomposition and the formation of Ph• radicals. Parallel to this, chalcone can also react in the excited state with EDB, in a reductive process, generating α-aminoalkyl radicals EDB•$_{(-H)}$. Efficiency of the photoinitiating system also relies in the ability of the photosensitizer to be regenerated. Indeed, dye$^{+•}$ can be reduced by the sacrificial amine EDB. Parallel to this, dye•$^-$ can also react with EDB, regenerating the dye to its initial redox state (See Figure 6).
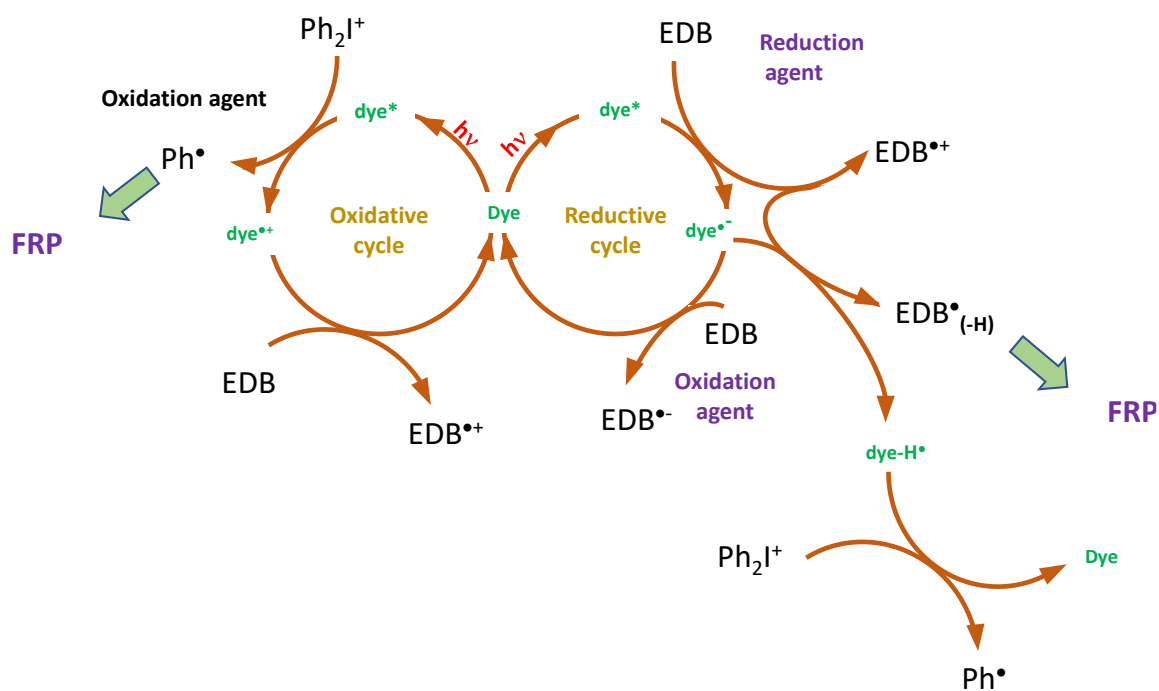
Figure 6. The concomitant oxidative and reductive cycles involved in the FRP of PEG-diacrylate using the three-component photoinitiating systems.

In 2021, a series of anthracene-based chalcones in which anthracene was used as the electron donor was examined as photoinitiators for 3D printing applications (See Figure 7).[104] In this series of dyes and considering that the same electron donor was used, similar absorption maxima could be determined between 387 and 389 nm. It therefore clearly indicates the weak contribution of the acetophenone group on the electronic delocalization. Indeed, even when the methoxy-substituted aromatic ring of acetophenone was replaced by a pyridine, a thiophene or a pyrrole moiety, no modification of the absorption maxima was detected. Due to the polyaromaticity of anthracene, a broad absorption band extending from 350 until 500 nm could be found for all chalcones, making CPD-12-CPD-18 suitable candidates for photopolymerization experiments carried out at 405 nm. For comparison, a narrower absorption spectrum was found for 9,10-dibutoxyanthracene (DBA), no absorption existing beyond 420 nm. (See Table 2 and Figure 8).
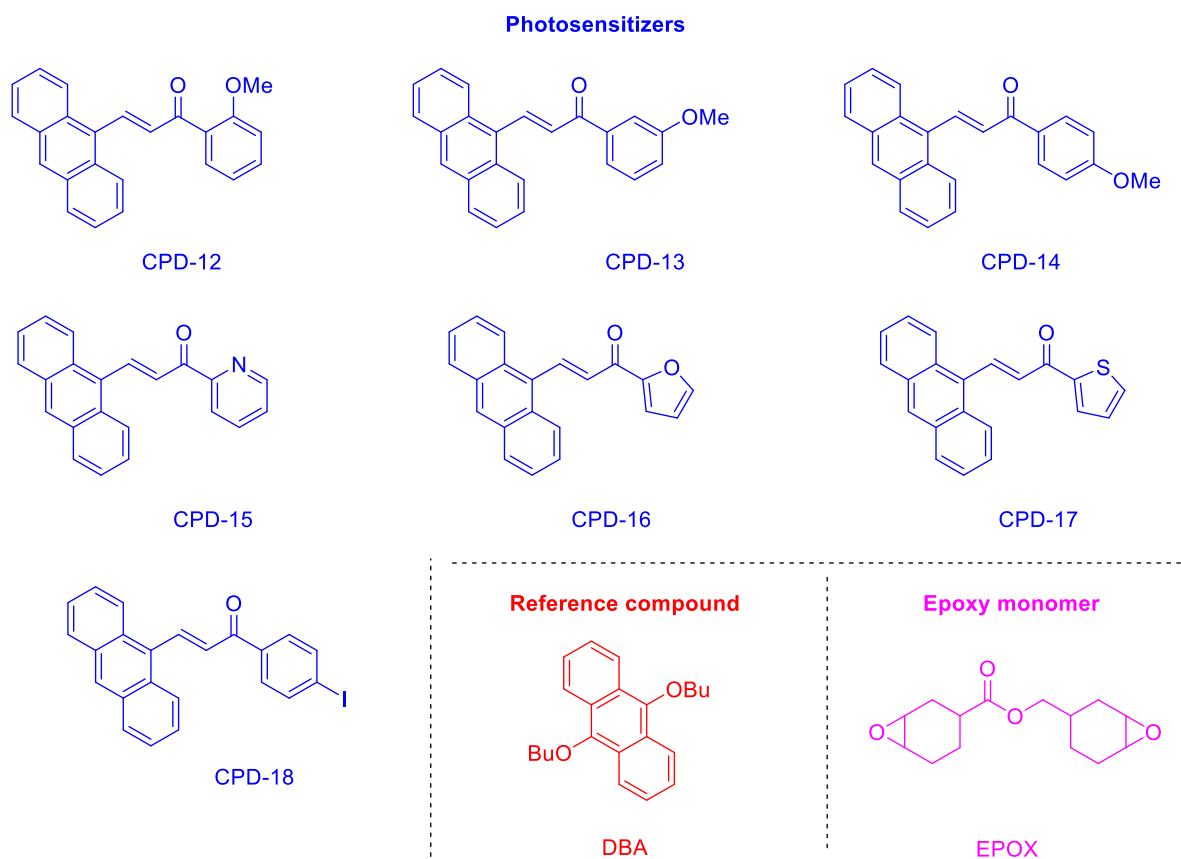
Figure 7. Chemical structures of chalcones CPD-12-CPD-18.

Table 2. Light absorption properties of anthracene-based chalcones CPD-12-CPD-18.

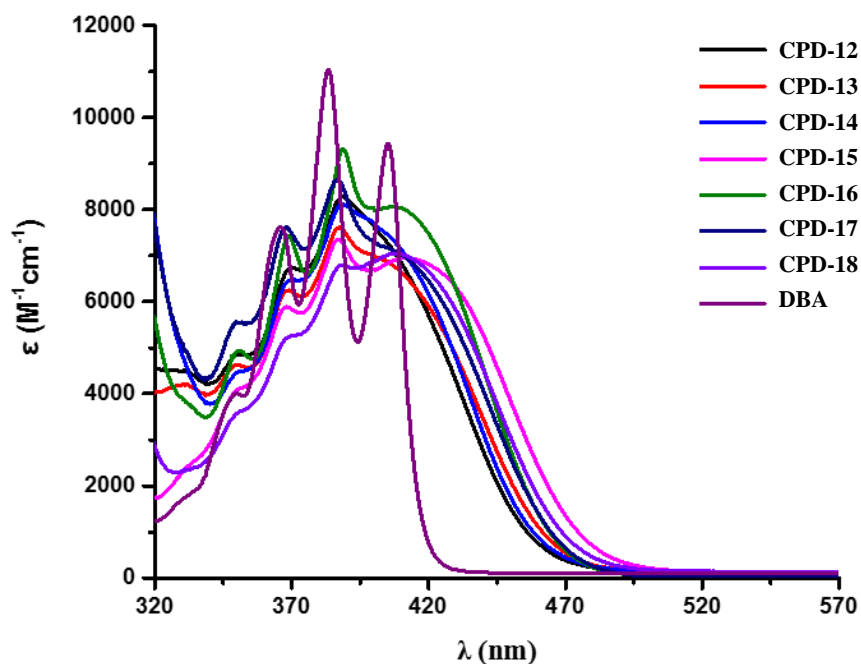|	λ_{max} /nm	ε_{max} /M^{-1}cm^{-1}	ε_{405nm} /M^{-1}cm^{-1}	ε_{470nm} /M^{-1}cm^{-1}
CPD-12	389	8300	7300	400
CPD-13	388	7600	6900	550
CPD-14	388	8100	7400	450
CPD-15	387	7300	6800	1350
CPD-16	389	9300	8000	600
CPD-17	387	8700	7200	650
CPD-18	389	6800	7000	900
DBA	384	11000	9400	0

Figure 8. UV-visible absorption spectra of chalcones CPD-12-CPD-18 and the reference dye DBA in acetonitrile. Reprinted with permission from Liu et al. [104]

To investigate the FRP of TMPTA in laminate, in thin films and upon irradiation at 405 nm with a LED, different three-component chalcone/Iod2/EDB (0.5%/1%/1%, w/w/w) photoinitiating systems were used. Noticeably, the seven chalcones gave final monomer conversions ranging from 45% for CPD-14 and CPD-18 up to 61% for CPD-17. Noticeably, best monomer conversions could be obtained for all chalcones comprising on the acetophenone moiety a group different from an aromatic ring. The highest monomer conversions were obtained with CPD-15-CPD-17 (~61%), comprising a pyridine, a thiophene or a pyrrole moiety. (See Table 3). For comparison, only a conversion of 5% was obtained with the two-component Iod2/EDB (1%/1%, w/w) system, evidencing the crucial role of chalcones in radical generation.

The higher reactivity of chalcones bearing heterocycles was confirmed during the CP of (3,4-epoxycyclohexane) methyl 3,4- epoxycyclohexylcarboxylate (EPOX) investigated under air at two different wavelengths, namely 405 and 470 nm. Here again, the two-component photoinitiating systems based on compounds CPD-15-CPD-17 could give higher monomer conversions than the reference DBA/Iod2 (0.5%/1%, w/w) system (43, 52 and 47% vs. 38% for the DBA-based system) at 405 nm. The same holds true at 470 nm, with EPOX conversions of 33, 36 and 27% after 600 s for CPD-15-CPD-17. Conversely, only a monomer conversion of 6% was obtained with DBA at 470 nm. This drastic difference can be assigned to the weak absorption of DBA at 470 nm, adversely affecting its photoinitiating ability. These results clearly demonstrate the crucial role of the substitution pattern of chalcones on their photoinitiating abilities. Indeed, from the optical viewpoint, no difference in terms of absorption maxima can be found between the different dyes. Other parameters than the absorption properties such as the rate constant of interaction with the different additives, the

reactivity of the generated radicals in turn govern the efficiency of the photoinitiating systems. Finally, investigation of the reactivity of CPD-15-CPD-17 by mean of photolysis experiments revealed similar photolysis kinetics for the chalcone/Iod2 and the chalcone/EDB combinations, certainly constituting the strength of the corresponding three-component photoinitiating systems. Consequently, both the oxidative and reductive processes can contribute to the generation of initiating species. Finally, 3D printing experiments could be carried out with the most reactive photoinitiating systems based on CPD-16. Upon irradiation at 405 nm, 3D patterns of remarkable spatial resolutions could be obtained (See Figure 9). Especially, EPOX was selected as the appropriate monomer for 3D printing experiments as a lower shrinkage is observed with this monomer compared to monomers such as TMPTA. Indeed, shrinkage is a major issue in the 3D printing technology.

Table 3. TMPTA and EPOX conversions obtained upon irradiation for 600 s with LEDs emitting at 405 and 470 nm

PISs	TMPTA/%	EPOX/%	
	dyes/Iod2/EDB[a]	dyes/Iod2[a]	dyes/Iod2[b]
CPD-12	57	39	21
CPD-13	51	37	24
CPD-14	45	21	15
CPD-15	60	43	33
CPD-16	60	52	36
CPD-17	61	47	27
CPD-18	45	33	19
Blank	5	-	-
DBA	-	38	6

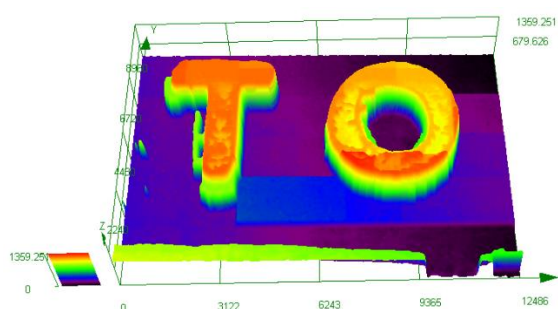[a] under LED@405 nm irradiation; [b] under LED@470 nm irradiation.

Figure 9. 3D patterns obtained upon polymerization of EPOX at 405 nm using the two-component CPD-16/Iod2 (0.5%/1%, w/w) system. Reprinted with permission from Liu et al.[80]

In 2021, CPD-14 was revisited by another group, except that the methoxy group of CPD-14 was replaced by an ethoxy group in CPD-19, unaffecting the optical properties (See Figure 10).[253] In this interesting work, influence of the *cis/trans* isomerization of chalcones on the photoinitiating ability was studied. A comparison between an anthracene and a triphenylamine-based chalcone (CPD-19 and CPD-20) was also established.
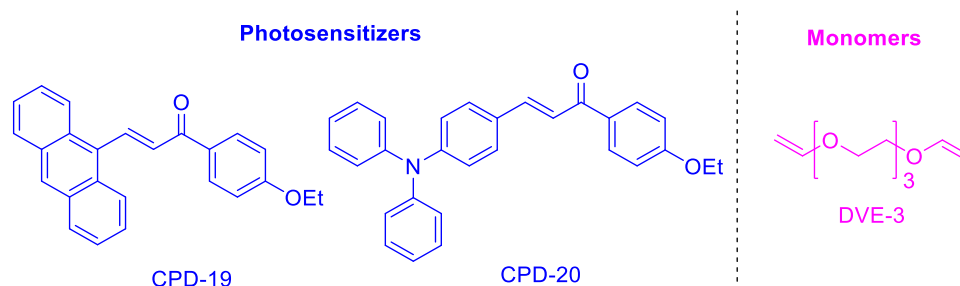

Figure 10. Chemical structures of CPD-19 and CPD-20, and DVE-3.

Indeed, photolysis experiments done in acetonitrile as the solvent revealed CPD-19 to rapidly isomerize contrarily to CPD-20, for which no isomerization was detected in solution. While examining the CP of triethyleneglycol divinyl ether (DVE-3) upon irradiation at 405 nm with a LED (45 mW/cm²), a final monomer conversion of 88% could be obtained with CPD-20 using the two-component CPD-20/Iod2 (1.0%/2.0%, w/w) photoinitiating system contrarily to only 62% with the two-component CPD-19/Iod2 (1.0%/2.0%, w/w) system. Therefore, the structure/performance relationship was clearly evidenced.

Monochalcones were not the only structures to be studied as photoinitiators of polymerization and a series of six *bis*-chalcones based on anthracene CPD-21-CPD-26 were also examined as potential photoinitiators (See Figure 11).[191] Interestingly, in these structures, the substitution pattern of the central cyclic ketones had no incidence on the absorption spectra of the different dyes so that all dyes showed an absorption maximum at 250 nm. An additional broad absorption band extending from 300 until 450 nm could be observed for all dyes so that polymerization tests could be carried out at 405 nm (See Figure 12 and Table 4).
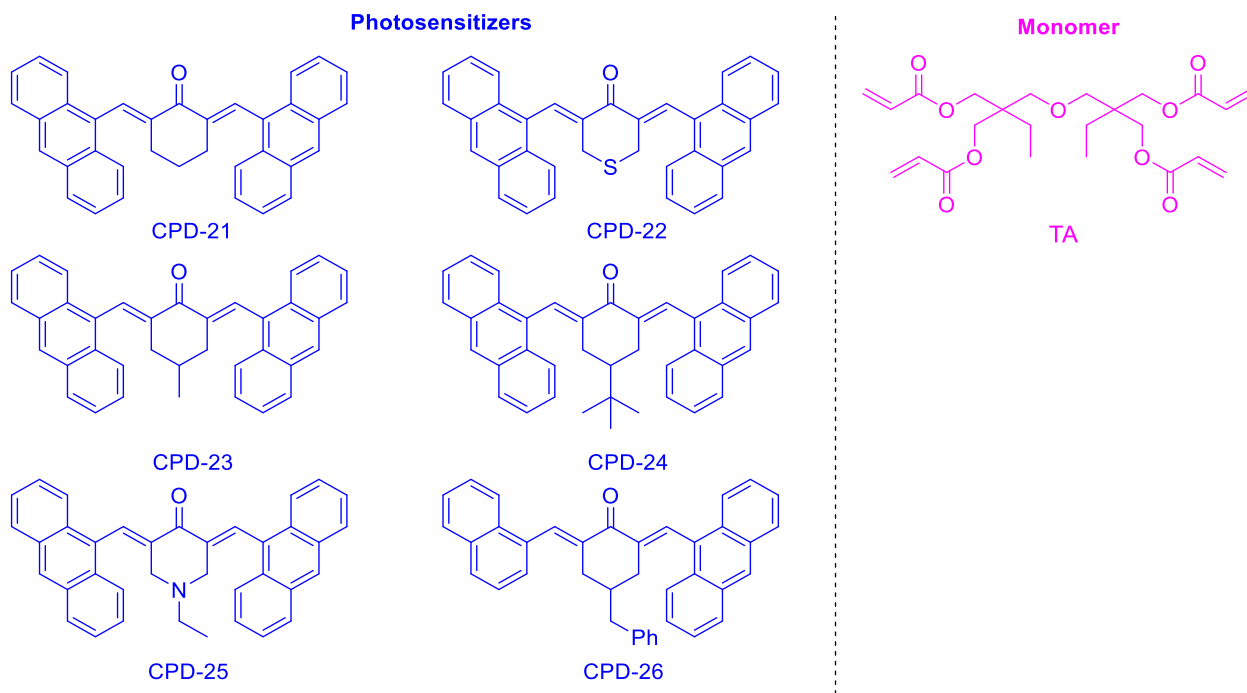
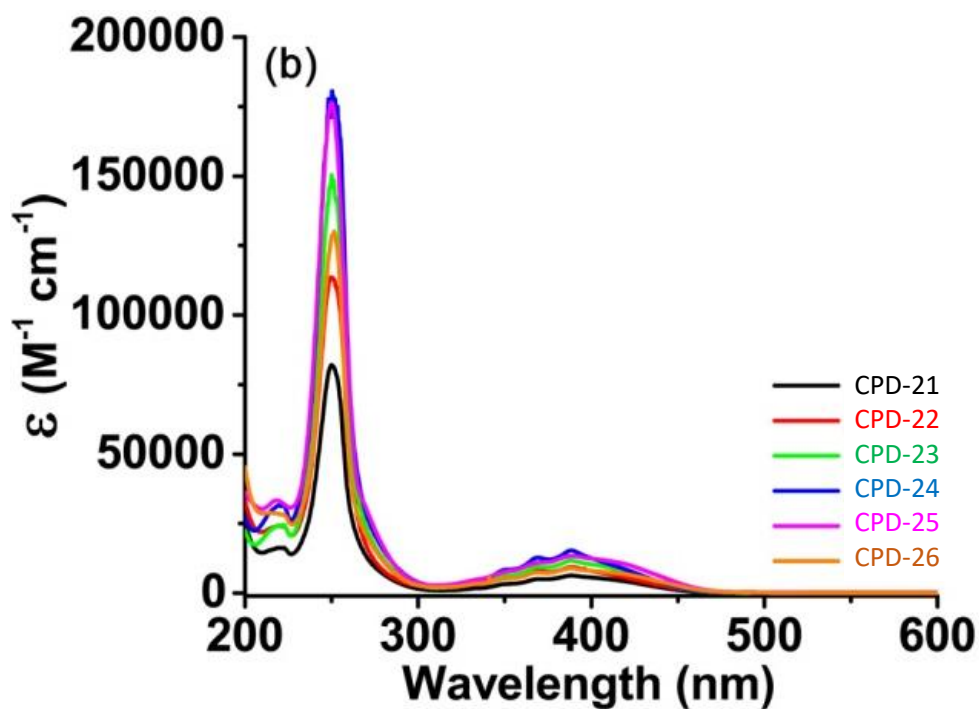**Figure 11.** Chemical structures of CPD-21-CPD-26 and TA.

Figure 12. UV-visible absorption spectra of CPD-21-CPD-26 in acetonitrile. Reproduced with permission of Xu et al. [191]

Table 4. Light absorption properties of CPD-21-CPD-26: absorption maxima wavelength (λ_{max}) as well as the molar extinction coefficients at λ_{max} (ε_{max}) and at 405 nm ($\varepsilon_{405\,nm}$), respectively.

	λ_{max} (nm)	ε_{max} (M^{-1} cm^{-1})	$\varepsilon_{405\,nm}$ (M^{-1} cm^{-1})
CPD-21	250	81800	5400
CPD-22	250	113300	7400
CPD-23	250	149600	9900
CPD-24	250	178400	11500
CPD-25	250	175900	12000
CPD-26	250	129500	7800

Noticeably, investigation of the FRP of (oxybis(methylene))*bis*(2-ethylpropane-2,1,3-triyl) tetraacrylate (TA) upon irradiation at 405 nm in thick and in thin films using the three-component chalcone/Iod2/EDB (0.1%/2%/2%, w/w/w) systems revealed that no direct correlation was existing between molar extinction coefficients and final monomer conversions. Indeed, as shown in the Table 5, if CPD-24 could maintain a higher TA conversion both in thick and thin films (81 and 74% respectively), conversely CPD-25 and CPD-26 were efficient dyes in thin films (73 and 76% yield respectively) whereas low conversions were obtained in thick films (41 and 53% respectively). On the opposite, CPD-21 could reach a TA conversion as high as 90% in thick film whereas the conversion was limited to 66% in thin films.

Table 5 Final monomer conversions obtained during the FRP of TA upon irradiation at 405 nm with a LED for 400 s using the three-component chalcone/Iod2/EDB (0.1%/2%/2%, w/w/w) systems.

FCs	CPD-21	CPD-22	CPD-23	CPD-24	CPD-25	CPD-26
(in thick films)	~90%	~41%	~68%	~81%	~41%	~53%
FCs	CPD-21	CPD-22	CPD-23	CPD-24	CPD-25	CPD-26
(in thin films)	~66%	~68%	~60%	~74%	~73%	~76%

2.2. Anthracene-based acridinedione

Acridinediones (ADs) are a class of laser dyes operating in the blue-green region.[254] Due to the simultaneous presence of an heterocyclic nitrogen atom and two carbonyl groups that respectively act as electron donor and as electron acceptors, an efficient push-pull effect exists within these structures.[255–257] In 2013, an anthracene-substituted acridine-1,8-dione CPD-27 was synthesized and its photoinitiating ability compared to that of a pyrene analogue CPD-28 (See Figure 13).[215]
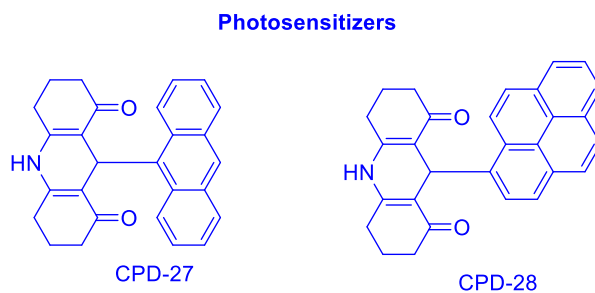
Photosensitizers

CPD-27   CPD-28

Figure 13. Chemical structures of CPD-27 and CPD-28.

From the absorption viewpoint, shapes of the absorption spectra of CPD-27 and CPD-28 were similar except that the absorption spectrum of CPD-28 was redshifted by ca. 50 nm compared to CPD-27. Molar extinction coefficients around 15 000 $M^{-1}.cm^{-1}$ were found for the two dyes at the absorption maximum (See Figure 14).
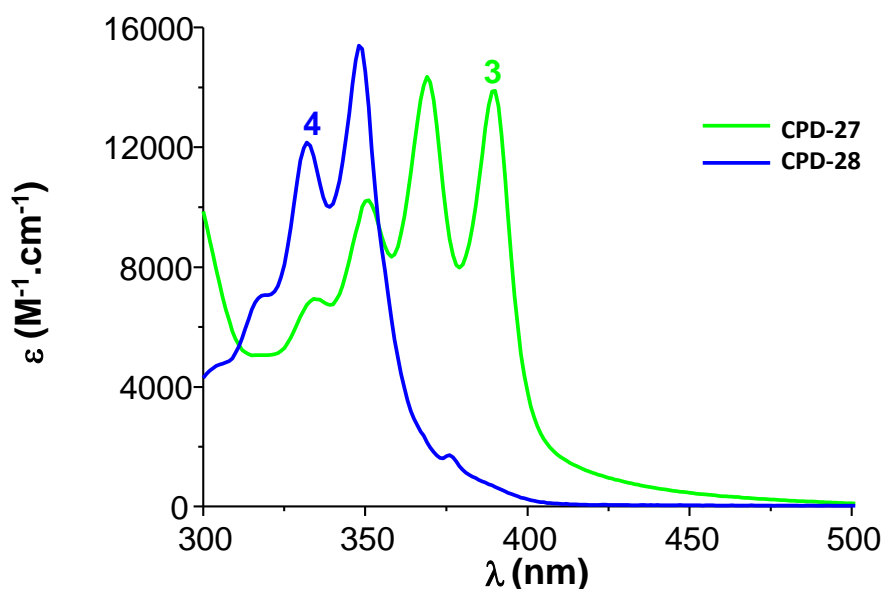

Figure 14. UV-visible absorption spectra of CPD-27 and CPD-28 in acetonitrile. Reprinted with permission of Xiao et al. [215]

Photopolymerization of EPOX in the presence of the three-component AD/Iod/NVK (3%/2%/3%, w/w/w) system under air upon irradiation with a Xe-Hg lamp (> 330 nm, 56 mW/cm²) furnished monomer conversions of 34 and 48% after 500 s of irradiation with CPD-27 and CPD-28 respectively. While using a LED emitting at 405 nm, only CPD-28 could initiate a polymerization, peaking at 28% despite the weak absorption of CPD-28 at this wavelength. Conversely, despite the high molar extinction coefficient at 405 nm, no polymerization was detected with the three-component CPD-27/Iod/NVK (3%/2%/3%, w/w/w) system. While using a halogen lamp of low intensity (370-800 nm range, 12 mW/cm²), similar monomer conversions were obtained with the two-component CPD-28/Iod (3%/2%, w/w) system and the three-component CPD-28/Iod/NVK (3%/2%/3%, w/w/w) system, the monomer conversions being respectively of 59 and 60%. Consistent with the results obtained with the Xe-Hg lamp, no polymerization was detected with CPD-27, the halogen lamp displaying a lower light intensity than the Xe-Hg lamp. Once again, the crucial importance of the

substitution pattern was demonstrated with this comparison between the photoinitiating ability of anthracene and pyrene-based dyes.

2.3. Anthracene-based 1,8-naphthalimides

1,8-Naphthalimides are fluorescent compounds that found applications in research fields such as light emitting devices for the design of electroluminescent materials,[258] as electron transport materials for inverted solar cells [259] electron acceptors for polymer solar cells,[260] or fluorescent probes for optical sensors.[261–264] Due to the easiness of synthesis, 1,8-naphthalimides were also used as photoinitiators of polymerization.[46,80–95] In 2014, the first anthracene-substituted 1,8-naphthalimide CPD-29 was proposed by Lalevée and coworkers (See Figure 15). Unfortunately, due to the lack of substitution on the naphthalimide core, absorption of CPD-29 remained located in the UV range so that this dye was unsuitable for visible light experiments.[89] Face to these considerations, in 2016, another strategy was used, consisting in incorporating the anthracene moiety in the naphthalimide core.[93] As specificity, CPD-30 is a well-known anticancer agent named azonafide which is still under use in medicine.[265,266] By extending the aromaticity of the naphthalimide core, a significant redshift of the absorption spectrum could be found compared to CPD-29. As shown in the Figure 16, the absorption spectrum of CPD-30 was broad, extending from 350 to 500 nm, the maximum being located at 431 nm ($\varepsilon = 7970$ M^{-1}.cm^{-1}). Based on its absorption, CPD-30 was an appropriate dye for irradiation at 405 and 455 nm with LEDs. Noticeably, examination of its photoinitiating ability at 405 and 455 nm during the CP of EPOX with two-component and three-component systems revealed the two-component CPD-30/Iod (0.5%/2%, w/w) system to be unable to initiate polymerizations at the two wavelengths. Conversely, upon introduction of NVK, conversions of 63 and 57% could be obtained at 405 and 455 nm respectively while using the three-component CPD-30/Iod/NVK (0.5%/2%/3%, w/w/w) system. By analogy with previous photoinitiating systems reported in the literature, the formation of Ph-NVK$^+$ cation was proposed as the initiating species in the three-component photoinitiating system. Indeed, as demonstrated with the two-component CPD-30/Iod (0.5%/2%, w/w) system, the radical cation CPD-30$^{\bullet+}$ is not sufficiently reactive to initiate the CP of EPOX. However, CPD-30$^{\bullet+}$ can react with NVK, producing the highly reactive Ph-NVK$^+$ cation, capable to initiate the CP of EPOX. Noticeably, bleaching properties could be evidenced with the two-component CPD-30/Iod system, enabling to manufacture colourless coatings.
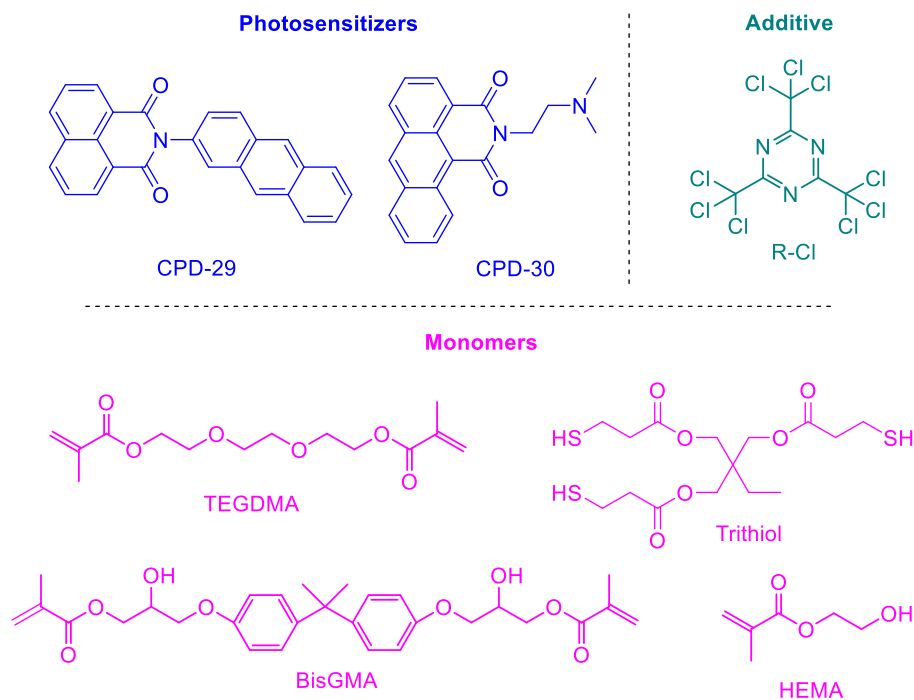
Figure 15. Chemical structures of CDP-29 and CPD-30, different monomers and additive.
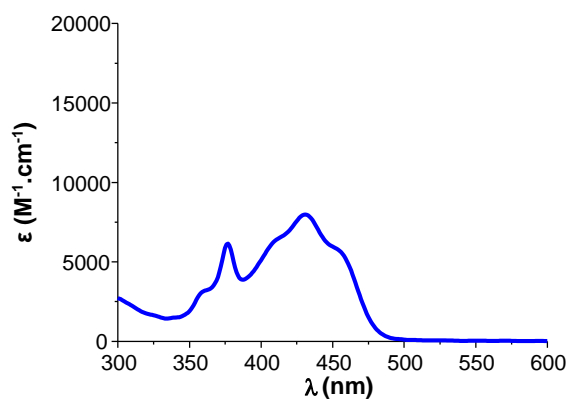
Figure 16. UV-visible absorption spectra of CPD-30 in acetonitrile. Reprinted with permission of Zivic et al. [93]

Table 6. EPOX conversions obtained under air upon exposure to different light sources for 800 s in the presence of CPD-30/Iod (0.5%/2%, w/w) or CPD-30/Iod/NVK (0.5%/2%/3%, w/w/w).

PIS	LED (405 nm)	LED (455 nm)
CPD-30/Iod	np[a]	np[a]
CPD-30/Iod/NVK	63%	57%

[a] np: no photopolymerization.

$$dye \rightarrow {}^1dye \ (hv) \quad and \quad {}^1dye \rightarrow {}^3dye \tag{r4}$$
$$^{1,3}dye + Ph_2I^+ \rightarrow dye^{\bullet+} + Ph_2I^\bullet \tag{r5}$$
$$Ph_2I^\bullet \rightarrow Ph^\bullet + Ph\text{-}I \tag{r6}$$
$$Ph^\bullet + NVK \rightarrow Ph\text{-}NVK^\bullet \tag{r7}$$
$$Ph\text{-}NVK^\bullet + Ph_2I^+ \rightarrow Ph\text{-}NVK^+ + Ph^\bullet + Ph\text{-}I \tag{r8}$$
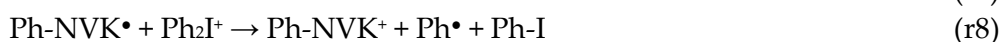
During the FRP of TMPTA, the low reactivity of the two-component CPD-30/Iod (0.5%/2%, w/w) photoinitiating system was confirmed. Indeed, if a moderate conversion was detected at 405 nm, no polymerization was observed at 455 nm. While using the three-component CPD-30/Iod/NVK system, a two-fold enhancement of the TMPTA conversion was detected at 405 nm (55% conversion) whereas a conversion of 49% could be obtained at 455 nm. Comparison with the benchmark *bis*-acylphosphine oxide (BAPO) revealed CPD-30 to furnish similar conversions.

Table 7. TMPTA conversions obtained in laminate upon exposure to different light sources for 400 s in the presence of CPD-30 based PISs (DNNDs: 0.5 wt%; Iod 2wt%; NVK 3 wt% in the formulations). BAPO (0.5 wt%) PISs as references.

PIS	LED 405 nm	LED 455nm
CPD-30/Iod	29%	
CPD-30/Iod/NVK	55%	49%
BAPO	56%	54%

Considering that the three-component CPD-30/Iod/NVK system can initiate both the FRP of TMPTA and the CP of EPOX upon irradiation at 405 nm, the concomitant cationic/radical polymerization of an EPOX/TMPTA blend (50%/50% w/w) was examined under air and in laminate, generating interpenetrated polymer networks (IPNs) (See Figure 17).
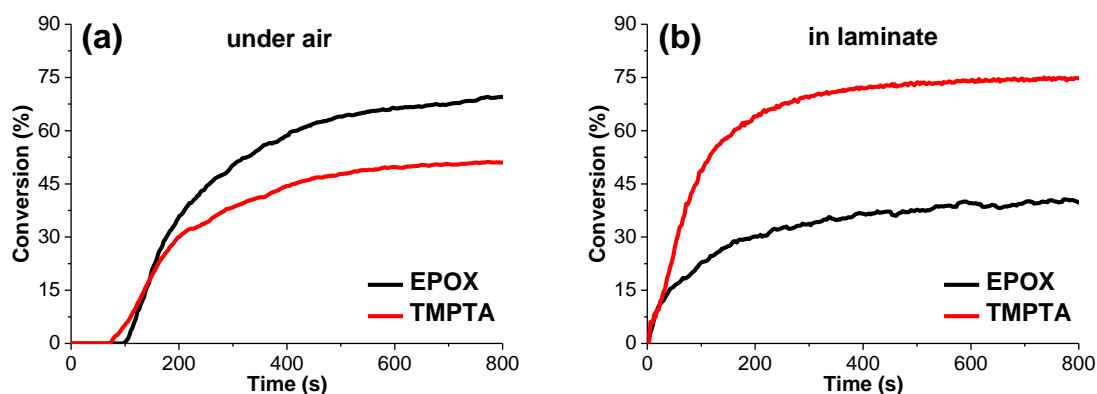

Figure 17. Photopolymerization profile of an EPOX/TMPTA blend (50%/50%, w/w) using the three-component CPD-30/Iod/NVK (0.5%/2%/3%, w/w/w) system under air (a) or in laminate (b). upon irradiation with a LED emitting at 405 nm. Reprinted with permission of Zivic et al. [93]

Interestingly, difference of EPOX and TMPTA conversions were found in laminate and under air. Thus, if EPOX and TMPTA conversion of 70% and 51% were respectively obtained under air, these values varied in laminate with a decrease of the EPOX conversion (40%) and a drastic improvement of the TMPTA conversion (75%) in laminate. Similar variations of the EPOX/TMPTA conversions have previously been reported in the literature for other photoinitiating systems.[89,94] Notably, part of the generated radicals are consumed by oxygen, adversely affecting the TMPTA conversion. Conversely, in laminate, the higher reactivity of radicals vs. cations support the higher TMPTA conversion compared to EPOX.

Thiol-ene photopolymerization of a trithiol/DVE-3 blend (57%/43%, w/w) in laminate using the two-component CPD-30/Iod (0.5%/2%, w/w) system upon irradiation with a LED emitting at 405 nm was also examined. Noticreably, an almost quantitative conversion of DVE-3 was observed whereas the conversion of trithiol remained limited to 41%. The high DVE-3 conversion can be assigned to the cationic polymerization of DVE-3 competing with the thiol-ene polymerization (See Figure 18). To support the thiol-ene polymerization, the mechanism detailed in equations r9-r11 was proposed.
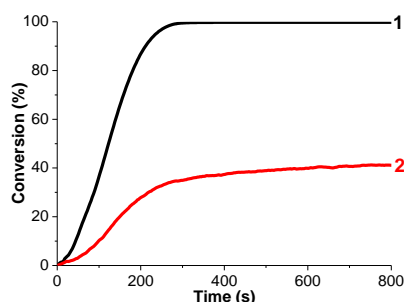

Figure 18. Photopolymerization profile of a trithiol/DVE-3 blend (40%/60%, n/n; 57%/43%, w/w) in laminate in the presence of CPD-30/Iod (0.5%/2%, w/w) upon the LED at 405 nm exposure; curve 1: DVE-3 (vinyl double bond) conversion; curve 2: trithiol (S–H) conversion. Reprinted with permission of Zivic et al. [93]

$$Ph^\bullet + RS\text{-}H \rightarrow Ph\text{-}H + RS^\bullet \tag{r9}$$

$$RS^\bullet + R'\text{-}CH{=}CH_2 \rightarrow R'\text{-}CH^\bullet\text{-}CH_2SR \tag{r10}$$

$$R'\text{-}CH^\bullet\text{-}CH_2SR + RS\text{-}H \rightarrow R'\text{-}CH_2\text{-}CH_2SR + RS^\bullet \tag{r11}$$

Finally, polymerization in water was examined with CPD-30, using an original approach. Indeed, in order to render the photoinitiator water-soluble, appropriate functional groups such as sulfonate, carboxylate or ammonium can be introduced, implying a chemical modification of the dye. In this work, a chemistry-free approach was examined, consisting in encapsulating the dye in β-cyclodextrin. Precisely, after searching the macrocycle of appropriate size for azonafide, sulfobutylether-β-cyclodextrin was selected as the best candidate.[267] When tested as photoinitiator for the two-component [CPD-30/SBE-β-

CD]/MDEA (0.3%/4%, w/w) system for hydroxyethylmethacrylate (HEMA) in water, hydrogels could be obtained after one hour or irradiation at 405 nm with a laser diode (110 mW/cm²). A monomer conversion of 68% and a water content of 70% were respectively determined. Interestingly, a clear photobleaching of the polymer was observed.

2.4. 9,10-*Bis*(ethynyl)-substituted anthracene

Polycyclic aromatic hydrocarbons (PAHs) are a large group of organic compounds only composed of carbons and hydrogens and comprising dyes such as anthracene, pentacene or rubrene. Due to their planarities and their polyaromaticities, these structures are often insoluble. To address this issue, introduction of triisopropylsilyl)ethynyl group proved to be an effective strategy and among structures 6,13-*bis*(triisopropylsilylethynyl)pentacene (TIPS-pentacene) is a well-known semiconductor extensively used for the design of organic field effect transistors by solution process.[268,269] By introducing two triisopropylsilyl)ethynyl groups, TIPS-pentacene is soluble in most of the common organic solvents. This strategy was also applied to improve the solubility of anthracene. In 2012, CPD-31 was used in combination with Iod and *tris*(trimethylsilyl)silane ((TMS)₃SiH).[270] By the presence of two triisopropylsilyl)ethynyl groups, a significant redshift of the absorption spectrum of CPD-31 was found compared to anthracene (See Figure 19). By theoretical calculations, contribution of the ethynyl groups both in the HOMO and LUMO levels (where HOMO and LUMO respectively stand for highest occupied molecular orbital and lowest unoccupied molecular orbital) was demonstrated, resulting in an extension of the π-conjugation and reducing the HOMO-LUMO gap. An absorption maximum was found at 440 nm (ε = 40 000 M⁻¹.cm⁻¹) for CPD-31, perfectly fitting with the emission of the blue LED emitting at 462 nm or the emission of Xe lamp (380-740 nm range) (See Figure 19).
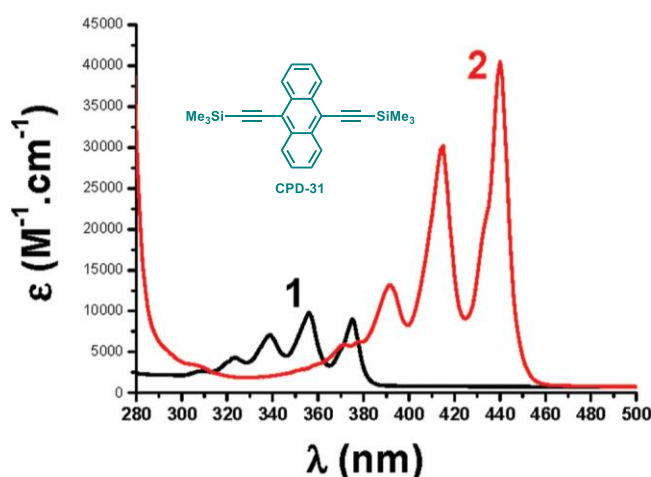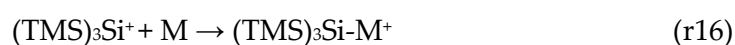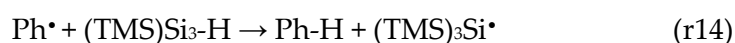

Figure 19. UV-visible absorption spectra of anthracene (1) and CDP-31 (2) in *tert*-butylbenzene. Reprinted with permission of Tefhe et al. [270]

From the fluorescence experiments, a strong interaction between Iod and CPD-31 could be evidenced, generating Ph• radicals detectable by electron-spin resonance spin-trapping (ESR-ST) experiments. By hydrogen abstraction, Ph• radicals can be converted as silyl radicals (TMS)₃Si•, capable to initiate the FRP of acrylates. Interestingly, photolysis of the three-

component CPD-31/(TMS)₃Si-H/Iod (0.5%/3%/2% w/w/w) system was slower than that of the two-component CPD-31/Iod (0.5%/2% w/w) system, evidencing that CPD-31 was partially regenerated during photolysis experiments. Regeneration of CPD-31 was assigned to the reaction of $(TMS)_3Si^\bullet$ with $An\text{-}Si^{\bullet+}$, generating silylium cations $(TMS)_3Si^+$ capable to initiate the CP of epoxides. Overall, a mechanism summarized in equations r12-r16 was proposed.

$$CPD\text{-}31 \rightarrow {}^1CPD\text{-}31 \quad (h\nu) \tag{r12}$$

$${}^1CPD\text{-}31 + Ph_2I^+ \rightarrow CPD\text{-}31^{\bullet+} + Ph^\bullet + Ph\text{-}I \tag{r13}$$

$$Ph^\bullet + (TMS)Si_3\text{-}H \rightarrow Ph\text{-}H + (TMS)_3Si^\bullet \tag{r14}$$

$$(TMS)_3Si^\bullet + CPD\text{-}31^{\bullet+} \rightarrow (TMS)_3Si^+ + CPD\text{-}31 \tag{r15}$$

$$(TMS)_3Si^+ + M \rightarrow (TMS)_3Si\text{-}M^+ \tag{r16}$$
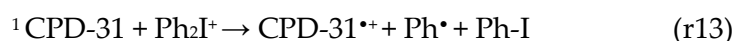
By cyclic voltammetry, the high reactivity of $CPD\text{-}31^{\bullet+}$ towards the residual water existing in solvents or monomers was demonstrated, explaining why CPD-31 was only partially regenerated in equation (r15).[271] Examination of the photoinitiating ability of the two-component CPD-31/Iod (0.5%/2% w/w) system and the three-component CPD-31/(TMS)₃Si-H/Iod (0.5%/3%/2% w/w/w) system under air upon irradiation with a Xe-lamp confirmed the partial regeneration of the photosensitizer with the three-component system. Indeed, as shown in the Figure 20, a conversion of 83% was obtained with the three-component system vs. 45% for the two-component system after 400 s of irradiation.
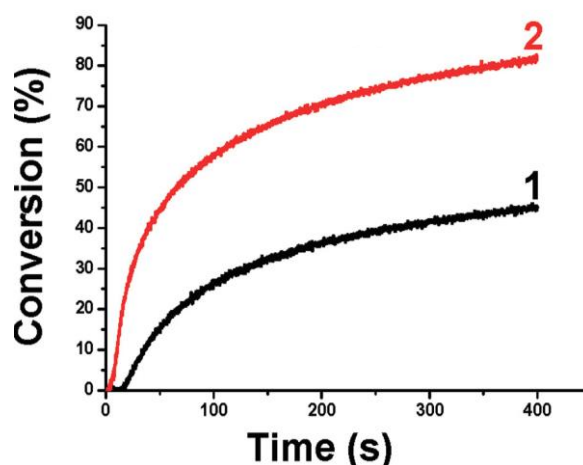

Figure 20. Photopolymerization profiles of EPOX under air upon irradiation with a Xe-lamp using (1) CPD-31/Iod (0.5/2% w/w); (2) CPD-31/(TMS)₃Si-H/Iod (0.5/3/2% w/w). Reprinted with permission of Tefhe et al. [270]

It therefore demonstrated the higher photoinitiating ability of silylium $(TMS)_3Si^+$ cations compared to the $CPD\text{-}31^{\bullet+}$ cations. The high reactivity of the three-component photoinitiating system was also assigned to the ability of silanes to convert the none initiating peroxyl radicals (formed by addition of oxygen) as new silyl radicals.[272–279] By using a LED

emitting at 462 nm, a slightly lower conversion was obtained with the three-component system, even after elongation of the polymerization time. Thus, a conversion of 70% was obtained after 700 s of irradiation, consistent with the low molar extinction coefficient of CPD-31 at 462 nm. Considering the photocatalytic behaviour of CPD-31 in three-component systems, comparisons were established with a reference metal complex i.e. Ir(ppy)$_3$. Interestingly, CPD-31 could compete with the two reference photoinitiating systems, evidencing that purely organic compounds can rival with transition metal complexes (See Figure 21).
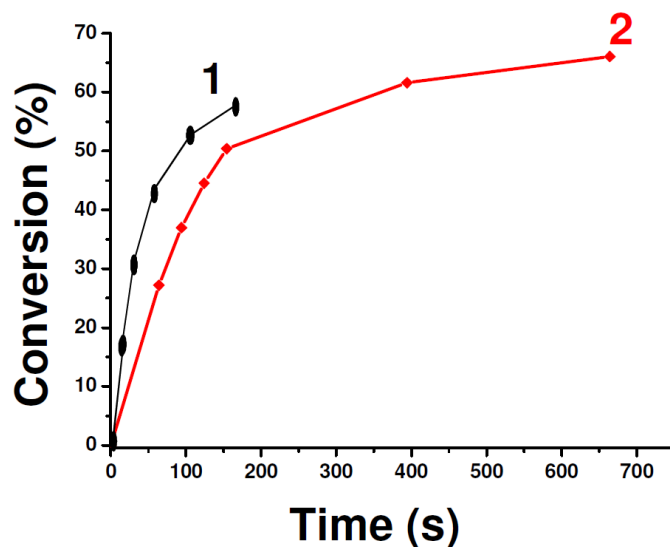

Figure 21. Comparison of the photoinitiating ability of (1) Ir(ppy)$_3$/(TMS)$_3$Si-H/Iod (0.2 %/3 %/ 2% w/w); (2) CPD-31/(TMS)$_3$Si-H/Iod (0.5 %/3 %/ 2% w/w) during the CP of EPOX under air upon irradiation at 462 nm. Reprinted with permission of Tefhe et al. [270]

Ph$^\bullet$ and (TMS)$_3$Si$^\bullet$ are good initiating radicals formed in equations r13 and r14 so that their photoinitiating abilities was examined during the FRP of TMPTA. As shown in the Figure 22, a final monomer conversion of 45% could be obtained with the three-component photoinitiating system upon irradiation with a Xe lamp, greatly higher than that obtained with its parent structure i.e. anthracene (almost no conversion detected).
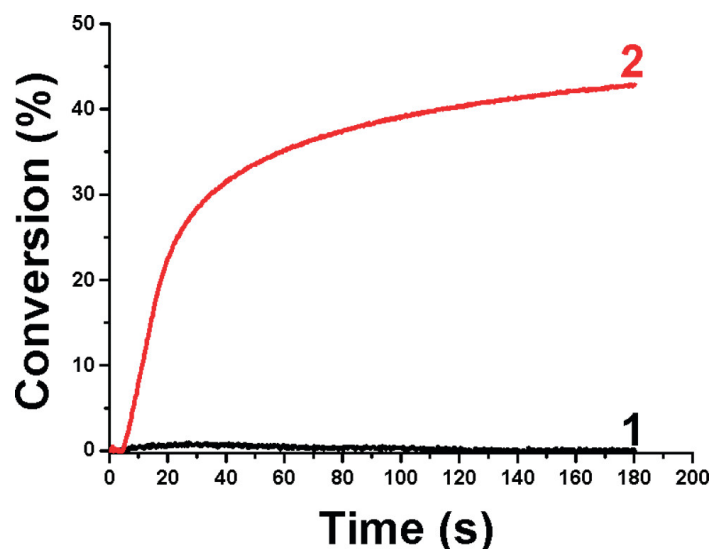
Figure 22. Conversion determined during the FRP of TMPTA in laminate using (1) CPD-31 (0.5%) and (2) CPD-31/(TMS)$_3$Si–H/Iod (0.5%/3%/2% w/w/w) upon irradiation with a Xe lamp. Reprinted with permission of Tefhe et al. [270]

With aim at designing soluble dyes, an interesting approach was developed in 2004 with the synthesis of 9,10-*bis*(phenylethynyl)-1,8-dimethoxyanthracene (CPD-32) in which the two methoxy groups could improve the solubility of dyes while red-shifting the absorption of CPD-32 towards the visible range. Interestingly, CPD-32 was used as a photosensitizer for the sensitization of photoacid generators such as *N*-trifluoromethyldulfonyloxy-1,8-naphthalimide (NAI-105) or Iod2 (See Figure 23).[280] All experiments were carried out at 488 nm with an Ar ion laser.
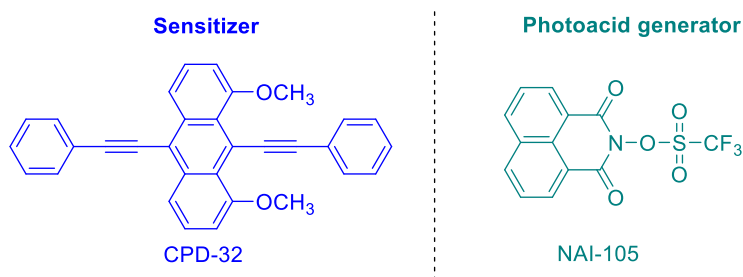

Figure 23. Chemical structures of CPD-32 and the photoacid generator.

Interestingly, sensitivity of the CPD-32/NAI-105 combination was greatly higher than that of the CPD-32/Iod2 combination. Besides, examination of photoacid generation in solution with an acid-base indicator revealed the acid concentration to be lower for the CPD-32/NAI-105 system compared to that of the CPD-32/Iod2 combination. To support these unexpected results, an unfavorable back electron transfer from the photoacid generator to the photosensitizer was suggested as the main explanation.[281–283]

2.5. Anthracene-based phenothiazine

Phenothiazine as well as carbazole or triphenylamine are aryl amines commonly used for the design of photoinitiators due to their good electron donating abilities. In 2019, a series of anthracenes substituted with different electron-donating groups CPD-33-CPD-36 was designed and synthesized as initiators for the FRP of hexanediol diacrylate (HDDA) (See Figure 24).[284]

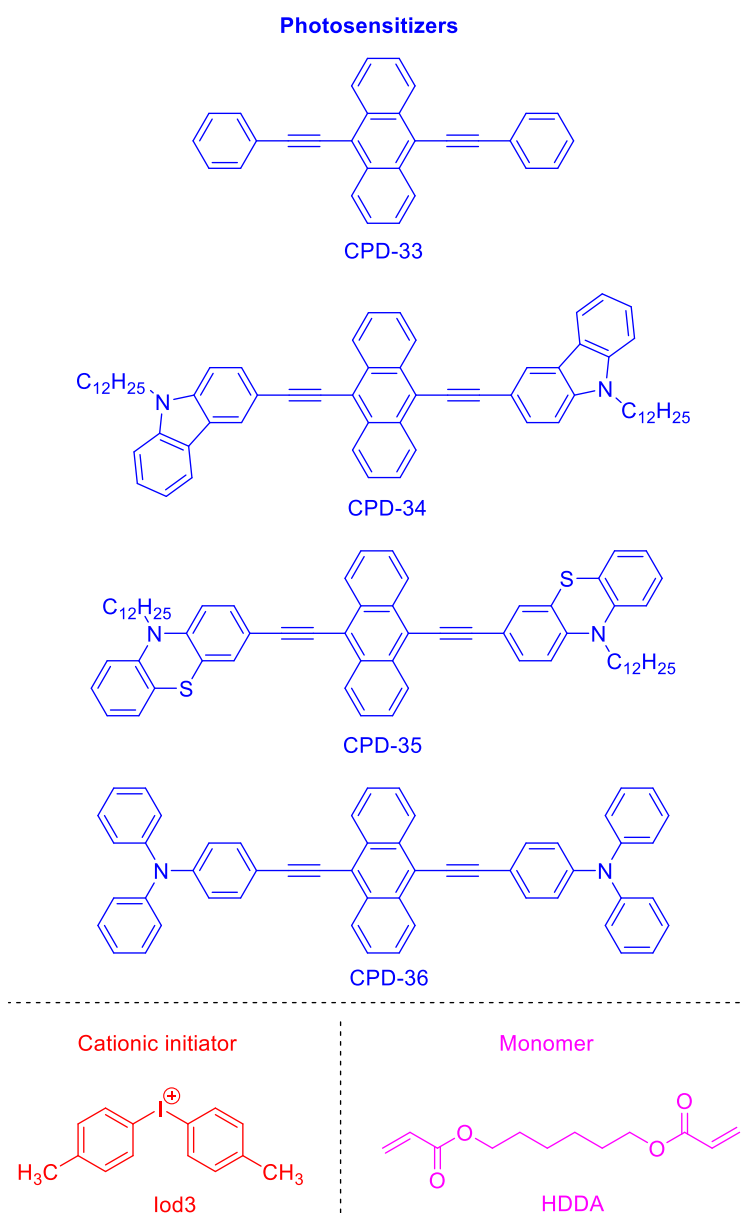**Figure 24.** Chemical structures of anthracene-based phenothiazine CPD-35, different reference compounds, Iod3 and HDDA.

In this series of dyes, the most redshifted absorption was found for the dye comprising phenothiazine as the electron-donating group (494 nm) i.e. CPD-35. This absorption maximum is close to that observed for CPD-34 (See Figure 25 and Table 3). Considering their absorption

spectra extending from 380 to 550 nm, polymerization tests were carried out at 460 and 520 nm. Unfortunately, due to the lack of solubility of CPD-36 in HDDA, this dye was not investigated for further experiments.
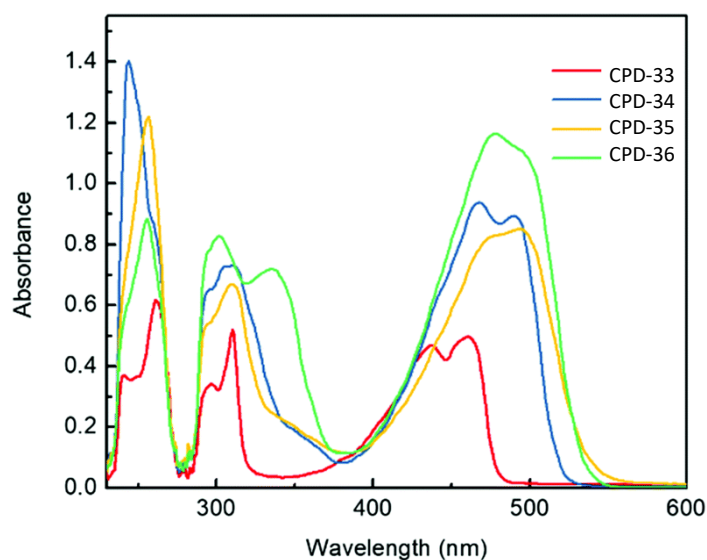

Figure 25. UV-visible absorption spectra of CPD-33-CPD-36 in THF. Reprinted with permission of Xue et al. [284]

Under blue light, all two-component dye/Iod3 (0.2%/2% w/w) photoinitiating systems showed higher polymerization rates than the reference camphorquinone (CQ)/triethanolamine (TEOA) (0.2%/2% w/w) system. Besides, after 100 s of irradiation at 460 nm, almost similar HDDA conversions could be obtained. A different situation was found at 520 nm, based on differences of molar extinction coefficients. Thus, monomer conversions followed the order of molar extinction coefficients, the highest monomer conversion being obtained for CPD-35, with a monomer conversion of 70% after 250 s similar to that obtained for the reference CQ/TEOA system (See Figure 26). Conversely, due to the lower absorption of CPD-33 at 520 nm, the HDDA conversion remained limited to 50%.

Table 8. Light absorption properties of AND1-AND4.

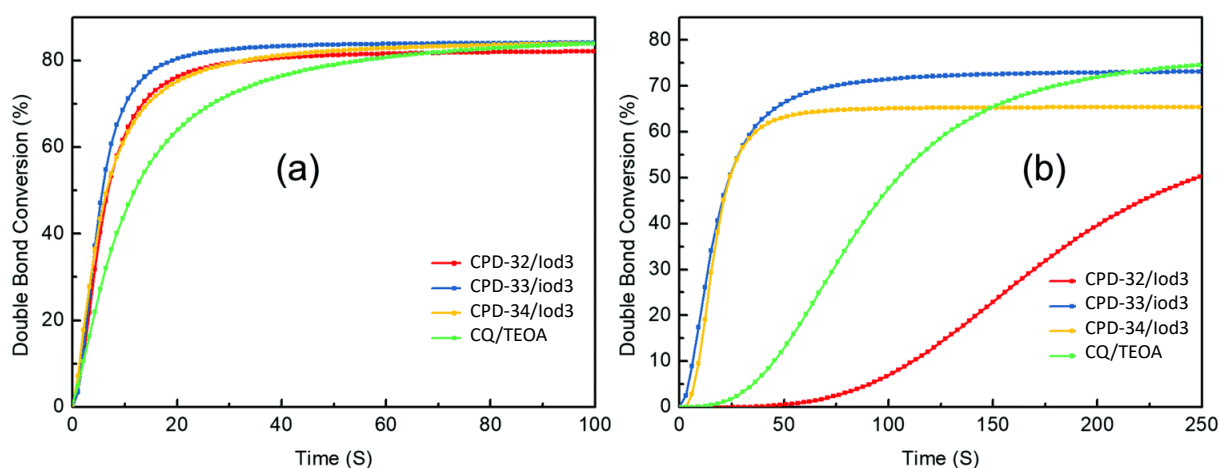|	λ_{max} /nm	ε_{max} /M^{-1}cm^{-1}	ε_{460max} /M^{-1}cm^{-1}	ε_{520max} /M^{-1}cm^{-1}
CPD-33	437	38 300	40 400	1 100
	461	40 200		
CPD-34	468	50 300	47 600	3 900
	490	48 600		
CPD-35	494	40 600	33 700	16 800
CPD-36	478	53 700	-	-

Figure 26. Polymerization profiles of HDDA using dye/Iod3 (0.2%/2%, w/w) and CQ/TEA (0.2%/2% w/w) upon irradiation at (a) 460 nm (b) 520 nm. Reprinted with permission of Xue et al. [284]

In 2020, the group of Tang and coworkers revisited phenothiazine-based anthracenes by modifying the spacer between the two partners (CPD-37 and CPD-38).[285] In this case, a double bond was introduced instead of a triple bond (See Figure 27).
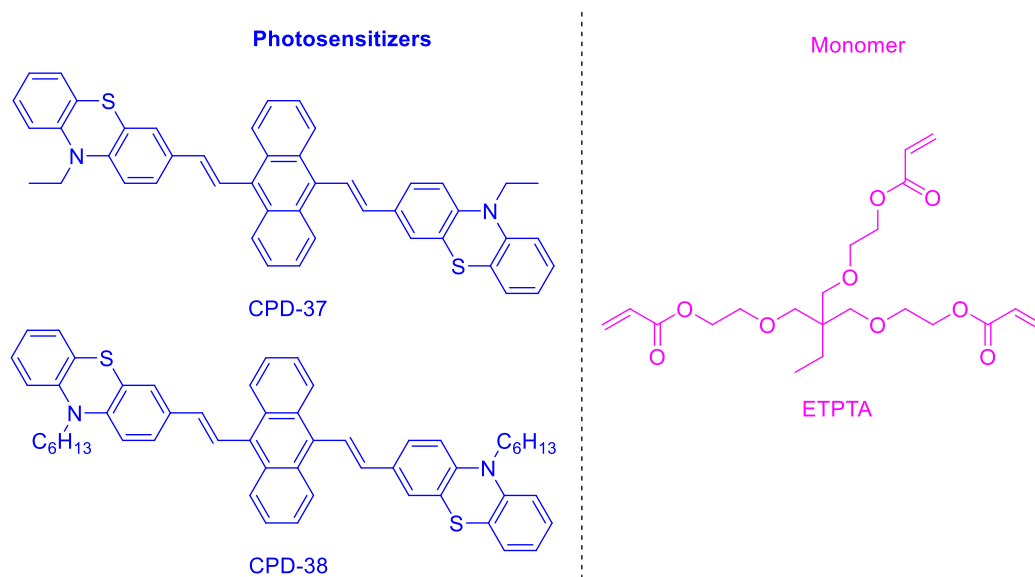
Figure 27. chemical structure of CPD-37 and CPD-38, and the monomer.

Considering the similarity of structures between CPD-37, CPD-38 and CPD-35, similar absorption spectra were found for the three dyes. Notably, for CPD-37 and CPD-38, a broad absorption band extending from 300 until 530 nm could be determined, the absorption maxima peaking at 430 nm (See Figure 28). Considering their respective absorption, light-induced polymerization reactions could be carried out at 405, 460, and 520 nm with LEDs.

Figure 28. UV-visible absorption spectra of CPD-37 and CPD-38 in THF. Reprinted with permission of Zhao et al.[285]

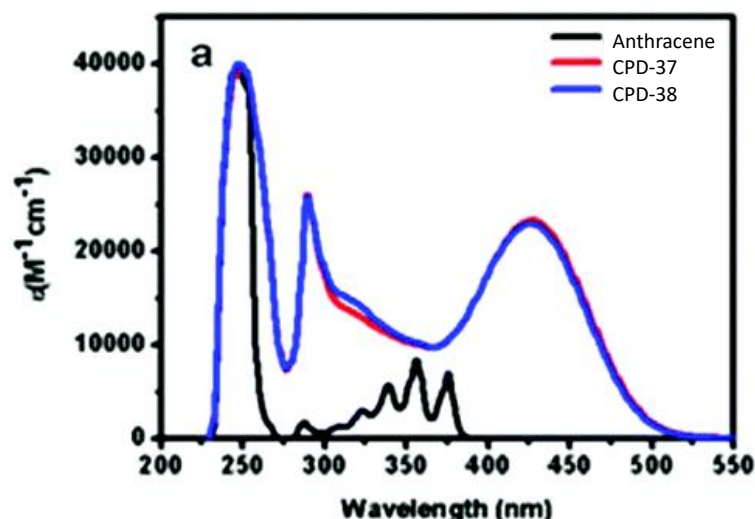Examination of the FRP of ethoxylated trimethylolpropane triacrylate (ETPTA) using the two-component dye/Iod3 (0.2%/2% w/w) system upon irradiation at different wavelengths revealed a direct correlation between ETPTA conversion and molar extinction coefficients (See Figure 29). Noticeably, upon irradiation at 405 nm, conversions of 98% within 2 s were obtained with the two dyes. Consistent with a low absorption at 520 nm, a decrease of the monomer conversion was observed. Besides, it could still reach monomer conversions of 83 and 90% with CPD-37 and CPD-38 respectively after 120 s of irradiation. Besides, while increasing the photosensitizer content from 0.2 to 0.4 wt%, the ETPTA conversion could increase from 83 to 90% using the two-component CPD-38/Iod3 (0.2%/2% w/w) system.
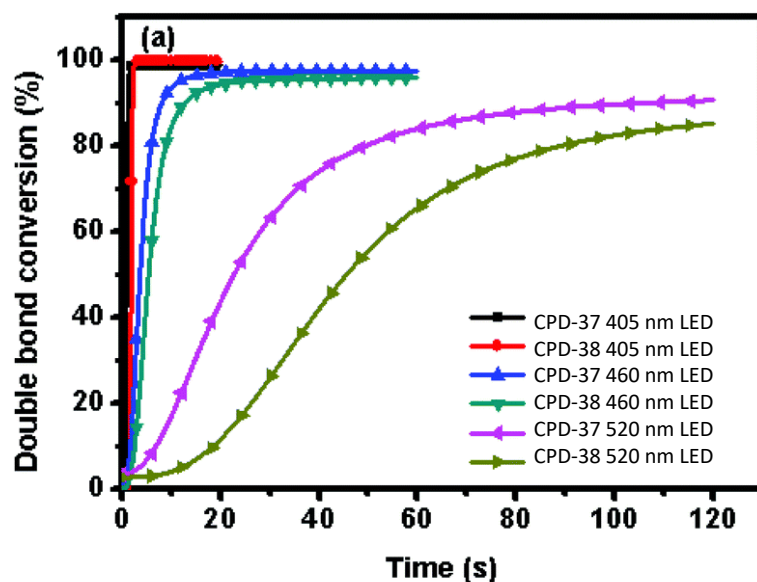

Figure 29. Photopolymerization profiles of ETPTA using the two-component dye/Iod3 (0.2%/2% w/w) using different light sources. Reprinted with permission of Zhao et al.[285]

2.6. Triazine derivatives

Increase of the molecular weight constitutes an effective strategy to address the migratability issue. In 2012, a trifunctional photoinitiator based on the triazine core and anthracene CPD-41 was proposed and its photoinitiating ability compared to that of a trifunctional photoinitiator based on pyrene or benzophenone CPD-38 and CPD-39 (See Figure 30).[148]
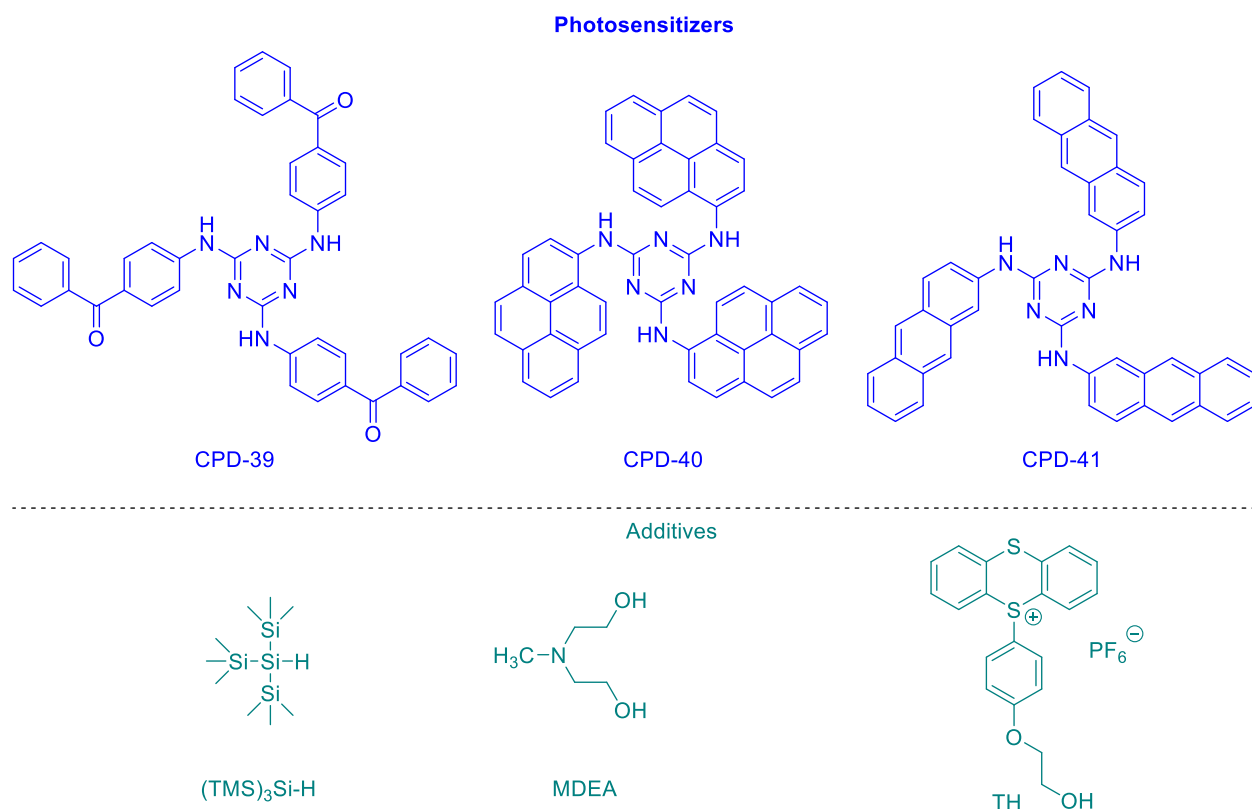
Figure 30. Chemical structure of the different triazine-based photoinitiators CPD-39-CPD-41, and different additives.

In fact, several other reasons can be cited to support the development of polyfunctional photoinitiators: reduced release of photolysis products or less smell resulting from a reduced volatility. Due to the presence of three functional groups per photoinitiator, high molar extinction coefficients could be determined, notably for CPD-40 (ε = 38 000 M^{-1}.cm^{-1}) or CPD-41 (ε = 8 500 M^{-1}.cm^{-1}). Interestingly, while replacing pyrene by anthracene, a redshift of the absorption maximum was found (404 nm for CPD-41 vs. 348 nm for CPD-40). Conversely, for CPD-39, the molar extinction coefficient remained low (330 M^{-1}.cm^{-1} at 330 nm) (See Figure 31).

Figure 31. UV-visible absorption spectra of the different triazine derivatives (CPD-40 in toluene; CPD-39 and CPD-41 in toluene/acetonitrile). Reprinted with permission of Tefhe et al.[148]

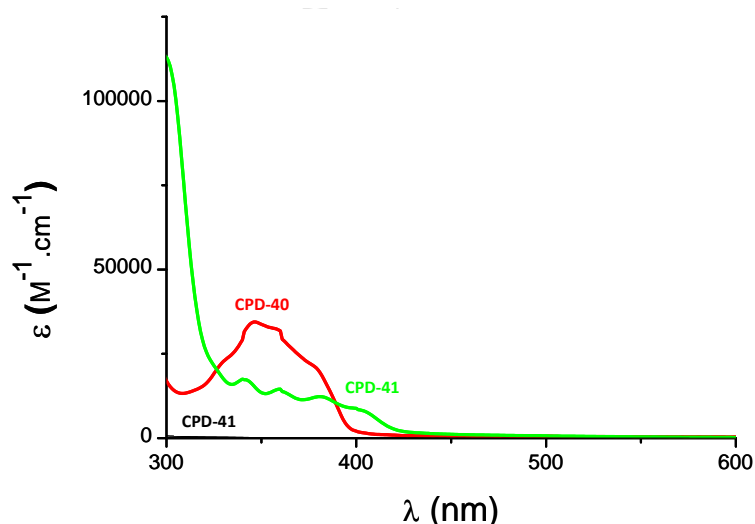When tested as photoinitiators of polymerization for the CP of EPOX, addition of silane to the dye/Iod combination greatly improved the monomer conversions as well as the polymerization rates. In fact, no EPOX conversion was detected with the different two-component photoinitiating systems (See Figure 32). Conversely, conversions of 90, 80 and 70% were respectively obtained with CPD-39, CPD-40, and CPD-41 incorporated in three-component dye/(TMS)$_3$Si–H/Iod (1%/3%/2% w/w/w) upon irradiation with a Xe-Hg lamp for 400 s under air. Benefits of designing trifunctional photoinitiators was demonstrated by comparing the EPOX conversion obtained with pyrene and CPD-40. Thus, the conversion increased from 50 to 70% upon irradiation with a Xe–Hg lamp. Upon visible light irradiation, a decrease of the polymerization efficiency from CPD-41 to CPD-40 and CPD-39 was determined, consistent with the molar extinction coefficients of the different dyes. Notably, due to the lack of absorption of CPD-39 in the visible range, no polymerization was detected with the three-component system for this dye. Noticeably, an efficient photobleaching was found with the CPD-41 and CPD-40-based photoinitiating systems during the CP of EPOX under visible light (use of halogen lamp).

Examination of the FRP of TMPTA upon a Xe–Hg lamp irradiation revealed the use of the three-component dye/(TMS)$_3$Si–H/Iod system to be required in order to get a monomer conversion both in laminates and under air. Indeed, while using the two-component dye/Iod systems, no polymerization could be detected. The high reactivity of the three-component systems was ascribed to the concomitant formation of Ph• and R$_3$Si• free radicals capable to overcome the oxygen inhibition.
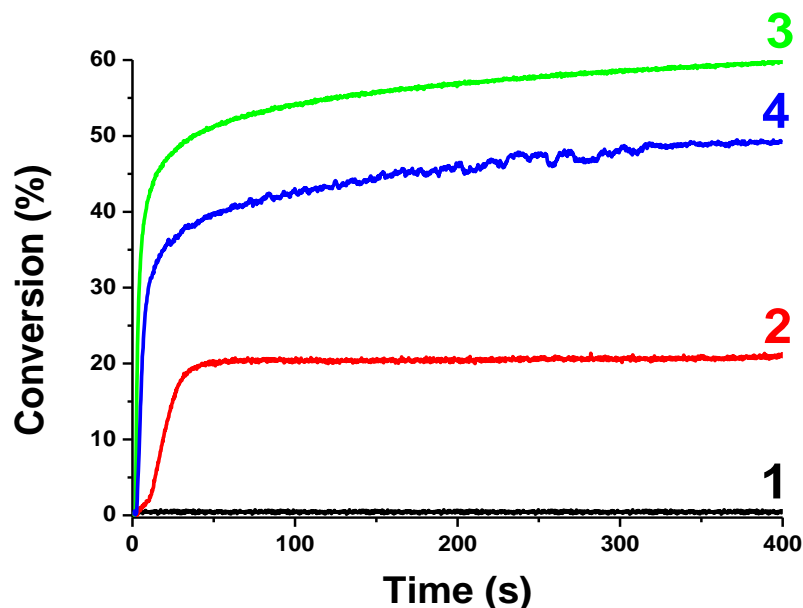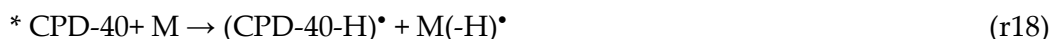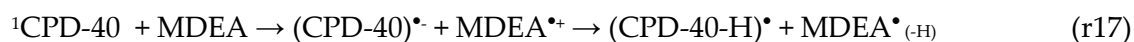
Figure 32. Photopolymerization profiles of TMPTA upon irradiation with a Xe-Hg lamp in laminate in the presence of (1) CPD-39/Iod (1%/2% w/w), (2) CPD-39/(TMS)₃Si−H/Iod (1%/3%/2% w/w), (3) CPD-40/(TMS)₃Si−H/Iod (1%/3%/2% w/w), and (4) CPD-41/(TMS)₃Si−H/Iod (1%/3%/2% w/w). Reprinted with permission of Tefhe et al.[148]

Trifunctional photoinitiators also proved to be efficient photoinitiators in combination with amines such as *N*-methyl diethanolamine MDEA. In fact, comparison of the TMPTA conversions obtained under laminates and upon irradiation with a Xe-Hg lamp revealed the monomers conversion to be higher with the two-component CPD-40/MDEA (1%/5% w/w) system (70% conversion after 400 s) vs. 60% for the three-component CPD-40/(TMS)₃Si−H/Iod (1%/3%/2% w/w) system. This remarkable reactivity was assigned to the formation of MDEA$^\bullet$(-H) radicals well-known to be sufficiently reactive to initiate the FRP of TMPTA[286] but also, to a lesser extent to CPD-40 to induce a hydrogen abstraction reaction with the monomer upon photoexcitation (See equations r17 and r18).

$$^1CPD\text{-}40 + MDEA \rightarrow (CPD\text{-}40)^{\bullet-} + MDEA^{\bullet+} \rightarrow (CPD\text{-}40\text{-}H)^\bullet + MDEA^\bullet_{(-H)} \qquad (r17)$$

$$* CPD\text{-}40 + M \rightarrow (CPD\text{-}40\text{-}H)^\bullet + M(\text{-}H)^\bullet \qquad (r18)$$

2.7. Push-pull dyes

Push-pull dyes are promising structures for the design of photoinitiators due to the possibility to finely tune the position of the intramolecular charge transfer (ICT) band by controlling the strength of both the electron-donating and electron-accepting groups.[287] Besides, beyond the position of the ICT band, solubility of dyes in resins is another major issue that should be considered. Thus, if CPD-42 and CPD-43,[133] CPD-44[128] or CPD-45[127]

showed suitable absorption properties, the lack of solubility in EPOX impeded photopolymerization of this monomer (See Figure 33).
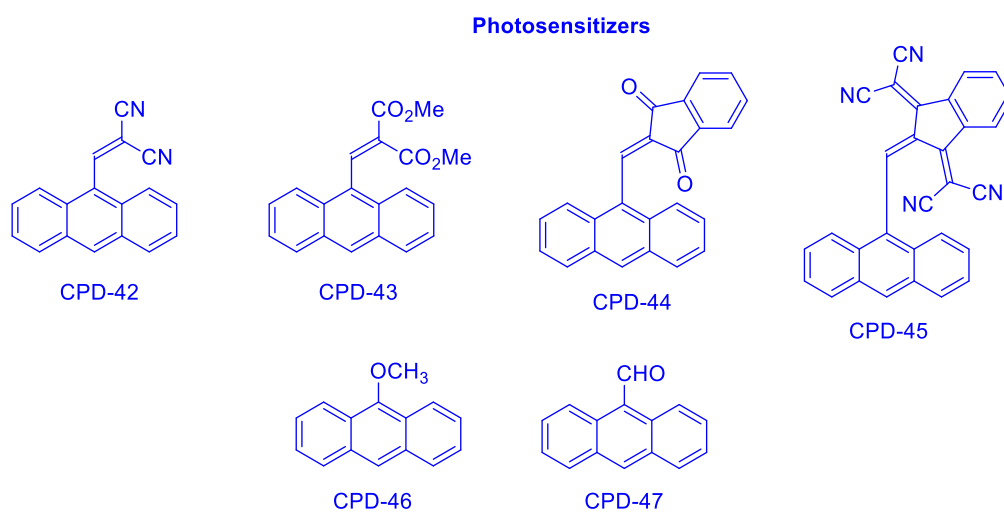
Figure 33. Chemical structures of different anthracene-based push-pull dyes.

In light of these results, in 2021, less extended push-pull dyes based on anthracene were proposed as photoinitiators for HDDA.[288] In the work developed by Nie and coworkers, an extremely weak electron acceptor was used for CPD-47, namely a formyl group (See Figure 33). For comparison, an anthracene substituted with a methoxy group i.e. CPD-46 was also examined. As shown in the Figure 34, CPD-46 exhibited a similar absorption spectrum than anthracene, with four broad absorption bands. However, compared to anthracene, a redshift by ca 15 nm was observed. Upon introduction of an electron-withdrawing group, a complete modification of the absorption spectrum was found for CPD-47, with the appearance of an ICT band at 437 nm. Compared to CPD-46, a more extended absorption spectrum was found for CPD-47.

Figure 34. UV-visible absorption spectra in methanol. Reprinted with permission of Xue et al.[288]

Examination of the FRP of HDDA at 385 nm revealed unexpected photopolymerization results in laminate. Thus, at low light intensity (2 mW/cm²), no polymerization was detected with the two-component CPD-47/Iod3 (0.2%/1% w/w) whereas a conversion as high as 80% could be obtained after 600 s of irradiation at 385 nm (See Figure 35). While increasing the LED intensity to 10 mW/cm², a conversion of 35% could be obtained with CPD-47. Besides, 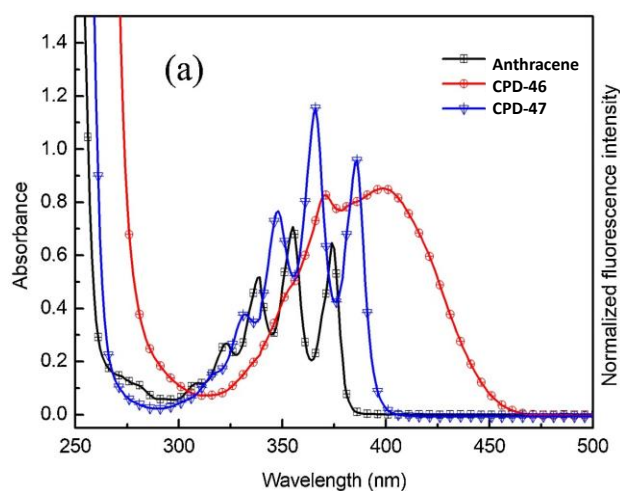an unusual inhibition time of 200 s was determined. Noticeably, if anthracene exhibits the lowest molar extinction coefficient of the series, upon irradiation with a LED of 10 mW/cm², a slower polymerization was observed but the final monomer conversion obtained after 600 s of irradiation was similar to that of the two-component CPD-46/Iod3 system, evidencing that the molar extinction coefficient was not the only parameter governing the reactivity of photosensitizer. The rate constant of interaction with Iod3, the redox properties of photosensitizers are other parameters governing the reactivity.
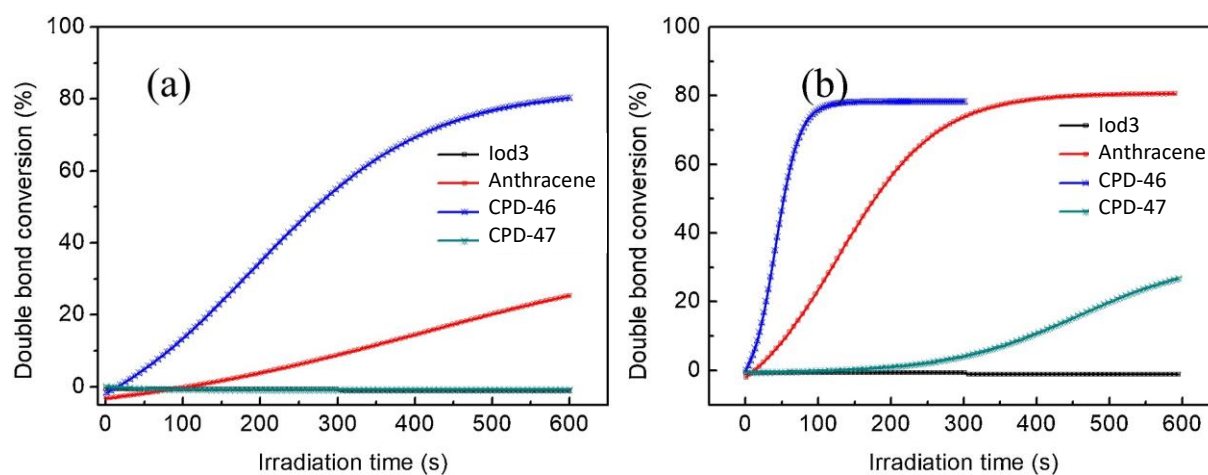
Figure 35. Photopolymerization profiles of HDDA in the presence of dye/Iod3 (Iod3: 1 wt%; dye: 0.2 wt%) under 385 nm LED irradiation; (a) 2 mW/cm²; (b) 10 mW/cm². Reprinted with permission of Xue et al.[288]

The unexpected behaviour of CPD-47 was confirmed during the photolysis experiments. Experiments done in acetonitrile revealed CPD-47 to photodimerize in solution within a few minutes. When combined with Iod3, an induction time of four minutes was evidenced, followed by a fast photobleaching of the solution. From these different experiments, it was concluded that CPD-47 was unable to directly photosensitize Iod3 whereas its photodimer could do.

2.8. 9,10-Dialkylthio/dialkoxy-anthracene

Hexaarylbiimidazoles are commonly used as initiators for free radical polymerization in industry. Hexaarylbiimidazoles are notably characterized by a low sensitivity to oxygen but also to a good thermal stability facilitating their storage.[289–292] In this family, 2,2-*bis*(2-chlorophenyl)-4,4,5,5-tetraphenyl-1,2-biimidazole (BCIM) is the most representative example. However, their absorptions are strongly UV centered so that these initiators need to be

sensitized in the visible range. In 2019, a series of six anthracene derivatives CPD-48-CPD-53 substituted by dialkylthio or dialkyloxo substituents at the 9,10-positions was developed for the sensitization of hexaarylbiimidazoles (See Figure 36).[293]
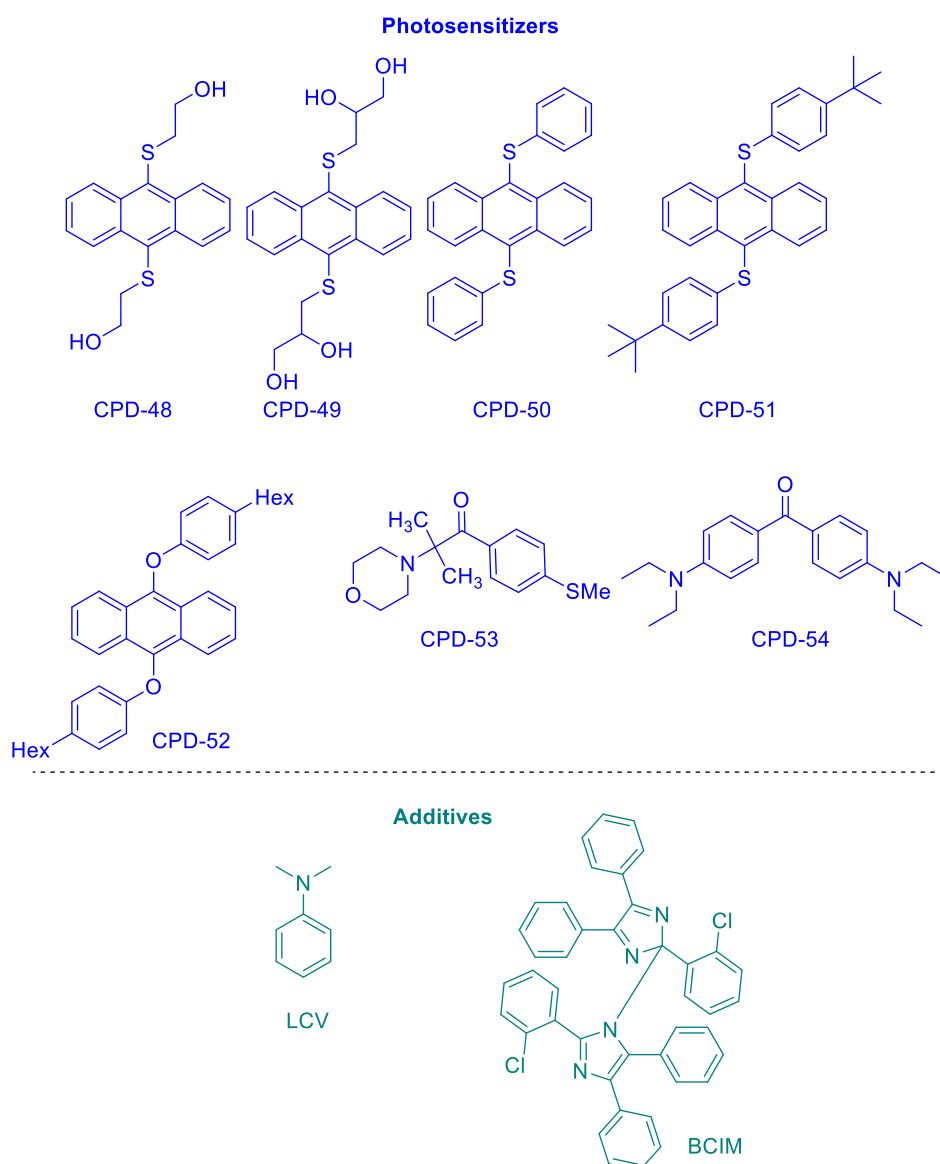
Figure 36. Chemical structures of dialkylthio and dialkyloxy-substituted anthracenes CPD-48-CPD-53, different additives and reference compounds.

Due to the presence of electron donating groups, all dyes showed a broad absorption extending from 325 nm until 450 nm. Considering that for all dyes, molar extinction coefficients higher than 6 000 $M^{-1}.cm^{-1}$ could be determined at 405 nm, polymerization experiments could be carried out in the visible range. In this series of dyes, compared to 9,10-dibutoxyanthracene (DBA) which is a benchmark photoinitiator,[55] all thio-substituted dyes CPD-48-CPD-51 showed a redshifted absorption compared to the alkoxy-substituted ones (CPD-52 and DBA), evidencing that thioalkyl groups were better electron donating groups than alkoxy groups (See Figure 37). Upon irradiation at 365 nm with a LED, an enhancement of the polymerization rate and final monomer conversions could be evidenced for all alkylthio-substituted dyes compared to the alkoxy-substituted dyes (See Figure 38). Comparisons with

reference photoinitiating systems based on 4,4′,4″-methanetriyltris(*N*,*N*-dimethylaniline) (LCV)/BCIM, 2-methyl-1-(4-methylthiophenyl)-2-morpholine-1-propanone (CPD-54)/BCIM or 4,4′-*bis*(diethylamino)benzophenone (CPD)/BCIM systems revealed the anthracene-based photoinitiating systems to outperform the reference ones.
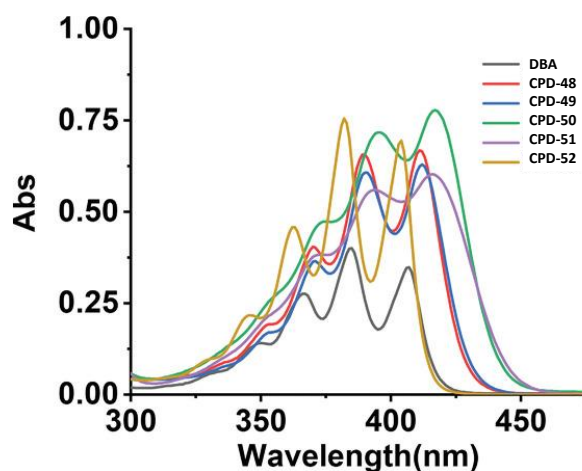
Figure 37. UV-visible absorption spectra of dyes in THF. Reprinted with permission of Lei et al.[293]

Table 9. UV-visible absorption properties of dyes in THF.

dyes	λ_{max} (nm)	$\varepsilon_{(\lambda max)}$ $M^{-1}.cm^{-1}$	$\varepsilon_{(365\ nm)}$ $M^{-1}.cm^{-1}$	$\varepsilon_{(405\ nm)}$ $M^{-1}.cm^{-1}$
DBA	385	8000	5400	6640
CPD-48	411	13 360	6500	10 100
CPD-49	412	12 580	5700	9500
CPD-50	417	15 560	7240	12 860
CPD-51	416	12 060	6400	10 560
CPD-52	382	15 100	8500	13 300

Figure 38. Polymerization profiles of HDDA upon irradiation at 365 nm with different photoinitiating systems dye/BCIM, CPD-53 and BCIM without dye UV-LED, [BCIM] = 5 × 10^{-2} M, [dye] = 5 × 10^{-3} M, [CPD-54] = 5 × 10^{-3} M, [LCV] = 3 × 10^{-2} M, [CPD-53] = 5 × 10^{-2} M. Reprinted with permission of Lei et al.[293]

Finally, DBA and CPD-48 were tested as photosensitizers for the photolithography of dry film photoresist upon irradiation at 405 nm. Micro-patterns of high resolution could be obtained with the two dyes used as photosensitizers for BCIM. Interestingly, colorless photoresists could be obtained with the two dyes, resulting from the ability of anthracene to dimerize. Noticeably, alkylthio-substituted anthracene showed faster photobleaching abilities than the alkoxy ones, enabling to avoid inner filter effect and to improve the depth of cure of the different patterns.

2.9. Anthracene-based metal organic frameworks (MOFs).

Organic dyes have been extensively used as visible light photosensitizers. However, inorganic structures or hybrid structures have not been excluded from this interest. In this field, metal organic frameworks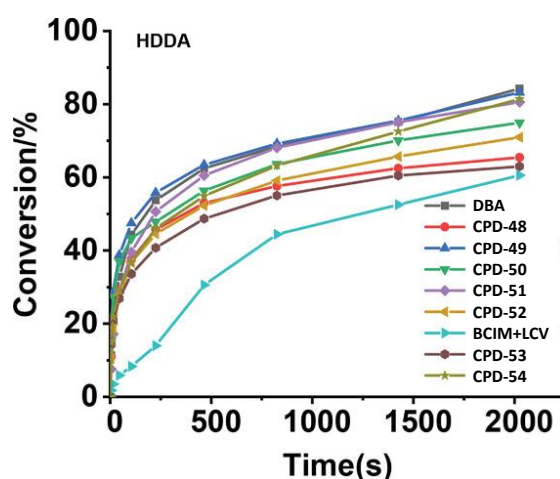 (MOFs) that are composed of metal cations coordinated to organic ligands have been used as photocatalysts for various chemical transformations.[294–299] MOFs have also been the focus of intense research efforts as photoinitiators of polymerization. In this field, iron-based metal organic frameworks have been developed as photocatalysts for free radical and cationic polymerizations in the near UV/visible range.[64] Atom transfer radical polymerization (ATRP) mediated by transition metal catalysts constitutes an efficient tool for designing polymers of complex architectures.[300–306] Recently, photoinduced ATRP has been proposed as an efficient strategy enabling to get a spatial and a temporal control of the chain extension.[307–310] Typically, photoinduced ATRP relies in the in-situ generation of a Cu(I) complex by reduction of a Cu(II) precursor by the photocatalyst. In 2016, an anthracene-based MOF i.e. NNU-32 was examined as photocatalyst for photoinduced ATRP.[311] In order to incorporate anthracene inside the indium-based MOF, a tetracarboxylated anthracene derivative was used (See Figure 39).
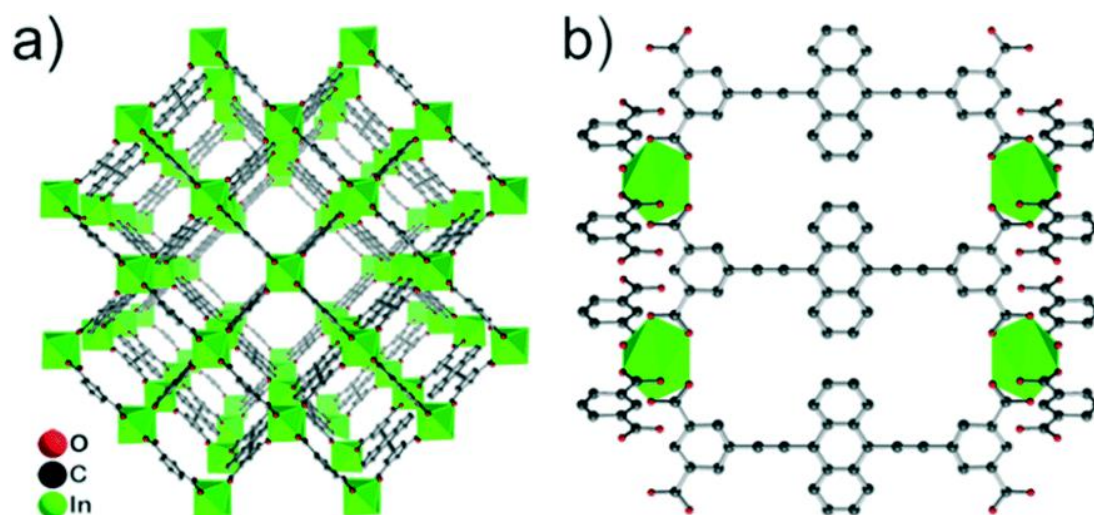

Figure 39. Chemical structure of NNU-32. Reprinted with permission of Li et al. [311]

From the absorption viewpoint, these structures are promising due to their panchromatic behaviours. Indeed, as shown in the Figure 40, the absorption spectrum extends

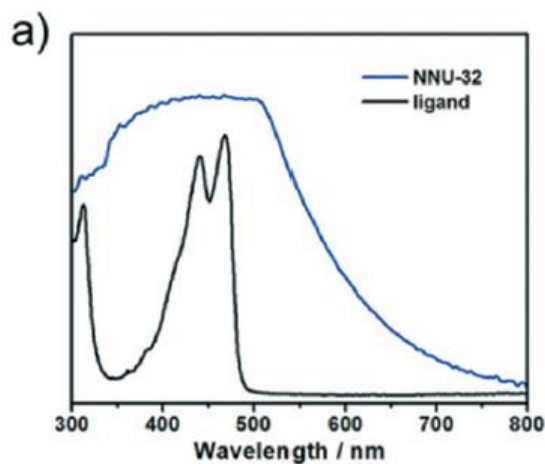from 300 until 800 nm, resulting from energy and/or ligand-to-metal charge transfer processes.[312,313]

Figure 40. UV-visible absorption spectrum of NNU-32 and the anthracene-based ligand. Reprinted with permission of Li et al. [311]

By electron paramagnetic resonance (EPR), appearance of an EPR signal upon visible light irradiation of MOF was evidenced, suggesting the formation of free radicals on the ligand. Interestingly, this ability to photogenerate radicals was also demonstrated with the free ligand. While monitoring the intensity of the EPR signal over time, a rapid increase of the signal could be demonstrated, reaching a saturation within 3 min. In order to investigate photoiniduced ATRP processes, the following four-component NNU-32/ ethyl α-bromo-isobutyrate/Cu(Br)$_2$/ *N,N,N',N'',N'''*-pentamethyldiethylenetriamine (PMDETA) system was used for the FRP of *iso*-butyl methacrylate (iso-BMA) upon irradiation at 520 nm with a monochromatic light. After 10 hours of irradiation, polymer chains of controlled size could be obtained (polydispersity index = 1.11) with a monomer conversion of 71%. Living nature of the polymerization process was also demonstrated, no monomer conversion being detected in the absence of light.

2.10. Anthracene-based thioxanthone

Thioxanthones are efficient photoinitiators in combination with tertiary amines. However, with aim at red-shifting the absorption of thioxanthone, the combination of thioxanthone and anthracene within a unique structure was examined as soon as 2007.[314] Previous to this work, the same authors, namely the group of Yagci and coworkers have developed a series of thioxanthone comprising a thiol group[315] or an acetic acid group[316,317] so that the hydrogen donor was directly connected to the dye, enabling to develop mono-component photoinitiating system. In the present case, the thioxanthone-anthracene combination could act as a mono-component system without additional hydrogen donors. From the absorption viewpoint, CPD-55 could be prepared in one step upon reaction of anthracene with thiosalicylic acid in concentrated acid. The dye could be prepared in 80% yield, according to the synthesis depicted in the Scheme 1.
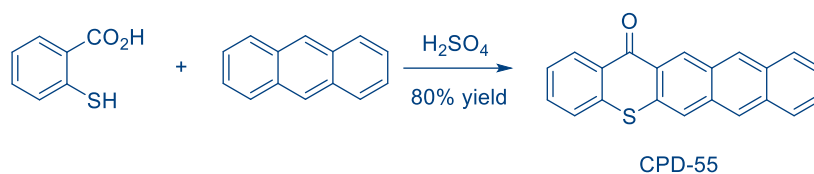
Scheme 1. Synthetic route to CPD-55.

Interestingly, absorption spectrum of CPD-55 was broad, extending from 300 to 450 nm so that a Hg-lamp was used as the light source for photopolymerization (See Figure 41).
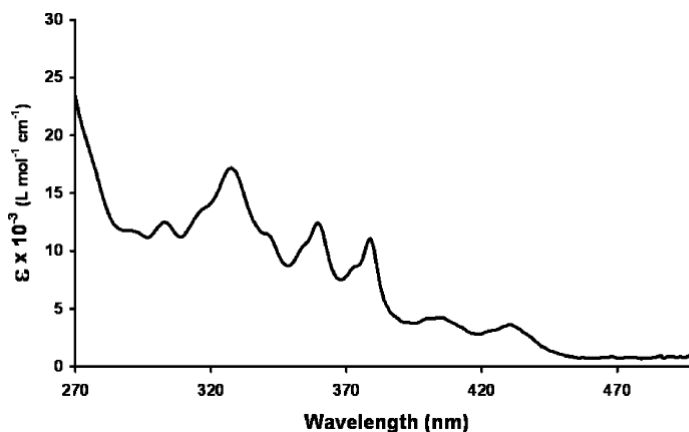
Figure 41. UV-visible absorption spectrum of CPD-55 in DMF. Reprinted with permission of Balta et al. [314]

Photopolymerization of MMA under air, in DMF, and in the absence of air revealed the crucial role of oxygen for photoinitiating. Indeed, under inert atmosphere, no polymerization processes could be carried out. This behaviour is unexpected considering that for most of the radical initiators, oxygen inhibits FRP processes. Noticeably, the CPD-55/MDEA combination only furnished a low monomer conversion, evidencing its poor reactivity with the co-initiator. Comparison of the monomer conversions obtained by using CPD-55 or a mixture of anthracene, thioxanthone and MDEA revealed the conversion to be improved for CPD-55. Especially, for the thioxanthone-anthracene combination, no polymerization was detected in the absence of MDEA, evidencing that for the mixture, presence of a hydrogen donor was required.

As other advantage of CPD-55, photopolymerization of styrene could be efficiently initiated with this dye whereas most of the radical photoinitiators only exhibit low reactivity towards styrene due to high quenching rate constants. Noticeably, an improvement of the monomer conversion could even be obtained upon introduction of MDEA in the solutions. Based on the different experiments, an initiating mechanism could be postulated. Notably, presence of oxygen being required to get high monomer conversion and the presence of hydrogen donors being not required to get a polymerization, the formation of instable endoperoxides by reaction of CPD-55 with oxygen upon irradiation was proposed. Precisely, upon photoexcitation of CPD-55, triplet excited states of CPD-55 can be quenched by oxygen, generating singlet oxygen. Singlet oxygen can add on the anthracene moiety, leading to CPD-

55-O2. In a second step, photoexcitation of the endoperoxide CPD-55-O2 can form alkoxy or peroxy radicals capable to initiate free-radical polymerization. Indeed, endoperoxides are well-known to be photochemically and thermally instable so that initiating radicals can be formed by decomposition of endoperoxides (See Scheme 2). In 2013, initiating species formed by CPD-55 upon photoexcitation with oxygen were identified by mean of laser flash photolysis, fluorescence and phosphorescence spectroscopy.[318] Notably, photoluminescence experiments carried out on photopolymerized PMMA revealed CPD-55 to be connected to the polymer chains. Besides, a deeper insight into the photoluminescence properties of polymers revealed the π-conjugation of the thioxanthone chromophore to be interrupted so that two decomposition products issued from the endoperoxide adducts were suggested as being the initiating species (See Scheme 2).
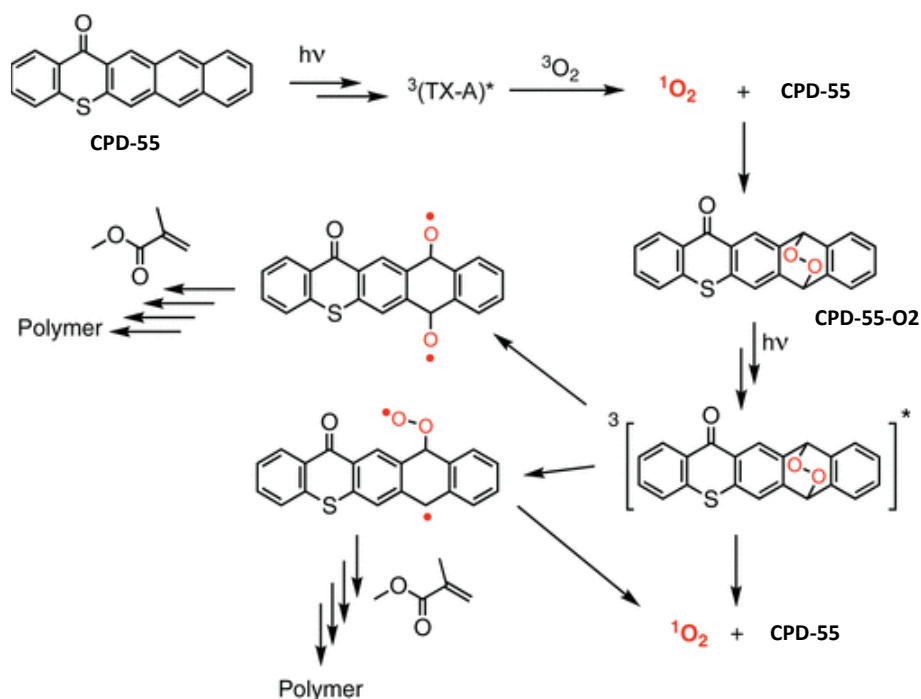
Scheme 2. Mechanism of FRP of methyl methacrylate using CPD-55 as photoinitiator in the presence of oxygen. Reprinted with permission of Balta et al. [318]

In 2013, a more soluble version of CPD-55 was proposed, bearing an alkyl chain for improving its solubility.[319] Interestingly, CPD-56 was soluble in highly polar solvents such as DMF and even water, but also in less polar solvents such as chloroform or THF. From the absorption viewpoint, an absorption spectrum superimposing that of CPD-55 was found, except that an additional tail was detected in the visible range due to the contribution of the triazole ring. With this dye, a dual behaviour could be evidenced. Indeed, if CPD-56 is an efficient mono-component photoinitiator, in the presence of triethylamine, an improvement of the butyl acrylate (BA) conversion was demonstrated, meaning that the amine was interacting with the thioxanthone moiety. Conversely, in the presence of oxygen, efficiency of the polymerization process was assigned to the formation of endoperoxides resulting from the reaction between oxygen and the anthracene moiety. Noticeably, if CPD-55 was an efficient initiator for the polymerization of styrene in combination with triethylamine, a different behaviour was found for CPD-56, resulting in low styrene conversions. Therefore, the

following mechanism could be proposed to support the polymerization efficiency in the different aforementioned conditions (See Scheme 3).
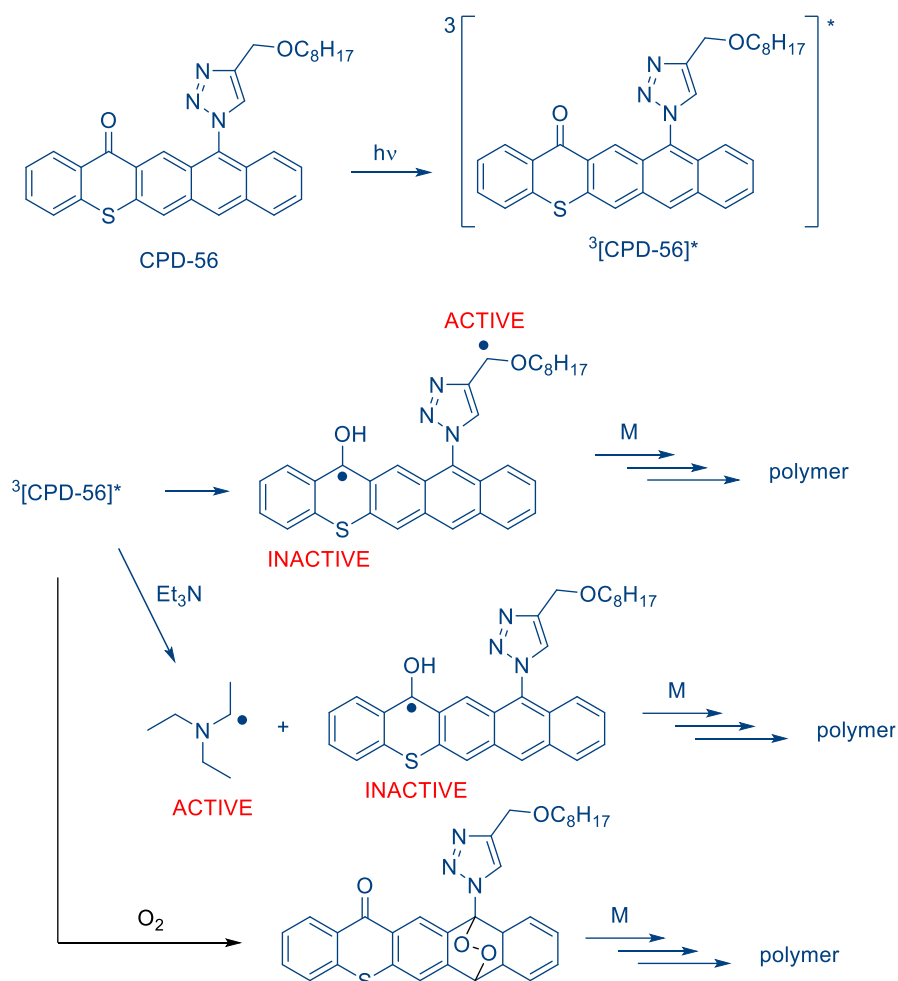
Scheme 3. The different mechanism occurring with CPD-56.

Over the years, several derivatives of CPD-55 have been prepared, based on 2-ethylanthracene (CPD-57)[320], anthracene-9-carboxylic acid (CPD-58)[321] and even 9,10-diphenylanthracene (CPD-59)[197] (See Figure 42). For all these derivatives, presence of oxygen was determined as being necessary to initiate a polymerization process. Considering that anthracene provides unexpected photoinitiating abilities to CPD-58, photoinitiating ability of the CPD-55 dimer i.e. CPD-60 was examined (See Figure 42). Using this approach, a traditional type II photoinitiator behavior could be recovered for CPD-60.[322] Notably, the FRP of MMA could only proceed under inert atmosphere. Comparison with the monomer conversion obtained with thioxanthone revealed CPD-60 to exhibit lower photoinitiating ability than its parent structure i.e. thioxanthone.
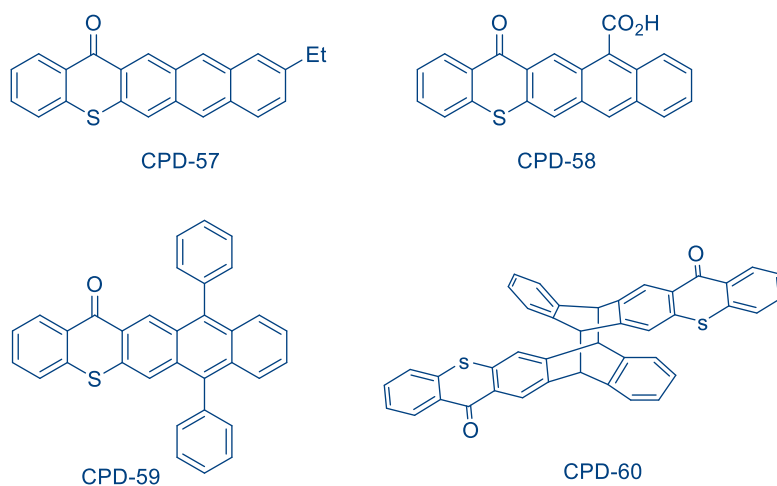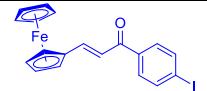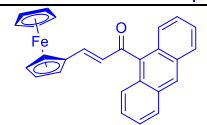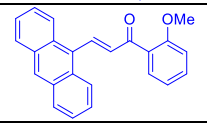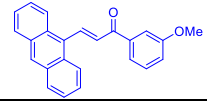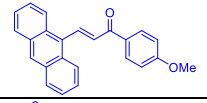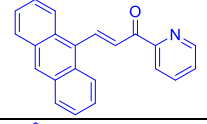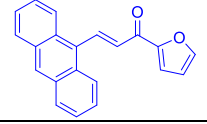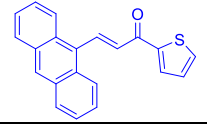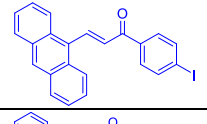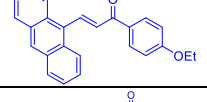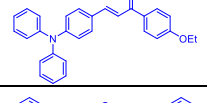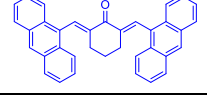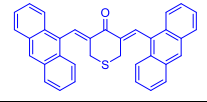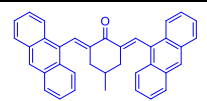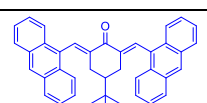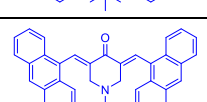
Figure 42. Chemical structures of CPD-57–CPD-60.

A summary of the different optical properties and the polymerization results is presented in the Table 10.

Table 10. Chemical structures, optical characteristics and summary of the polymerization results.

Dye	Chemical structure	Maximum absorption wavelength (nm)	Photoinitiating systems	Monomers	Light source	Monomer conversion	Ref.
2.1. Anthracene-based chalcones							
CPD-1		315	CPD/Iod/NVK (0.5%/3%/3% w/w/w)	TMPTA	457 nm	n.p.[a]	[107]
CPD-2		329	CPD/Iod/NVK (0.5%/3%/3% w/w/w)	TMPTA	457 nm	n.p.[a]	[107]
CPD-3		361	CPD/Iod/NVK (0.5%/3%/3% w/w/w)	TMPTA	457 nm	n.p.[a]	[107]
CPD-4		401	CPD/Iod/NVK (0.5%/3%/3% w/w/w)	TMPTA	457 nm	25% (400 s)	[107]
CPD-5		435	CPD/Iod/NVK (0.5%/3%/3% w/w/w)	TMPTA	457 nm	55% (400 s)	[107]
CPD-6		-	CPD/Iod2/EDB (1.5%/1.5%/1.5 % w/w/w)	PEG-diacrylate	405 nm	79.5% (200 s)	[99]
CPD-7		-	CPD/Iod2/EDB (1.5%/1.5%/1.5 % w/w/w)	PEG-diacrylate	405 nm	73.5% (200 s)	[99]
CPD-8		-	CPD/Iod2/EDB (1.5%/1.5%/1.5 % w/w/w)	PEG-diacrylate	405 nm	40.3% (200 s)	[99]
CPD-9		-	CPD/Iod2/EDB (1.5%/1.5%/1.5 % w/w/w)	PEG-diacrylate	405 nm	74.7% (200 s)	[99]

CPD-10		-	CPD/Iod2/EDB (1.5%/1.5%/1.5% w/w/w)	PEG-diacrylate	405 nm	30.5% (200 s)	[99]
CPD-11		-	CPD/Iod2/EDB (1.5%/1.5%/1.5% w/w/w)	PEG-diacrylate	405 nm	79.5% (200 s)	[99]
CPD-12		389	CPD/Iod2 (0.5%/1%, w/w)	EPOX	405 nm	39% (600 s)	[104]
CPD-13		388	CPD/Iod2 (0.5%/1%, w/w)	EPOX	405 nm	37% (600 s)	[104]
CPD-14		388	CPD/Iod2 (0.5%/1%, w/w)	EPOX	405 nm	21% (600 s)	[104]
CPD-15		387	CPD/Iod2 (0.5%/1%, w/w)	EPOX	405 nm	43% (600 s)	[104]
CPD-16		389	CPD/Iod2 (0.5%/1%, w/w)	EPOX	405 nm	52% (600 s)	[104]
CPD-17		387	CPD/Iod2 (0.5%/1%, w/w)	EPOX	405 nm	47% (600 s)	[104]
CPD-18		389	CPD/Iod2 (0.5%/1%, w/w)	EPOX	405 nm	33% (600 s)	[104]
CPD-19		400	CPD/Iod2 (1%/2%, w/w)	DVE-3	405 nm	62% (300 s)	[253]
CPD-20		405	CPD/Iod2 (1%/2%, w/w)	DVE-3	405 nm	88% (300 s)	[253]
CPD-21		250	CPD/Iod2/EBD (0.1%/2%/2%, w/w/w)	TA	405 nm	90% (400 s)	[191]
CPD-22		250	CPD/Iod2/EBD (0.1%/2%/2%, w/w/w)	TA	405 nm	41% (400 s)	[191]
CPD-23		250	CPD/Iod2/EBD (0.1%/2%/2%, w/w/w)	TA	405 nm	68% (400 s)	[191]
CPD-24		250	CPD/Iod2/EBD (0.1%/2%/2%, w/w/w)	TA	405 nm	81% (400 s)	[191]
CPD-25		250	CPD/Iod2/EBD (0.1%/2%/2%, w/w/w)	TA	405 nm	41% (400 s)	[191]

CPD-26		250	CPD/Iod2/EBD (0.1%/2%/2%, w/w/w)	TA	405 nm	53% (400 s)	[191]

2.2. Anthracene-based acridinedione

CPD-27		369	AD/Iod/NVK (3%/2%/3%, w/w/w)	EPOX	Xe-Hg lamp	34% (500 s)	[215]
CPD-28		348	AD/Iod/NVK (3%/2%/3%, w/w/w)	EPOX	Xe-Hg lamp	48% (500 s)	[215]

2.3. Anthracene-based 1,8-naphthalimides

CPD-29		< 400	CPD/Iod/NVK (0.5%/2%/3%, w/w/w)	EPOX	405 nm	n.p.	[89]
CPD-30		431	CPD/Iod/NVK (0.5%/2%/3%, w/w/w)	EPOX	405 nm	63% (800 s)	[89]

2.4. 9,10-*Bis*(ethynyl)-substituted anthracene

CPD-31		440	CPD/(TMS)$_3$Si–H/Iod (0.5 %/3 %/ 2% w/w)	EPOX	462 nm	70% (700 s)	[270]
CPD-32		462	CPD/NAI-105	-	488 nm	-	[280]

2.5. Anthracene-based phenothiazine

CPD-33		437, 461	CPD/Iod3 (0.2%/2%, w/w)	HDDA	460 nm	~ 80% (100 s)	[284]
CPD-34		468, 490	CPD/Iod3 (0.2%/2%, w/w)	HDDA	460 nm	~ 80% (100 s)	[284]
CPD-35		494	CPD/Iod3 (0.2%/2%, w/w)	HDDA	460 nm	~ 80% (100 s)	[284]
CPD-36		478	CPD/Iod3 (0.2%/2%, w/w)	HDDA	460 nm	~ 80% (100 s)	[284]
CPD-37		430	CPD/Iod3 (0.2%/2% w/w)	ETPTA	405 nm	100% (20 s)	[285]
CPD-38		430	CPD/Iod3 (0.2%/2% w/w)	ETPTA	405 nm	100% (20 s)	[285]

2.6. Triazine derivatives

CPD-39		330	CPD/(TMS)$_3$Si–H/Iod (1%/3%/2% w/w/w)	EPOX	Xe-Hg lamp	90% (400 s)	[148]

CPD-40		348	CPD/(TMS)₃Si–H/Iod (1%/3%/2% w/w/w)	EPOX	Xe-Hg lamp	90% (400 s)	[148]
CPD-41		404	CPD/(TMS)₃Si–H/Iod (1%/3%/2% w/w/w)	EPOX	Xe-Hg lamp	90% (400 s)	[148]
2.7. Push-pull dyes							
CPD-46		392	CPD/Iod3 (0.2%/1% w/w)	HDDA	385 nm	30% (600 s)	[288]
CPD-47		437	CPD/Iod3 (0.2%/1% w/w)	HDDA	385 nm	80% (600 s)	[288]
CPD-48		411	CPD/BCIM	HDDA	365 nm	67% (2000 s)	[293]
CPD-49		412	CPD/BCIM	HDDA	365 nm	80% (2000 s)	[293]
CPD-50		417	CPD/BCIM	HDDA	365 nm	-	[293]
CPD-51		416	CPD/BCIM	HDDA	365 nm	-	[293]
CPD-52		382	CPD/BCIM	HDDA	365 nm	-	[293]
2.9. Anthracene-based metal organic frameworks (MOFs)							
NNU-32		300-800	NNU-32/ ethyl α-bromo-isobutyrate/ Cu(Br)₂/PMDETA	iso-BMA	520	71% (10 hours)	[311]

[a] n.p.

3. Conclusion

To conclude, anthracene is a versatile scaffold that was at the basis of numerous visible light photoinitiators. Over the years, around 60 different structures have been investigated. Anthracene was notably used for the design of bioinspired chalcones and this family of dyes constitutes the most important group of molecules since more than 25 derivatives have been examined during the last three years. As the main finding, the different investigations revealed that used of anthracene as an electron donor in these structures was less favourable in terms of photoinitiating ability than when incorporated into the acetophenone moiety. Besides, polymerization results also revealed that use of heterocycles in the acetophenone moiety could greatly improve the final monomer conversions compared to chalcones comprising aromatic rings. When incorporated in naphthalimides, photoinitiators exhibiting good photobleaching properties could be obtained. Anthracene is a polyaromatic structure that can drastically reduce the solubility of dyes in resins and this point was evidenced with a series of push-pull dyes bearing indane-1,3-dione derivatives as electron acceptors. A great deal of efforts was also devoted to elaborate anthracene-based thioxanthone. In this case, and contrarily to what is commonly observed with type II photoinitiators, higher monomer conversions could be obtained in the presence of oxygen, what is rarely observed. Even if remarkable photoinitiating abilities have been demonstrated with anthracene-based dyes, a lot of works remains to be done. Indeed, future prospects will notably consist in developing water-soluble dyes, no anthracene-based chromophores being reported to date in the literature. Similarly, anthracene has only been investigated for the design of Type II photoinitiators. Besides, design of glyoxylate derivatives or oxime esters could contribute to drastically simplify the photocurable resins while maintaining high monomer conversions.

Conflicts of Interest

The authors declare no conflict of interest.

References

[1] J. Lalevée, H. Mokbel, J.-P. Fouassier, Recent Developments of Versatile Photoinitiating Systems for Cationic Ring Opening Polymerization Operating at Any Wavelengths and under Low Light Intensity Sources, Molecules. 20 (2015) 7201–7221. https://doi.org/10.3390/molecules20047201.

[2]   M.A. Tehfe, F. Louradour, J. Lalevée, J.-P. Fouassier, Photopolymerization Reactions: On the Way to a Green and Sustainable Chemistry, Applied Sciences. 3 (2013) 490–514. https://doi.org/10.3390/app3020490.

[3]   P. Xiao, J. Zhang, F. Dumur, M.A. Tehfe, F. Morlet-Savary, B. Graff, D. Gigmes, J.P. Fouassier, J. Lalevée, Visible light sensitive photoinitiating systems: Recent progress in cationic and radical photopolymerization reactions under soft conditions, Progress in Polymer Science. 41 (2015) 32–66. https://doi.org/10.1016/j.progpolymsci.2014.09.001.

[4]   K. Sun, P. Xiao, F. Dumur, J. Lalevée, Organic dye-based photoinitiating systems for visible-light-induced photopolymerization, Journal of Polymer Science. 59 (2021) 1338–1389. https://doi.org/10.1002/pol.20210225.

[5]   J. Lalevée, S. Telitel, P. Xiao, M. Lepeltier, F. Dumur, F. Morlet-Savary, D. Gigmes, J.-P. Fouassier, Metal and metal-free photocatalysts: mechanistic approach and application as photoinitiators of photopolymerization, Beilstein J. Org. Chem. 10 (2014) 863–876. https://doi.org/10.3762/bjoc.10.83.

[6]   P. Xiao, F. Dumur, B. Graff, J.P. Fouassier, D. Gigmes, J. Lalevée, Cationic and Thiol–Ene Photopolymerization upon Red Lights Using Anthraquinone Derivatives as Photoinitiators, Macromolecules. 46 (2013) 6744–6750. https://doi.org/10.1021/ma401513b.

[7]   M.-A. Tehfe, D. Gigmes, F. Dumur, D. Bertin, F. Morlet-Savary, B. Graff, J. Lalevée, J.-P. Fouassier, Cationic photosensitive formulations based on silyl radical chemistry for green and red diode laser exposure, Polym. Chem. 3 (2012) 1899–1902. https://doi.org/10.1039/C1PY00460C.

[8]   P. Garra, C. Dietlin, F. Morlet-Savary, F. Dumur, D. Gigmes, J.-P. Fouassier, J. Lalevée, Redox two-component initiated free radical and cationic polymerizations: Concepts, reactions and applications, Progress in Polymer Science. 94 (2019) 33–56. https://doi.org/10.1016/j.progpolymsci.2019.04.003.

[9]   Y. Zhang, Y. Xu, A. Simon-Masseron, J. Lalevée, Radical photoinitiation with LEDs and applications in the 3D printing of composites, Chem. Soc. Rev. 50 (2021) 3824–3841. https://doi.org/10.1039/D0CS01411G.

[10]   F. Dumur, Recent Advances on Visible Light Metal-Based Photocatalysts for Polymerization under Low Light Intensity, Catalysts. 9 (2019). https://doi.org/10.3390/catal9090736.

[11]   C. Pigot, G. Noirbent, D. Brunel, F. Dumur, Recent advances on push–pull organic dyes as visible light photoinitiators of polymerization, European Polymer Journal. 133 (2020) 109797. https://doi.org/10.1016/j.eurpolymj.2020.109797.

[12]   P. Garra, C. Dietlin, F. Morlet-Savary, F. Dumur, D. Gigmes, J.-P. Fouassier, J. Lalevée, Photopolymerization processes of thick films and in shadow areas: a review for the access to composites, Polym. Chem. 8 (2017) 7088–7101. https://doi.org/10.1039/C7PY01778B.

[13]   W. Tomal, J. Ortyl, Water-Soluble Photoinitiators in Biomedical Applications, Polymers. 12 (2020) 1073. https://doi.org/10.3390/polym12051073.

[14]   N. Corrigan, J. Yeow, P. Judzewitsch, J. Xu, C. Boyer, Seeing the Light: Advancing Materials Chemistry through Photopolymerization, Angewandte Chemie International Edition. 58 (2019) 5170–5189. https://doi.org/10.1002/anie.201805473.

[15]   A. Banerji, K. Jin, K. Liu, M.K. Mahanthappa, C.J. Ellison, Cross-Linked Nonwoven Fibers by Room-Temperature Cure Blowing and in Situ Photopolymerization, Macromolecules. 52 (2019) 6662–6672. https://doi.org/10.1021/acs.macromol.9b01002.

[16] G. Yilmaz, Y. Yagci, Light-induced step-growth polymerization, Progress in Polymer Science. 100 (2020) 101178. https://doi.org/10.1016/j.progpolymsci.2019.101178.

[17] M. Layani, X. Wang, S. Magdassi, Novel Materials for 3D Printing by Photopolymerization, Advanced Materials. 30 (2018) 1706344. https://doi.org/10.1002/adma.201706344.

[18] C. Dietlin, S. Schweizer, P. Xiao, J. Zhang, F. Morlet-Savary, B. Graff, J.-P. Fouassier, J. Lalevée, Photopolymerization upon LEDs: new photoinitiating systems and strategies, Polym. Chem. 6 (2015) 3895–3912. https://doi.org/10.1039/C5PY00258C.

[19] S. Shanmugam, J. Xu, C. Boyer, Photocontrolled Living Polymerization Systems with Reversible Deactivations through Electron and Energy Transfer, Macromolecular Rapid Communications. 38 (2017) 1700143. https://doi.org/10.1002/marc.201700143.

[20] F. Jasinski, P.B. Zetterlund, A.M. Braun, A. Chemtob, Photopolymerization in dispersed systems, Progress in Polymer Science. 84 (2018) 47–88. https://doi.org/10.1016/j.progpolymsci.2018.06.006.

[21] C. Noè, M. Hakkarainen, M. Sangermano, Cationic UV-Curing of Epoxidized Biobased Resins, Polymers. 13 (2021) 89. https://doi.org/10.3390/polym13010089.

[22] Y. Yuan, C. Li, R. Zhang, R. Liu, J. Liu, Low volume shrinkage photopolymerization system using hydrogen-bond-based monomers, Progress in Organic Coatings. 137 (2019) 105308. https://doi.org/10.1016/j.porgcoat.2019.105308.

[23] I.V. Khudyakov, J.C. Legg, M.B. Purvis, B.J. Overton, Kinetics of Photopolymerization of Acrylates with Functionality of 1–6, Ind. Eng. Chem. Res. 38 (1999) 3353–3359. https://doi.org/10.1021/ie990306i.

[24] S.H. Dickens, J.W. Stansbury, K.M. Choi, C.J.E. Floyd, Photopolymerization Kinetics of Methacrylate Dental Resins, Macromolecules. 36 (2003) 6043–6053. https://doi.org/10.1021/ma021675k.

[25] A. Maffezzoli, A.D. Pietra, S. Rengo, L. Nicolais, G. Valletta, Photopolymerization of dental composite matrices, Biomaterials. 15 (1994) 1221–1228. https://doi.org/10.1016/0142-9612(94)90273-9.

[26] T. Dikova, J. Maximov, V. Todorov, G. Georgiev, V. Panov, Optimization of Photopolymerization Process of Dental Composites, Processes. 9 (2021) 779. https://doi.org/10.3390/pr9050779.

[27] A. Andreu, P.-C. Su, J.-H. Kim, C.S. Ng, S. Kim, I. Kim, J. Lee, J. Noh, A.S. Subramanian, Y.-J. Yoon, 4D printing materials for vat photopolymerization, Additive Manufacturing. 44 (2021) 102024. https://doi.org/10.1016/j.addma.2021.102024.

[28] H. Chen, G. Noirbent, Y. Zhang, K. Sun, S. Liu, D. Brunel, D. Gigmes, B. Graff, F. Morlet-Savary, P. Xiao, F. Dumur, J. Lalevée, Photopolymerization and 3D/4D applications using newly developed dyes: Search around the natural chalcone scaffold in photoinitiating systems, Dyes and Pigments. 188 (2021) 109213. https://doi.org/10.1016/j.dyepig.2021.109213.

[29] A. Bagheri, J. Jin, Photopolymerization in 3D Printing, ACS Appl. Polym. Mater. 1 (2019) 593–611. https://doi.org/10.1021/acsapm.8b00165.

[30] B.K. Armstrong, A. Kricker, The epidemiology of UV induced skin cancer, Journal of Photochemistry and Photobiology B: Biology. 63 (2001) 8–18. https://doi.org/10.1016/S1011-1344(01)00198-1.

[31] F.R. de Gruijl, Skin cancer and solar UV radiation, European Journal of Cancer. 35 (1999) 2003–2009. https://doi.org/10.1016/S0959-8049(99)00283-X.

[32] D.L. Narayanan, R.N. Saladi, J.L. Fox, Review: Ultraviolet radiation and skin cancer, International Journal of Dermatology. 49 (2010) 978–986. https://doi.org/10.1111/j.1365-4632.2010.04474.x.

[33] J. Shao, Y. Huang, Q. Fan, Visible light initiating systems for photopolymerization: status, development and challenges, Polym. Chem. 5 (2014) 4195–4210. https://doi.org/10.1039/C4PY00072B.

[34] F. Petko, A. Świeży, J. Ortyl, Photoinitiating systems and kinetics of frontal photopolymerization processes – the prospects for efficient preparation of composites and thick 3D structures, Polym. Chem. 12 (2021) 4593–4612. https://doi.org/10.1039/D1PY00596K.

[35] A.H. Bonardi, F. Dumur, T.M. Grant, G. Noirbent, D. Gigmes, B.H. Lessard, J.-P. Fouassier, J. Lalevée, High Performance Near-Infrared (NIR) Photoinitiating Systems Operating under Low Light Intensity and in the Presence of Oxygen, Macromolecules. 51 (2018) 1314–1324. https://doi.org/10.1021/acs.macromol.8b00051.

[36] F. Dumur, Recent advances on carbazole-based photoinitiators of polymerization, European Polymer Journal. 125 (2020) 109503. https://doi.org/10.1016/j.eurpolymj.2020.109503.

[37] F. Dumur, Recent advances on pyrene-based photoinitiators of polymerization, European Polymer Journal. 126 (2020) 109564. https://doi.org/10.1016/j.eurpolymj.2020.109564.

[38] F. Dumur, Recent advances on ferrocene-based photoinitiating systems, European Polymer Journal. 147 (2021) 110328. https://doi.org/10.1016/j.eurpolymj.2021.110328.

[39] F. Dumur, Recent advances on visible light photoinitiators of polymerization based on Indane-1,3-dione and related derivatives, European Polymer Journal. 143 (2021) 110178. https://doi.org/10.1016/j.eurpolymj.2020.110178.

[40] F. Dumur, Recent advances on iron-based photoinitiators of polymerization, European Polymer Journal. 139 (2020) 110026. https://doi.org/10.1016/j.eurpolymj.2020.110026.

[41] F. Dumur, Recent advances on perylene-based photoinitiators of polymerization, European Polymer Journal. 159 (2021) 110734. https://doi.org/10.1016/j.eurpolymj.2021.110734.

[42] F. Dumur, Recent advances on coumarin-based photoinitiators of polymerization, European Polymer Journal. 163 (2022) 110962. https://doi.org/10.1016/j.eurpolymj.2021.110962.

[43] N. Giacoletto, M. Ibrahim-Ouali, F. Dumur, Recent advances on squaraine-based photoinitiators of polymerization, European Polymer Journal. 150 (2021) 110427. https://doi.org/10.1016/j.eurpolymj.2021.110427.

[44] N. Giacoletto, F. Dumur, Recent Advances in bis-Chalcone-Based Photoinitiators of Polymerization: From Mechanistic Investigations to Applications, Molecules. 26 (2021) 3192. https://doi.org/10.3390/molecules26113192.

[45] M. Ibrahim-Ouali, F. Dumur, Recent Advances on Chalcone-based Photoinitiators of Polymerization, European Polymer Journal. (2021) 110688. https://doi.org/10.1016/j.eurpolymj.2021.110688.

[46] G. Noirbent, F. Dumur, Recent advances on naphthalic anhydrides and 1,8-naphthalimide-based photoinitiators of polymerization, European Polymer Journal. 132 (2020) 109702. https://doi.org/10.1016/j.eurpolymj.2020.109702.

[47] G. Noirbent, F. Dumur, Recent Advances on Copper Complexes as Visible Light Photoinitiators and (Photo) Redox Initiators of Polymerization, Catalysts. 10 (2020). https://doi.org/10.3390/catal10090953.

[48] P. Xiao, F. Dumur, J. Zhang, J.P. Fouassier, D. Gigmes, J. Lalevée, Copper Complexes in Radical Photoinitiating Systems: Applications to Free Radical and Cationic Polymerization upon Visible LEDs, Macromolecules. 47 (2014) 3837–3844. https://doi.org/10.1021/ma5006793.

[49] P. Xiao, F. Dumur, J. Zhang, D. Gigmes, J.P. Fouassier, J. Lalevée, Copper complexes: the effect of ligands on their photoinitiation efficiencies in radical polymerization reactions under visible light, Polym. Chem. 5 (2014) 6350–6357. https://doi.org/10.1039/C4PY00925H.

[50] P. Xiao, J. Zhang, D. Campolo, F. Dumur, D. Gigmes, J.P. Fouassier, J. Lalevée, Copper and iron complexes as visible-light-sensitive photoinitiators of polymerization, Journal of Polymer Science Part A: Polymer Chemistry. 53 (2015) 2673–2684. https://doi.org/10.1002/pola.27762.

[51] P. Garra, M. Carré, F. Dumur, F. Morlet-Savary, C. Dietlin, D. Gigmes, J.-P. Fouassier, J. Lalevée, Copper-Based (Photo)redox Initiating Systems as Highly Efficient Systems for Interpenetrating Polymer Network Preparation, Macromolecules. 51 (2018) 679–688. https://doi.org/10.1021/acs.macromol.7b02491.

[52] P. Garra, F. Dumur, F. Morlet-Savary, C. Dietlin, D. Gigmes, J.P. Fouassier, J. Lalevée, Mechanosynthesis of a Copper complex for redox initiating systems with a unique near infrared light activation, Journal of Polymer Science Part A: Polymer Chemistry. 55 (2017) 3646–3655. https://doi.org/10.1002/pola.28750.

[53] P. Garra, F. Dumur, A.A. Mousawi, B. Graff, D. Gigmes, F. Morlet-Savary, C. Dietlin, J.P. Fouassier, J. Lalevée, Mechanosynthesized copper(I) complex based initiating systems for redox polymerization: towards upgraded oxidizing and reducing agents, Polym. Chem. 8 (2017) 5884–5896. https://doi.org/10.1039/C7PY01244F.

[54] H. Mokbel, D. Anderson, R. Plenderleith, C. Dietlin, F. Morlet-Savary, F. Dumur, D. Gigmes, J.-P. Fouassier, J. Lalevée, Copper photoredox catalyst "G1": a new high performance photoinitiator for near-UV and visible LEDs, Polym. Chem. 8 (2017) 5580–5592. https://doi.org/10.1039/C7PY01016H.

[55] H. Mokbel, D. Anderson, R. Plenderleith, C. Dietlin, F. Morlet-Savary, F. Dumur, D. Gigmes, J.P. Fouassier, J. Lalevée, Simultaneous initiation of radical and cationic polymerization reactions using the "G1" copper complex as photoredox catalyst: Applications of free radical/cationic hybrid photopolymerization in the composites and 3D printing fields, Progress in Organic Coatings. 132 (2019) 50–61. https://doi.org/10.1016/j.porgcoat.2019.02.044.

[56] A.A. Mousawi, A. Kermagoret, D.-L. Versace, J. Toufaily, T. Hamieh, B. Graff, F. Dumur, D. Gigmes, J.P. Fouassier, J. Lalevée, Copper photoredox catalysts for polymerization upon near UV or visible light: structure/reactivity/efficiency relationships and use in LED projector 3D printing resins, Polym. Chem. 8 (2017) 568–580. https://doi.org/10.1039/C6PY01958G.

[57] A. Mau, G. Noirbent, C. Dietlin, B. Graff, D. Gigmes, F. Dumur, J. Lalevée, Panchromatic Copper Complexes for Visible Light Photopolymerization, Photochem. 1 (2021). https://doi.org/10.3390/photochem1020010.

[58] A. Mau, C. Dietlin, F. Dumur, J. Lalevée, Concomitant initiation of radical and cationic polymerisations using new copper complexes as photoinitiators: Synthesis and

characterisation of acrylate/epoxy interpenetrated polymer networks, European Polymer Journal. 152 (2021) 110457. https://doi.org/10.1016/j.eurpolymj.2021.110457.

[59]   P. Garra, F. Dumur, D. Gigmes, A. Al Mousawi, F. Morlet-Savary, C. Dietlin, J.P. Fouassier, J. Lalevée, Copper (Photo)redox Catalyst for Radical Photopolymerization in Shadowed Areas and Access to Thick and Filled Samples, Macromolecules. 50 (2017) 3761–3771. https://doi.org/10.1021/acs.macromol.7b00622.

[60]   P. Garra, F. Dumur, F. Morlet-Savary, C. Dietlin, J.P. Fouassier, J. Lalevée, A New Highly Efficient Amine-Free and Peroxide-Free Redox System for Free Radical Polymerization under Air with Possible Light Activation, Macromolecules. 49 (2016) 6296–6309. https://doi.org/10.1021/acs.macromol.6b01615.

[61]   P. Garra, A. Kermagoret, A.A. Mousawi, F. Dumur, D. Gigmes, F. Morlet-Savary, C. Dietlin, J.P. Fouassier, J. Lalevée, New copper(I) complex based initiating systems in redox polymerization and comparison with the amine/benzoyl peroxide reference, Polym. Chem. 8 (2017) 4088–4097. https://doi.org/10.1039/C7PY00726D.

[62]   T. Borjigin, G. Noirbent, D. Gigmes, P. Xiao, F. Dumur, J. Lalevée, The new LED-Sensitive photoinitiators of Polymerization: Copper complexes in free radical and cationic photoinitiating systems and application in 3D printing, European Polymer Journal. 162 (2022) 110885. https://doi.org/10.1016/j.eurpolymj.2021.110885.

[63]   A. Al Mousawi, P. Garra, X. Sallenave, F. Dumur, J. Toufaily, T. Hamieh, B. Graff, D. Gigmes, J.P. Fouassier, J. Lalevée, π-Conjugated Dithienophosphole Derivatives as High Performance Photoinitiators for 3D Printing Resins, Macromolecules. 51 (2018) 1811–1821. https://doi.org/10.1021/acs.macromol.8b00044.

[64]   J. Zhang, F. Dumur, P. Horcajada, C. Livage, P. Xiao, J.P. Fouassier, D. Gigmes, J. Lalevée, Iron-Based Metal-Organic Frameworks (MOF) as Photocatalysts for Radical and Cationic Polymerizations under Near UV and Visible LEDs (385–405 nm), Macromolecular Chemistry and Physics. 217 (2016) 2534–2540. https://doi.org/10.1002/macp.201600352.

[65]   P. Garra, D. Brunel, G. Noirbent, B. Graff, F. Morlet-Savary, C. Dietlin, V.F. Sidorkin, F. Dumur, D. Duché, D. Gigmes, J.-P. Fouassier, J. Lalevée, Ferrocene-based (photo)redox polymerization under long wavelengths, Polym. Chem. 10 (2019) 1431–1441. https://doi.org/10.1039/C9PY00059C.

[66]   S. Telitel, F. Dumur, D. Campolo, J. Poly, D. Gigmes, J.P. Fouassier, J. Lalevée, Iron complexes as potential photocatalysts for controlled radical photopolymerizations: A tool for modifications and patterning of surfaces, Journal of Polymer Science Part A: Polymer Chemistry. 54 (2016) 702–713. https://doi.org/10.1002/pola.27896.

[67]   J. Zhang, D. Campolo, F. Dumur, P. Xiao, J.P. Fouassier, D. Gigmes, J. Lalevée, Iron complexes as photoinitiators for radical and cationic polymerization through photoredox catalysis processes, Journal of Polymer Science Part A: Polymer Chemistry. 53 (2015) 42–49. https://doi.org/10.1002/pola.27435.

[68]   J. Zhang, D. Campolo, F. Dumur, P. Xiao, J.P. Fouassier, D. Gigmes, J. Lalevée, Visible-light-sensitive photoredox catalysis by iron complexes: Applications in cationic and radical polymerization reactions, Journal of Polymer Science Part A: Polymer Chemistry. 54 (2016) 2247–2253. https://doi.org/10.1002/pola.28098.

[69]   J. Zhang, D. Campolo, F. Dumur, P. Xiao, J.P. Fouassier, D. Gigmes, J. Lalevée, Iron Complexes in Visible-Light-Sensitive Photoredox Catalysis: Effect of Ligands on Their Photoinitiation Efficiencies, ChemCatChem. 8 (2016) 2227–2233. https://doi.org/10.1002/cctc.201600320.

[70] M. Ghali, M. Benltifa, C. Brahmi, L. Elbassi, F. Dumur, C. Simonnet-Jégat, L. Bousselmi, J. Lalevée, LED and solar photodecomposition of erythrosine B and rose Bengal using H3PMo12O40/polymer photocatalyst, European Polymer Journal. 159 (2021) 110743. https://doi.org/10.1016/j.eurpolymj.2021.110743.

[71] C. Brahmi, M. Benltifa, M. Ghali, F. Dumur, C. Simonnet-Jégat, M. Valérie, F. Morlet-Savary, L. Bousselmi, J. Lalevée, Performance improvement of the photocatalytic process for the degradation of pharmaceutical compounds using new POM/polymer photocatalysts, Journal of Environmental Chemical Engineering. 9 (2021) 106015. https://doi.org/10.1016/j.jece.2021.106015.

[72] J. Lalevée, M. Peter, F. Dumur, D. Gigmes, N. Blanchard, M.-A. Tehfe, F. Morlet-Savary, J.P. Fouassier, Subtle Ligand Effects in Oxidative Photocatalysis with Iridium Complexes: Application to Photopolymerization, Chemistry – A European Journal. 17 (2011) 15027–15031. https://doi.org/10.1002/chem.201101445.

[73] J. Lalevée, M.-A. Tehfe, F. Dumur, D. Gigmes, N. Blanchard, F. Morlet-Savary, J.P. Fouassier, Iridium Photocatalysts in Free Radical Photopolymerization under Visible Lights, ACS Macro Lett. 1 (2012) 286–290. https://doi.org/10.1021/mz2001753.

[74] J. Lalevée, F. Dumur, C.R. Mayer, D. Gigmes, G. Nasr, M.-A. Tehfe, S. Telitel, F. Morlet-Savary, B. Graff, J.P. Fouassier, Photopolymerization of N-Vinylcarbazole Using Visible-Light Harvesting Iridium Complexes as Photoinitiators, Macromolecules. 45 (2012) 4134–4141. https://doi.org/10.1021/ma3005229.

[75] M.-A. Tehfe, M. Lepeltier, F. Dumur, D. Gigmes, J.-P. Fouassier, J. Lalevée, Structural Effects in the Iridium Complex Series: Photoredox Catalysis and Photoinitiation of Polymerization Reactions under Visible Lights, Macromolecular Chemistry and Physics. 218 (2017) 1700192. https://doi.org/10.1002/macp.201700192.

[76] S. Telitel, F. Dumur, S. Telitel, O. Soppera, M. Lepeltier, Y. Guillaneuf, J. Poly, F. Morlet-Savary, P. Fioux, J.-P. Fouassier, D. Gigmes, J. Lalevée, Photoredox catalysis using a new iridium complex as an efficient toolbox for radical, cationic and controlled polymerizations under soft blue to green lights, Polym. Chem. 6 (2014) 613–624. https://doi.org/10.1039/C4PY01358A.

[77] S. Telitel, F. Dumur, M. Lepeltier, D. Gigmes, J.-P. Fouassier, J. Lalevée, Photoredox process induced polymerization reactions: Iridium complexes for panchromatic photoinitiating systems, Comptes Rendus Chimie. 19 (2016) 71–78. https://doi.org/10.1016/j.crci.2015.06.016.

[78] F. Dumur, D. Bertin, D. Gigmes, Iridium (III) complexes as promising emitters for solid–state Light–Emitting Electrochemical Cells (LECs), International Journal of Nanotechnology. 9 (2012) 377–395. https://doi.org/10.1504/IJNT.2012.045343.

[79] F. Dumur, G. Nasr, G. Wantz, C.R. Mayer, E. Dumas, A. Guerlin, F. Miomandre, G. Clavier, D. Bertin, D. Gigmes, Cationic iridium complex for the design of soft salt-based phosphorescent OLEDs and color-tunable light-emitting electrochemical cells, Organic Electronics. 12 (2011) 1683–1694. https://doi.org/10.1016/j.orgel.2011.06.014.

[80] N. Zivic, M. Bouzrati-Zerrelli, S. Villotte, F. Morlet-Savary, C. Dietlin, F. Dumur, D. Gigmes, J.P. Fouassier, J. Lalevée, A novel naphthalimide scaffold based iodonium salt as a one-component photoacid/photoinitiator for cationic and radical polymerization under LED exposure, Polym. Chem. 7 (2016) 5873–5879. https://doi.org/10.1039/C6PY01306F.

[81] A.-H. Bonardi, S. Zahouily, C. Dietlin, B. Graff, F. Morlet-Savary, M. Ibrahim-Ouali, D. Gigmes, N. Hoffmann, F. Dumur, J. Lalevée, New 1,8-Naphthalimide Derivatives as

Photoinitiators for Free-Radical Polymerization Upon Visible Light, Catalysts. 9 (2019) 637. https://doi.org/10.3390/catal9080637.

[82] J. Zhang, N. Zivic, F. Dumur, P. Xiao, B. Graff, J.P. Fouassier, D. Gigmes, J. Lalevée, Naphthalimide-Tertiary Amine Derivatives as Blue-Light-Sensitive Photoinitiators, ChemPhotoChem. 2 (2018) 481–489. https://doi.org/10.1002/cptc.201800006.

[83] P. Xiao, F. Dumur, J. Zhang, B. Graff, D. Gigmes, J.P. Fouassier, J. Lalevée, Naphthalimide Derivatives: Substituent Effects on the Photoinitiating Ability in Polymerizations under Near UV, Purple, White and Blue LEDs (385, 395, 405, 455, or 470 nm), Macromolecular Chemistry and Physics. 216 (2015) 1782–1790. https://doi.org/10.1002/macp.201500150.

[84] P. Xiao, F. Dumur, J. Zhang, B. Graff, D. Gigmes, J.P. Fouassier, J. Lalevée, Naphthalimide-phthalimide derivative based photoinitiating systems for polymerization reactions under blue lights, Journal of Polymer Science Part A: Polymer Chemistry. 53 (2015) 665–674. https://doi.org/10.1002/pola.27490.

[85] J. Zhang, N. Zivic, F. Dumur, P. Xiao, B. Graff, D. Gigmes, J.P. Fouassier, J. Lalevée, A benzophenone-naphthalimide derivative as versatile photoinitiator of polymerization under near UV and visible lights, Journal of Polymer Science Part A: Polymer Chemistry. 53 (2015) 445–451. https://doi.org/10.1002/pola.27451.

[86] J. Zhang, N. Zivic, F. Dumur, P. Xiao, B. Graff, J.P. Fouassier, D. Gigmes, J. Lalevée, N-[2-(Dimethylamino)ethyl]-1,8-naphthalimide derivatives as photoinitiators under LEDs, Polym. Chem. 9 (2018) 994–1003. https://doi.org/10.1039/C8PY00055G.

[87] J. Zhang, F. Dumur, P. Xiao, B. Graff, D. Bardelang, D. Gigmes, J.P. Fouassier, J. Lalevée, Structure Design of Naphthalimide Derivatives: Toward Versatile Photoinitiators for Near-UV/Visible LEDs, 3D Printing, and Water-Soluble Photoinitiating Systems, Macromolecules. 48 (2015) 2054–2063. https://doi.org/10.1021/acs.macromol.5b00201.

[88] J. Zhang, N. Zivic, F. Dumur, P. Xiao, B. Graff, J.P. Fouassier, D. Gigmes, J. Lalevée, UV-violet-blue LED induced polymerizations: Specific photoinitiating systems at 365, 385, 395 and 405 nm, Polymer. 55 (2014) 6641–6648. https://doi.org/10.1016/j.polymer.2014.11.002.

[89] P. Xiao, F. Dumur, B. Graff, D. Gigmes, J.P. Fouassier, J. Lalevée, Blue Light Sensitive Dyes for Various Photopolymerization Reactions: Naphthalimide and Naphthalic Anhydride Derivatives., Macromolecules. 47 (2014) 601–608. https://doi.org/10.1021/ma402376x.

[90] P. Xiao, F. Dumur, M. Frigoli, M.-A. Tehfe, B. Graff, J.P. Fouassier, D. Gigmes, J. Lalevée, Naphthalimide based methacrylated photoinitiators in radical and cationic photopolymerization under visible light, Polym. Chem. 4 (2013) 5440–5448. https://doi.org/10.1039/C3PY00766A.

[91] M. Rahal, H. Mokbel, B. Graff, V. Pertici, D. Gigmes, J. Toufaily, T. Hamieh, F. Dumur, J. Lalevée, Naphthalimide-Based Dyes as Photoinitiators under Visible Light Irradiation and their Applications: Photocomposite Synthesis, 3D printing and Polymerization in Water, ChemPhotoChem. 5 (2021) 476–490. https://doi.org/10.1002/cptc.202000306.

[92] M. Rahal, B. Graff, J. Toufaily, T. Hamieh, M. Ibrahim-Ouali, F. Dumur, J. Lalevée, Naphthyl-Naphthalimides as High-Performance Visible Light Photoinitiators for 3D Printing and Photocomposites Synthesis, Catalysts. 11 (2021). https://doi.org/10.3390/catal11111269.

[93] N. Zivic, J. Zhang, D. Bardelang, F. Dumur, P. Xiao, T. Jet, D.-L. Versace, C. Dietlin, F. Morlet-Savary, B. Graff, J.P. Fouassier, D. Gigmes, J. Lalevée, Novel naphthalimide–

amine based photoinitiators operating under violet and blue LEDs and usable for various polymerization reactions and synthesis of hydrogels, Polym. Chem. 7 (2015) 418–429. https://doi.org/10.1039/C5PY01617G.

[94] P. Xiao, F. Dumur, B. Graff, F. Morlet-Savary, D. Gigmes, J.P. Fouassier, J. Lalevée, Design of High Performance Photoinitiators at 385–405 nm: Search around the Naphthalene Scaffold, Macromolecules. 47 (2014) 973–978. https://doi.org/10.1021/ma402622v.

[95] P. Xiao, F. Dumur, J. Zhang, B. Graff, D. Gigmes, J.P. Fouassier, J. Lalevée, Amino and nitro substituted 2-amino-1H-benzo[de]isoquinoline-1,3(2H)-diones: as versatile photoinitiators of polymerization from violet-blue LED absorption to a panchromatic behavior, Polym. Chem. 6 (2015) 1171–1179. https://doi.org/10.1039/C4PY01409J.

[96] J. Zhang, J. Lalevée, J. Zhao, B. Graff, M.H. Stenzel, P. Xiao, Dihydroxyanthraquinone derivatives: natural dyes as blue-light-sensitive versatile photoinitiators of photopolymerization, Polym. Chem. 7 (2016) 7316–7324. https://doi.org/10.1039/C6PY01550F.

[97] C. Brahmi, M. Benltifa, C. Vaulot, L. Michelin, F. Dumur, A. Airoudj, F. Morlet-Savary, B. Raveau, L. Bousselmi, J. Lalevée, New hybrid perovskites/polymer composites for the photodegradation of organic dyes, European Polymer Journal. 157 (2021) 110641. https://doi.org/10.1016/j.eurpolymj.2021.110641.

[98] H. Mokbel, F. Dumur, B. Raveau, F. Morlet-Savary, C. Simonnet-Jégat, D. Gigmes, J. Toufaily, T. Hamieh, J.P. Fouassier, J. Lalevée, Perovskites as new radical photoinitiators for radical and cationic polymerizations, Tetrahedron. 72 (2016) 7686–7690. https://doi.org/10.1016/j.tet.2016.03.057.

[99] H. Chen, G. Noirbent, K. Sun, D. Brunel, D. Gigmes, F. Morlet-Savary, Y. Zhang, S. Liu, P. Xiao, F. Dumur, J. Lalevée, Photoinitiators derived from natural product scaffolds: monochalcones in three-component photoinitiating systems and their applications in 3D printing, Polym. Chem. 11 (2020) 4647–4659. https://doi.org/10.1039/D0PY00568A.

[100] L. Tang, J. Nie, X. Zhu, A high performance phenyl-free LED photoinitiator for cationic or hybrid photopolymerization and its application in LED cationic 3D printing, Polym. Chem. 11 (2020) 2855–2863. https://doi.org/10.1039/D0PY00142B.

[101] Y. Xu, G. Noirbent, D. Brunel, Z. Ding, D. Gigmes, B. Graff, P. Xiao, F. Dumur, J. Lalevée, Allyloxy ketones as efficient photoinitiators with high migration stability in free radical polymerization and 3D printing, Dyes and Pigments. 185 (2021) 108900. https://doi.org/10.1016/j.dyepig.2020.108900.

[102] Y. Xu, Z. Ding, H. Zhu, B. Graff, S. Knopf, P. Xiao, F. Dumur, J. Lalevée, Design of ketone derivatives as highly efficient photoinitiators for free radical and cationic photopolymerizations and application in 3D printing of composites, Journal of Polymer Science. 58 (2020) 3432–3445. https://doi.org/10.1002/pol.20200658.

[103] H. Chen, G. Noirbent, S. Liu, D. Brunel, B. Graff, D. Gigmes, Y. Zhang, K. Sun, F. Morlet-Savary, P. Xiao, F. Dumur, J. Lalevée, Bis-chalcone derivatives derived from natural products as near-UV/visible light sensitive photoinitiators for 3D/4D printing, Mater. Chem. Front. 5 (2021) 901–916. https://doi.org/10.1039/D0QM00755B.

[104] S. Liu, Y. Zhang, K. Sun, B. Graff, P. Xiao, F. Dumur, J. Lalevée, Design of photoinitiating systems based on the chalcone-anthracene scaffold for LED cationic photopolymerization and application in 3D printing, European Polymer Journal. 147 (2021) 110300. https://doi.org/10.1016/j.eurpolymj.2021.110300.

[105] H. Chen, G. Noirbent, S. Liu, Y. Zhang, K. Sun, F. Morlet-Savary, D. Gigmes, P. Xiao, F. Dumur, J. Lalevée, In situ generation of Ag nanoparticles during photopolymerization by using newly developed dyes-based three-component photoinitiating systems and the related 3D printing applications and their shape change behavior, Journal of Polymer Science. 59 (2021) 843–859. https://doi.org/10.1002/pol.20210154.

[106] H. Chen, M. Vahdati, P. Xiao, F. Dumur, J. Lalevée, Water-Soluble Visible Light Sensitive Photoinitiating System Based on Charge Transfer Complexes for the 3D Printing of Hydrogels, Polymers. 13 (2021). https://doi.org/10.3390/polym13183195.

[107] M.-A. Tehfe, F. Dumur, P. Xiao, M. Delgove, B. Graff, J.-P. Fouassier, D. Gigmes, J. Lalevée, Chalcone derivatives as highly versatile photoinitiators for radical, cationic, thiol–ene and IPN polymerization reactions upon exposure to visible light, Polym. Chem. 5 (2014) 382–390. https://doi.org/10.1039/C3PY00922J.

[108] K. Sun, Y. Xu, F. Dumur, F. Morlet-Savary, H. Chen, C. Dietlin, B. Graff, J. Lalevée, P. Xiao, In silico rational design by molecular modeling of new ketones as photoinitiators in three-component photoinitiating systems: application in 3D printing, Polym. Chem. 11 (2020) 2230–2242. https://doi.org/10.1039/C9PY01874C.

[109] H. Chen, C. Regeard, H. Salmi, F. Morlet-Savary, N. Giacoletto, M. Nechab, P. Xiao, F. Dumur, J. Lalevée, Interpenetrating polymer network hydrogels using natural based dyes initiating systems: antibacterial activity and 3D/4D performance, European Polymer Journal. (2022) 111042. https://doi.org/10.1016/j.eurpolymj.2022.111042.

[110] J. Zhang, N. Zivic, F. Dumur, C. Guo, Y. Li, P. Xiao, B. Graff, D. Gigmes, J.P. Fouassier, J. Lalevée, Panchromatic photoinitiators for radical, cationic and thiol-ene polymerization reactions: A search in the diketopyrrolopyrrole or indigo dye series, Materials Today Communications. 4 (2015) 101–108. https://doi.org/10.1016/j.mtcomm.2015.06.007.

[111] P. Xiao, W. Hong, Y. Li, F. Dumur, B. Graff, J.P. Fouassier, D. Gigmes, J. Lalevée, Diketopyrrolopyrrole dyes: Structure/reactivity/efficiency relationship in photoinitiating systems upon visible lights, Polymer. 55 (2014) 746–751. https://doi.org/10.1016/j.polymer.2014.01.003.

[112] P. Xiao, W. Hong, Y. Li, F. Dumur, B. Graff, J.P. Fouassier, D. Gigmes, J. Lalevée, Green light sensitive diketopyrrolopyrrole derivatives used in versatile photoinitiating systems for photopolymerizations, Polym. Chem. 5 (2014) 2293–2300. https://doi.org/10.1039/C3PY01599H.

[113] E.A. Kamoun, A. Winkel, M. Eisenburger, H. Menzel, Carboxylated camphorquinone as visible-light photoinitiator for biomedical application: Synthesis, characterization, and application, Arabian Journal of Chemistry. 9 (2016) 745–754. https://doi.org/10.1016/j.arabjc.2014.03.008.

[114] A. Santini, I.T. Gallegos, C.M. Felix, Photoinitiators in Dentistry: A Review, Prim Dent J. 2 (2013) 30–33. https://doi.org/10.1308/205016814809859563.

[115] H. Mokbel, J. Toufaily, T. Hamieh, F. Dumur, D. Campolo, D. Gigmes, J.P. Fouassier, J. Ortyl, J. Lalevée, Specific cationic photoinitiators for near UV and visible LEDs: Iodonium versus ferrocenium structures, Journal of Applied Polymer Science. 132 (2015). https://doi.org/10.1002/app.42759.

[116] S. Villotte, D. Gigmes, F. Dumur, J. Lalevée, Design of Iodonium Salts for UV or Near-UV LEDs for Photoacid Generator and Polymerization Purposes, Molecules. 25 (2020) 149. https://doi.org/10.3390/molecules25010149.

[117] M.A. Tasdelen, V. Kumbaraci, S. Jockusch, N.J. Turro, N. Talinli, Y. Yagci, Photoacid Generation by Stepwise Two-Photon Absorption: Photoinitiated Cationic Polymerization of Cyclohexene Oxide by Using Benzodioxinone in the Presence of Iodonium Salt, Macromolecules. 41 (2008) 295–297. https://doi.org/10.1021/ma7023649.

[118] J.V. Crivello, J.H.W. Lam, Diaryliodonium Salts. A New Class of Photoinitiators for Cationic Polymerization, Macromolecules. 10 (1977) 1307–1315. https://doi.org/10.1021/ma60060a028.

[119] Y. He, W. Zhou, F. Wu, M. Li, E. Wang, Photoreaction and photopolymerization studies on squaraine dyes/iodonium salts combination, Journal of Photochemistry and Photobiology A: Chemistry. 162 (2004) 463–471. https://doi.org/10.1016/S1010-6030(03)00390-3.

[120] L.I. Jun, L.I. Miaozhen, S. Huaihai, Y. Yongyuan, W. Erjian, Photopolymerization Initiated by Dimethylaminochalcone/Diphenyliodonium Salt Combination System Sensitive to Visible Light, Chinese J. Polym. Sci. 11 (1993) 163–170.

[121] N. Zivic, P.K. Kuroishi, F. Dumur, D. Gigmes, A.P. Dove, H. Sardon, Recent Advances and Challenges in the Design of Organic Photoacid and Photobase Generators for Polymerizations, Angewandte Chemie International Edition. 58 (2019) 10410–10422. https://doi.org/10.1002/anie.201810118.

[122] M.-A. Tehfe, A. Zein-Fakih, J. Lalevée, F. Dumur, D. Gigmes, B. Graff, F. Morlet-Savary, T. Hamieh, J.-P. Fouassier, New pyridinium salts as versatile compounds for dye sensitized photopolymerization, European Polymer Journal. 49 (2013) 567–574. https://doi.org/10.1016/j.eurpolymj.2012.10.010.

[123] P. Xiao, M. Frigoli, F. Dumur, B. Graff, D. Gigmes, J.P. Fouassier, J. Lalevée, Julolidine or Fluorenone Based Push–Pull Dyes for Polymerization upon Soft Polychromatic Visible Light or Green Light., Macromolecules. 47 (2014) 106–112. https://doi.org/10.1021/ma402196p.

[124] H. Mokbel, F. Dumur, B. Graff, C.R. Mayer, D. Gigmes, J. Toufaily, T. Hamieh, J.-P. Fouassier, J. Lalevée, Michler's Ketone as an Interesting Scaffold for the Design of High-Performance Dyes in Photoinitiating Systems Upon Visible Light, Macromolecular Chemistry and Physics. 215 (2014) 783–790. https://doi.org/10.1002/macp.201300779.

[125] M.-A. Tehfe, F. Dumur, B. Graff, F. Morlet-Savary, J.-P. Fouassier, D. Gigmes, J. Lalevée, New Push–Pull Dyes Derived from Michler's Ketone For Polymerization Reactions Upon Visible Lights., Macromolecules. 46 (2013) 3761–3770. https://doi.org/10.1021/ma400766z.

[126] H. Mokbel, F. Dumur, C.R. Mayer, F. Morlet-Savary, B. Graff, D. Gigmes, J. Toufaily, T. Hamieh, J.-P. Fouassier, J. Lalevée, End capped polyenic structures as visible light sensitive photoinitiators for polymerization of vinylethers, Dyes and Pigments. 105 (2014) 121–129. https://doi.org/10.1016/j.dyepig.2014.02.002.

[127] S. Telitel, F. Dumur, T. Kavalli, B. Graff, F. Morlet-Savary, D. Gigmes, J.-P. Fouassier, J. Lalevée, The 1,3-bis(dicyanomethylidene)indane skeleton as a (photo) initiator in thermal ring opening polymerization at RT and radical or cationic photopolymerization, RSC Adv. 4 (2014) 15930–15936. https://doi.org/10.1039/C3RA42819B.

[128] P. Xiao, F. Dumur, B. Graff, F. Morlet-Savary, L. Vidal, D. Gigmes, J.P. Fouassier, J. Lalevée, Structural Effects in the Indanedione Skeleton for the Design of Low Intensity 300–500 nm Light Sensitive Initiators., Macromolecules. 47 (2014) 26–34. https://doi.org/10.1021/ma402149g.

[129] K. Sun, S. Liu, C. Pigot, D. Brunel, B. Graff, M. Nechab, D. Gigmes, F. Morlet-Savary, Y. Zhang, P. Xiao, F. Dumur, J. Lalevée, Novel Push–Pull Dyes Derived from 1H-cyclopenta[b]naphthalene-1,3(2H)-dione as Versatile Photoinitiators for Photopolymerization and Their Related Applications: 3D Printing and Fabrication of Photocomposites, Catalysts. 10 (2020) 1196. https://doi.org/10.3390/catal10101196.

[130] K. Sun, S. Liu, H. Chen, F. Morlet-Savary, B. Graff, C. Pigot, M. Nechab, P. Xiao, F. Dumur, J. Lalevée, N-ethyl carbazole-1-allylidene-based push-pull dyes as efficient light harvesting photoinitiators for sunlight induced polymerization, European Polymer Journal. 147 (2021) 110331. https://doi.org/10.1016/j.eurpolymj.2021.110331.

[131] M.-A. Tehfe, F. Dumur, B. Graff, F. Morlet-Savary, D. Gigmes, J.-P. Fouassier, J. Lalevée, Push–pull (thio)barbituric acid derivatives in dye photosensitized radical and cationic polymerization reactions under 457/473 nm laser beams or blue LEDs, Polym. Chem. 4 (2013) 3866–3875. https://doi.org/10.1039/C3PY00372H.

[132] K. Sun, H. Chen, Y. Zhang, F. Morlet-Savary, B. Graff, P. Xiao, F. Dumur, J. Lalevée, High-performance sunlight induced polymerization using novel push-pull dyes with high light absorption properties, European Polymer Journal. 151 (2021) 110410. https://doi.org/10.1016/j.eurpolymj.2021.110410.

[133] H. Mokbel, F. Dumur, S. Telitel, L. Vidal, P. Xiao, D.-L. Versace, M.-A. Tehfe, F. Morlet-Savary, B. Graff, J.-P. Fouassier, D. Gigmes, J. Toufaily, T. Hamieh, J. Lalevée, Photoinitiating systems of polymerization and in situ incorporation of metal nanoparticles into polymer matrices upon exposure to visible light: push–pull malonate and malononitrile based dyes, Polym. Chem. 4 (2013) 5679–5687. https://doi.org/10.1039/C3PY00846K.

[134] S. Helmy, S. Oh, F.A. Leibfarth, C.J. Hawker, J. Read de Alaniz, Design and Synthesis of Donor–Acceptor Stenhouse Adducts: A Visible Light Photoswitch Derived from Furfural, J. Org. Chem. 79 (2014) 11316–11329. https://doi.org/10.1021/jo502206g.

[135] K. Sun, C. Pigot, Y. Zhang, T. Borjigin, F. Morlet-Savary, B. Graff, M. Nechab, P. Xiao, F. Dumur, J. Lalevée, Sunlight Induced Polymerization Photoinitiated by Novel Push–Pull Dyes: Indane-1,3-Dione, 1H-Cyclopenta[b]Naphthalene-1,3(2H)-Dione and 4-Dimethoxyphenyl-1-Allylidene Derivatives, Macromolecular Chemistry and Physics. n/a (2022) 2100439. https://doi.org/10.1002/macp.202100439.

[136] A.A. Mousawi, F. Dumur, P. Garra, J. Toufaily, T. Hamieh, F. Goubard, T.-T. Bui, B. Graff, D. Gigmes, J.P. Fouassier, J. Lalevée, Azahelicenes as visible light photoinitiators for cationic and radical polymerization: Preparation of photoluminescent polymers and use in high performance LED projector 3D printing resins, Journal of Polymer Science Part A: Polymer Chemistry. 55 (2017) 1189–1199. https://doi.org/10.1002/pola.28476.

[137] A. Al Mousawi, M. Schmitt, F. Dumur, J. Ouyang, L. Favereau, V. Dorcet, N. Vanthuyne, P. Garra, J. Toufaily, T. Hamieh, B. Graff, J.P. Fouassier, D. Gigmes, J. Crassous, J. Lalevée, Visible Light Chiral Photoinitiator for Radical Polymerization and Synthesis of Polymeric Films with Strong Chiroptical Activity, Macromolecules. 51 (2018) 5628–5637. https://doi.org/10.1021/acs.macromol.8b01085.

[138] J. Lalevée, F. Dumur, M.-A. Tehfe, A. Zein-Fakih, D. Gigmes, F. Morlet-Savary, B. Graff, J.-P. Fouassier, Dye photosensitized cationic ring-opening polymerization: Search for new dye skeletons, Polymer. 53 (2012) 4947–4954. https://doi.org/10.1016/j.polymer.2012.08.067.

[139] M.-A. Tehfe, F. Dumur, P. Xiao, B. Graff, F. Morlet-Savary, J.-P. Fouassier, D. Gigmes, J. Lalevée, New chromone based photoinitiators for polymerization reactions under visible light, Polym. Chem. 4 (2013) 4234–4244. https://doi.org/10.1039/C3PY00536D.

[140] J. You, H. Fu, D. Zhao, T. Hu, J. Nie, T. Wang, Flavonol dyes with different substituents in photopolymerization, Journal of Photochemistry and Photobiology A: Chemistry. 386 (2020) 112097. https://doi.org/10.1016/j.jphotochem.2019.112097.

[141] A. Al Mousawi, P. Garra, M. Schmitt, J. Toufaily, T. Hamieh, B. Graff, J.P. Fouassier, F. Dumur, J. Lalevée, 3-Hydroxyflavone and N-Phenylglycine in High Performance Photoinitiating Systems for 3D Printing and Photocomposites Synthesis, Macromolecules. 51 (2018) 4633–4641. https://doi.org/10.1021/acs.macromol.8b00979.

[142] S. Liu, H. Chen, Y. Zhang, K. Sun, Y. Xu, F. Morlet-Savary, B. Graff, G. Noirbent, C. Pigot, D. Brunel, M. Nechab, D. Gigmes, P. Xiao, F. Dumur, J. Lalevée, Monocomponent Photoinitiators based on Benzophenone-Carbazole Structure for LED Photoinitiating Systems and Application on 3D Printing, Polymers. 12 (2020) 1394. https://doi.org/10.3390/polym12061394.

[143] P. Xiao, F. Dumur, B. Graff, D. Gigmes, J.P. Fouassier, J. Lalevée, Variations on the Benzophenone Skeleton: Novel High Performance Blue Light Sensitive Photoinitiating Systems, Macromolecules. 46 (2013) 7661–7667. https://doi.org/10.1021/ma401766v.

[144] J. Zhang, M. Frigoli, F. Dumur, P. Xiao, L. Ronchi, B. Graff, F. Morlet-Savary, J.P. Fouassier, D. Gigmes, J. Lalevée, Design of Novel Photoinitiators for Radical and Cationic Photopolymerizations under Near UV and Visible LEDs (385, 395, and 405 nm)., Macromolecules. 47 (2014) 2811–2819. https://doi.org/10.1021/ma500612x.

[145] S. Liu, D. Brunel, G. Noirbent, A. Mau, H. Chen, F. Morlet-Savary, B. Graff, D. Gigmes, P. Xiao, F. Dumur, J. Lalevée, New multifunctional benzophenone-based photoinitiators with high migration stability and their applications in 3D printing, Mater. Chem. Front. 5 (2021) 1982–1994. https://doi.org/10.1039/D0QM00885K.

[146] S. Liu, D. Brunel, K. Sun, Y. Zhang, H. Chen, P. Xiao, F. Dumur, J. Lalevée, Novel Photoinitiators Based on Benzophenone-Triphenylamine Hybrid Structure for LED Photopolymerization, Macromolecular Rapid Communications. 41 (2020) 2000460. https://doi.org/10.1002/marc.202000460.

[147] S. Liu, D. Brunel, K. Sun, Y. Xu, F. Morlet-Savary, B. Graff, P. Xiao, F. Dumur, J. Lalevée, A monocomponent bifunctional benzophenone–carbazole type II photoinitiator for LED photoinitiating systems, Polym. Chem. 11 (2020) 3551–3556. https://doi.org/10.1039/D0PY00644K.

[148] M.-A. Tehfe, F. Dumur, B. Graff, F. Morlet-Savary, J.-P. Fouassier, D. Gigmes, J. Lalevée, Trifunctional Photoinitiators Based on a Triazine Skeleton for Visible Light Source and UV LED Induced Polymerizations, Macromolecules. 45 (2012) 8639–8647. https://doi.org/10.1021/ma301931p.

[149] J.-T. Lin, J. Lalevee, Efficacy Modeling of New Multi-Functional Benzophenone-Based System for Free-Radical/Cationic Hybrid Photopolymerization Using 405 nm LED, (2021). https://doi.org/10.20944/preprints202106.0502.v1.

[150] C. Brahmi, M. Benltifa, C. Vaulot, L. Michelin, F. Dumur, F. Millange, M. Frigoli, A. Airoudj, F. Morlet-Savary, L. Bousselmi, J. Lalevée, New hybrid MOF/polymer composites for the photodegradation of organic dyes, European Polymer Journal. 154 (2021) 110560. https://doi.org/10.1016/j.eurpolymj.2021.110560.

[151] C. Brahmi, M. Benltifa, C. Vaulot, L. Michelin, F. Dumur, E. Gkaniatsou, C. Sicard, A. Airoudj, F. Morlet-Savary, L. Bousselmi, J. Lalevée, New Hybrid Fe-based

MOFs/Polymer Composites for the Photodegradation of Organic Dyes, ChemistrySelect. 6 (2021) 8120–8132. https://doi.org/10.1002/slct.202102194.

[152] P. Xiao, F. Dumur, T.T. Bui, F. Goubard, B. Graff, F. Morlet-Savary, J.P. Fouassier, D. Gigmes, J. Lalevée, Panchromatic Photopolymerizable Cationic Films Using Indoline and Squaraine Dye Based Photoinitiating Systems, ACS Macro Lett. 2 (2013) 736–740. https://doi.org/10.1021/mz400316y.

[153] V. Launay, A. Caron, G. Noirbent, D. Gigmes, F. Dumur, J. Lalevée, NIR Organic Dyes as Innovative Tools for Reprocessing/Recycling of Plastics: Benefits of the Photothermal Activation in the Near-Infrared Range, Advanced Functional Materials. 31 (2021) 2006324. https://doi.org/10.1002/adfm.202006324.

[154] A. Bonardi, F. Bonardi, G. Noirbent, F. Dumur, C. Dietlin, D. Gigmes, J.-P. Fouassier, J. Lalevée, Different NIR dye scaffolds for polymerization reactions under NIR light, Polym. Chem. 10 (2019) 6505–6514. https://doi.org/10.1039/C9PY01447K.

[155] J. Zhang, D. Campolo, F. Dumur, P. Xiao, D. Gigmes, J.P. Fouassier, J. Lalevée, The carbazole-bound ferrocenium salt as a specific cationic photoinitiator upon near-UV and visible LEDs (365–405 nm), Polym. Bull. 73 (2016) 493–507. https://doi.org/10.1007/s00289-015-1506-1.

[156] A. Al Mousawi, F. Dumur, P. Garra, J. Toufaily, T. Hamieh, B. Graff, D. Gigmes, J.P. Fouassier, J. Lalevée, Carbazole Scaffold Based Photoinitiator/Photoredox Catalysts: Toward New High Performance Photoinitiating Systems and Application in LED Projector 3D Printing Resins, Macromolecules. 50 (2017) 2747–2758. https://doi.org/10.1021/acs.macromol.7b00210.

[157] A. Al Mousawi, D.M. Lara, G. Noirbent, F. Dumur, J. Toufaily, T. Hamieh, T.-T. Bui, F. Goubard, B. Graff, D. Gigmes, J.P. Fouassier, J. Lalevée, Carbazole Derivatives with Thermally Activated Delayed Fluorescence Property as Photoinitiators/Photoredox Catalysts for LED 3D Printing Technology, Macromolecules. 50 (2017) 4913–4926. https://doi.org/10.1021/acs.macromol.7b01114.

[158] A. Al Mousawi, P. Garra, F. Dumur, T.-T. Bui, F. Goubard, J. Toufaily, T. Hamieh, B. Graff, D. Gigmes, J.P. Fouassier, J. Lalevée, Novel Carbazole Skeleton-Based Photoinitiators for LED Polymerization and LED Projector 3D Printing, Molecules. 22 (2017) 2143. https://doi.org/10.3390/molecules22122143.

[159] A.A. Mousawi, A. Arar, M. Ibrahim-Ouali, S. Duval, F. Dumur, P. Garra, J. Toufaily, T. Hamieh, B. Graff, D. Gigmes, J.-P. Fouassier, J. Lalevée, Carbazole-based compounds as photoinitiators for free radical and cationic polymerization upon near visible light illumination, Photochem. Photobiol. Sci. 17 (2018) 578–585. https://doi.org/10.1039/C7PP00400A.

[160] M. Abdallah, D. Magaldi, A. Hijazi, B. Graff, F. Dumur, J.-P. Fouassier, T.-T. Bui, F. Goubard, J. Lalevée, Development of new high-performance visible light photoinitiators based on carbazole scaffold and their applications in 3d printing and photocomposite synthesis, Journal of Polymer Science Part A: Polymer Chemistry. 57 (2019) 2081–2092. https://doi.org/10.1002/pola.29471.

[161] S. Liu, B. Graff, P. Xiao, F. Dumur, J. Lalevée, Nitro-Carbazole Based Oxime Esters as Dual Photo/Thermal Initiators for 3D Printing and Composite Preparation, Macromolecular Rapid Communications. 42 (2021) 2100207. https://doi.org/10.1002/marc.202100207.

[162] F. Hammoud, A. Hijazi, S. Duval, J. Lalevée, F. Dumur, 5,12-Dihydroindolo[3,2-a]carbazole: A promising scaffold for the design of visible light photoinitiators of

polymerization, European Polymer Journal. 162 (2022) 110880. https://doi.org/10.1016/j.eurpolymj.2021.110880.

[163] F. Dumur, Recent advances on visible light Triphenylamine-based photoinitiators of polymerization, European Polymer Journal. 166 (2022) 111036. https://doi.org/10.1016/j.eurpolymj.2022.111036.

[164] M. Abdallah, H. Le, A. Hijazi, M. Schmitt, B. Graff, F. Dumur, T.-T. Bui, F. Goubard, J.-P. Fouassier, J. Lalevée, Acridone derivatives as high performance visible light photoinitiators for cationic and radical photosensitive resins for 3D printing technology and for low migration photopolymer property, Polymer. 159 (2018) 47–58. https://doi.org/10.1016/j.polymer.2018.11.021.

[165] J. Zhang, F. Dumur, M. Bouzrati, P. Xiao, C. Dietlin, F. Morlet-Savary, B. Graff, D. Gigmes, J.P. Fouassier, J. Lalevée, Novel panchromatic photopolymerizable matrices: N,N'-dibutylquinacridone as an efficient and versatile photoinitiator, Journal of Polymer Science Part A: Polymer Chemistry. 53 (2015) 1719–1727. https://doi.org/10.1002/pola.27615.

[166] M.-A. Tehfe, F. Dumur, S. Telitel, D. Gigmes, E. Contal, D. Bertin, F. Morlet-Savary, B. Graff, J.-P. Fouassier, J. Lalevée, Zinc-based metal complexes as new photocatalysts in polymerization initiating systems, European Polymer Journal. 49 (2013) 1040–1049. https://doi.org/10.1016/j.eurpolymj.2013.01.023.

[167] M. Abdallah, A. Hijazi, B. Graff, J.-P. Fouassier, G. Rodeghiero, A. Gualandi, F. Dumur, P.G. Cozzi, J. Lalevée, Coumarin derivatives as versatile photoinitiators for 3D printing, polymerization in water and photocomposite synthesis, Polym. Chem. 10 (2019) 872–884. https://doi.org/10.1039/C8PY01708E.

[168] M. Abdallah, F. Dumur, A. Hijazi, G. Rodeghiero, A. Gualandi, P.G. Cozzi, J. Lalevée, Keto-coumarin scaffold for photoinitiators for 3D printing and photocomposites, Journal of Polymer Science. 58 (2020) 1115–1129. https://doi.org/10.1002/pol.20190290.

[169] M. Abdallah, A. Hijazi, F. Dumur, J. Lalevée, Coumarins as Powerful Photosensitizers for the Cationic Polymerization of Epoxy-Silicones under Near-UV and Visible Light and Applications for 3D Printing Technology, Molecules. 25 (2020) 2063. https://doi.org/10.3390/molecules25092063.

[170] M. Abdallah, A. Hijazi, P.G. Cozzi, A. Gualandi, F. Dumur, J. Lalevée, Boron Compounds as Additives for the Cationic Polymerization Using Coumarin Derivatives in Epoxy Silicones, Macromolecular Chemistry and Physics. 222 (2021) 2000404. https://doi.org/10.1002/macp.202000404.

[171] Q. Chen, Q. Yang, P. Gao, B. Chi, J. Nie, Y. He, Photopolymerization of Coumarin-Containing Reversible Photoresponsive Materials Based on Wavelength Selectivity, Ind. Eng. Chem. Res. 58 (2019) 2970–2975. https://doi.org/10.1021/acs.iecr.8b05164.

[172] Z. Li, X. Zou, G. Zhu, X. Liu, R. Liu, Coumarin-Based Oxime Esters: Photobleachable and Versatile Unimolecular Initiators for Acrylate and Thiol-Based Click Photopolymerization under Visible Light-Emitting Diode Light Irradiation, ACS Appl. Mater. Interfaces. 10 (2018) 16113–16123. https://doi.org/10.1021/acsami.8b01767.

[173] M. Rahal, H. Mokbel, B. Graff, J. Toufaily, T. Hamieh, F. Dumur, J. Lalevée, Mono vs. Difunctional Coumarin as Photoinitiators in Photocomposite Synthesis and 3D Printing, Catalysts. 10 (2020) 1202. https://doi.org/10.3390/catal10101202.

[174] M. Rajeshirke, M.C. Sreenath, S. Chitrambalam, I.H. Joe, N. Sekar, Enhancement of NLO Properties in OBO Fluorophores Derived from Carbazole–Coumarin Chalcones

Containing Carboxylic Acid at the N-Alykl Terminal End, J. Phys. Chem. C. 122 (2018) 14313–14325. https://doi.org/10.1021/acs.jpcc.8b02937.

[175] M. Rahal, B. Graff, J. Toufaily, T. Hamieh, F. Dumur, J. Lalevée, Design of keto-coumarin based photoinitiator for Free Radical Photopolymerization: Towards 3D printing and photocomposites applications, European Polymer Journal. 154 (2021) 110559. https://doi.org/10.1016/j.eurpolymj.2021.110559.

[176] M. Rahal, B. Graff, J. Toufaily, T. Hamieh, G. Noirbent, D. Gigmes, F. Dumur, J. Lalevée, 3-Carboxylic Acid and Formyl-Derived Coumarins as Photoinitiators in Photo-Oxidation or Photo-Reduction Processes for Photopolymerization upon Visible Light: Photocomposite Synthesis and 3D Printing Applications, Molecules. 26 (2021). https://doi.org/10.3390/molecules26061753.

[177] F. Hammoud, N. Giacoletto, G. Noirbent, B. Graff, A. Hijazi, M. Nechab, D. Gigmes, F. Dumur, J. Lalevée, Substituent effects on the photoinitiation ability of coumarin-based oxime-ester photoinitiators for free radical photopolymerization, Mater. Chem. Front. 5 (2021) 8361–8370. https://doi.org/10.1039/D1QM01310F.

[178] M.-A. Tehfe, F. Dumur, P. Xiao, J. Zhang, B. Graff, F. Morlet-Savary, D. Gigmes, J.-P. Fouassier, J. Lalevée, Photoinitiators based on a phenazine scaffold: High performance systems upon near-UV or visible LED (385, 395 and 405 nm) irradiations, Polymer. 55 (2014) 2285–2293. https://doi.org/10.1016/j.polymer.2014.04.005.

[179] F. Dumur, Recent advances on visible light Phenothiazine-based photoinitiators of polymerization, European Polymer Journal. 165 (2022) 110999. https://doi.org/10.1016/j.eurpolymj.2022.110999.

[180] B. Corakci, S.O. Hacioglu, L. Toppare, U. Bulut, Long wavelength photosensitizers in photoinitiated cationic polymerization: The effect of quinoxaline derivatives on photopolymerization, Polymer. 54 (2013) 3182–3187. https://doi.org/10.1016/j.polymer.2013.04.008.

[181] P. Xiao, F. Dumur, D. Thirion, S. Fagour, A. Vacher, X. Sallenave, F. Morlet-Savary, B. Graff, J.P. Fouassier, D. Gigmes, J. Lalevée, Multicolor Photoinitiators for Radical and Cationic Polymerization: Monofunctional vs Polyfunctional Thiophene Derivatives, Macromolecules. 46 (2013) 6786–6793. https://doi.org/10.1021/ma401389t.

[182] A. Al Mousawi, C. Poriel, F. Dumur, J. Toufaily, T. Hamieh, J.P. Fouassier, J. Lalevée, Zinc Tetraphenylporphyrin as High Performance Visible Light Photoinitiator of Cationic Photosensitive Resins for LED Projector 3D Printing Applications, Macromolecules. 50 (2017) 746–753. https://doi.org/10.1021/acs.macromol.6b02596.

[183] G. Noirbent, Y. Xu, A.-H. Bonardi, D. Gigmes, J. Lalevée, F. Dumur, Metalated porphyrins as versatile visible light and NIR photoinitiators of polymerization, European Polymer Journal. 139 (2020) 110019. https://doi.org/10.1016/j.eurpolymj.2020.110019.

[184] J. Zhao, J. Lalevée, H. Lu, R. MacQueen, S.H. Kable, T.W. Schmidt, M.H. Stenzel, P. Xiao, A new role of curcumin: as a multicolor photoinitiator for polymer fabrication under household UV to red LED bulbs, Polym. Chem. 6 (2015) 5053–5061. https://doi.org/10.1039/C5PY00661A.

[185] J.V. Crivello, U. Bulut, Curcumin: A naturally occurring long-wavelength photosensitizer for diaryliodonium salts, Journal of Polymer Science Part A: Polymer Chemistry. 43 (2005) 5217–5231. https://doi.org/10.1002/pola.21017.

[186] W. Han, H. Fu, T. Xue, T. Liu, Y. Wang, T. Wang, Facilely prepared blue-green light sensitive curcuminoids with excellent bleaching properties as high performance

photosensitizers in cationic and free radical photopolymerization, Polym. Chem. 9 (2018) 1787–1798. https://doi.org/10.1039/C8PY00166A.

[187] A. Mishra, S. Daswal, Curcumin, A Novel Natural Photoinitiator for the Copolymerization of Styrene and Methylmethacrylate, Null. 42 (2005) 1667–1678. https://doi.org/10.1080/10601320500246974.

[188] J. Li, X. Zhang, S. Ali, M.Y. Akram, J. Nie, X. Zhu, The effect of polyethylene glycoldiacrylate complexation on type II photoinitiator and promotion for visible light initiation system, Journal of Photochemistry and Photobiology A: Chemistry. 384 (2019) 112037. https://doi.org/10.1016/j.jphotochem.2019.112037.

[189] J. Li, S. Li, Y. Li, R. Li, J. Nie, X. Zhu, In situ monitoring of photopolymerization by photoinitiator with luminescence characteristics, Journal of Photochemistry and Photobiology A: Chemistry. 389 (2020) 112225. https://doi.org/10.1016/j.jphotochem.2019.112225.

[190] J. Li, Y. Hao, M. Zhong, L. Tang, J. Nie, X. Zhu, Synthesis of furan derivative as LED light photoinitiator: One-pot, low usage, photobleaching for light color 3D printing, Dyes and Pigments. 165 (2019) 467–473. https://doi.org/10.1016/j.dyepig.2019.03.011.

[191] Y. Xu, G. Noirbent, D. Brunel, Z. Ding, D. Gigmes, B. Graff, P. Xiao, F. Dumur, J. Lalevée, Novel ketone derivative-based photoinitiating systems for free radical polymerization under mild conditions and 3D printing, Polym. Chem. 11 (2020) 5767–5777. https://doi.org/10.1039/D0PY00990C.

[192] P. Xiao, F. Dumur, M. Frigoli, B. Graff, F. Morlet-Savary, G. Wantz, H. Bock, J.P. Fouassier, D. Gigmes, J. Lalevée, Perylene derivatives as photoinitiators in blue light sensitive cationic or radical curable films and panchromatic thiol-ene polymerizable films, European Polymer Journal. 53 (2014) 215–222. https://doi.org/10.1016/j.eurpolymj.2014.01.024.

[193] P. Xiao, F. Dumur, B. Graff, D. Gigmes, J.P. Fouassier, J. Lalevée, Red-Light-Induced Cationic Photopolymerization: Perylene Derivatives as Efficient Photoinitiators, Macromolecular Rapid Communications. 34 (2013) 1452–1458. https://doi.org/10.1002/marc.201300383.

[194] M.-A. Tehfe, F. Dumur, B. Graff, D. Gigmes, J.-P. Fouassier, J. Lalevée, Green-Light-Induced Cationic Ring Opening Polymerization Reactions: Perylene-3,4:9,10-bis(Dicarboximide) as Efficient Photosensitizers, Macromolecular Chemistry and Physics. 214 (2013) 1052–1060. https://doi.org/10.1002/macp.201200728.

[195] N. Karaca, N. Ocal, N. Arsu, S. Jockusch, Thioxanthone-benzothiophenes as photoinitiator for free radical polymerization, Journal of Photochemistry and Photobiology A: Chemistry. 331 (2016) 22–28. https://doi.org/10.1016/j.jphotochem.2016.01.017.

[196] D.K. Balta, N. Cetiner, G. Temel, Z. Turgut, N. Arsu, An annelated thioxanthone as a new Type II initiator, Journal of Photochemistry and Photobiology A: Chemistry. 199 (2008) 316–321. https://doi.org/10.1016/j.jphotochem.2008.06.008.

[197] D.K. Balta, G. Temel, G. Goksu, N. Ocal, N. Arsu, Thioxanthone–Diphenyl Anthracene: Visible Light Photoinitiator, Macromolecules. 45 (2012) 119–125. https://doi.org/10.1021/ma202168m.

[198] S. Dadashi-Silab, C. Aydogan, Y. Yagci, Shining a light on an adaptable photoinitiator: advances in photopolymerizations initiated by thioxanthones, Polym. Chem. 6 (2015) 6595–6615. https://doi.org/10.1039/C5PY01004G.

[199] T.N. Eren, N. Yasar, V. Aviyente, F. Morlet-Savary, B. Graff, J.P. Fouassier, J. Lalevee, D. Avci, Photophysical and Photochemical Studies of Novel Thioxanthone-Functionalized Methacrylates through LED Excitation, Macromolecular Chemistry and Physics. 217 (2016) 1501–1512. https://doi.org/10.1002/macp.201600051.

[200] J. Qiu, J. Wei, Thioxanthone photoinitiator containing polymerizable N-aromatic maleimide for photopolymerization, J Polym Res. 21 (2014) 559. https://doi.org/10.1007/s10965-014-0559-4.

[201] H. Tar, D. Sevinc Esen, M. Aydin, C. Ley, N. Arsu, X. Allonas, Panchromatic Type II Photoinitiator for Free Radical Polymerization Based on Thioxanthone Derivative, Macromolecules. 46 (2013) 3266–3272. https://doi.org/10.1021/ma302641d.

[202] Q. Wu, X. Wang, Y. Xiong, J. Yang, H. Tang, Thioxanthone based one-component polymerizable visible light photoinitiator for free radical polymerization, RSC Adv. 6 (2016) 66098–66107. https://doi.org/10.1039/C6RA15349F.

[203] Q. Wu, K. Tang, Y. Xiong, X. Wang, J. Yang, H. Tang, High-Performance and Low Migration One-Component Thioxanthone Visible Light Photoinitiators, Macromolecular Chemistry and Physics. 218 (2017) 1600484. https://doi.org/10.1002/macp.201600484.

[204] X. Wu, M. Jin, J.-P. Malval, D. Wan, H. Pu, Visible light-emitting diode-sensitive thioxanthone derivatives used in versatile photoinitiating systems for photopolymerizations, Journal of Polymer Science Part A: Polymer Chemistry. 55 (2017) 4037–4045. https://doi.org/10.1002/pola.28871.

[205] J. Lalevée, M.-A. Tehfe, F. Dumur, D. Gigmes, B. Graff, F. Morlet-Savary, J.-P. Fouassier, Light-Harvesting Organic Photoinitiators of Polymerization, Macromolecular Rapid Communications. 34 (2013) 239–245. https://doi.org/10.1002/marc.201200578.

[206] D.S. Esen, F. Karasu, N. Arsu, The investigation of photoinitiated polymerization of multifunctional acrylates with TX-BT by Photo-DSC and RT-FTIR, Progress in Organic Coatings. 70 (2011) 102–107. https://doi.org/10.1016/j.porgcoat.2010.10.010.

[207] M.-A. Tehfe, F. Dumur, E. Contal, B. Graff, F. Morlet-Savary, D. Gigmes, J.-P. Fouassier, J. Lalevée, New insights into radical and cationic polymerizations upon visible light exposure: role of novel photoinitiator systems based on the pyrene chromophore, Polym. Chem. 4 (2013) 1625–1634. https://doi.org/10.1039/C2PY20950K.

[208] S. Telitel, F. Dumur, T. Faury, B. Graff, M.-A. Tehfe, D. Gigmes, J.-P. Fouassier, J. Lalevée, New core-pyrene π structure organophotocatalysts usable as highly efficient photoinitiators, Beilstein J. Org. Chem. 9 (2013) 877–890. https://doi.org/10.3762/bjoc.9.101.

[209] N. Uchida, H. Nakano, T. Igarashi, T. Sakurai, Nonsalt 1-(arylmethyloxy)pyrene photoinitiators capable of initiating cationic polymerization, Journal of Applied Polymer Science. 131 (2014). https://doi.org/10.1002/app.40510.

[210] A. Mishra, S. Daswal, 1-(Bromoacetyl)pyrene, a novel photoinitiator for the copolymerization of styrene and methylmethacrylate, Radiation Physics and Chemistry. 75 (2006) 1093–1100. https://doi.org/10.1016/j.radphyschem.2006.01.013.

[211] M.-A. Tehfe, F. Dumur, B. Graff, F. Morlet-Savary, D. Gigmes, J.-P. Fouassier, J. Lalevée, Design of new Type I and Type II photoinitiators possessing highly coupled pyrene–ketone moieties, Polym. Chem. 4 (2013) 2313–2324. https://doi.org/10.1039/C3PY21079K.

[212] M.-A. Tehfe, F. Dumur, N. Vilà, B. Graff, C.R. Mayer, J.P. Fouassier, D. Gigmes, J. Lalevée, A Multicolor Photoinitiator for Cationic Polymerization and Interpenetrated

Polymer Network Synthesis: 2,7-Di-tert-butyldimethyldihydropyrene, Macromolecular Rapid Communications. 34 (2013) 1104–1109. https://doi.org/10.1002/marc.201300302.

[213] S. Telitel, F. Dumur, D. Gigmes, B. Graff, J.P. Fouassier, J. Lalevée, New functionalized aromatic ketones as photoinitiating systems for near visible and visible light induced polymerizations, Polymer. 54 (2013) 2857–2864. https://doi.org/10.1016/j.polymer.2013.03.062.

[214] M.-A. Tehfe, F. Dumur, E. Contal, B. Graff, D. Gigmes, J.-P. Fouassier, J. Lalevée, Novel Highly Efficient Organophotocatalysts: Truxene–Acridine-1,8-diones as Photoinitiators of Polymerization, Macromolecular Chemistry and Physics. 214 (2013) 2189–2201. https://doi.org/10.1002/macp.201300362.

[215] P. Xiao, F. Dumur, M.-A. Tehfe, B. Graff, D. Gigmes, J.P. Fouassier, J. Lalevée, Difunctional acridinediones as photoinitiators of polymerization under UV and visible lights: Structural effects, Polymer. 54 (2013) 3458–3466. https://doi.org/10.1016/j.polymer.2013.04.055.

[216] P. Xiao, F. Dumur, M.-A. Tehfe, B. Graff, D. Gigmes, J.P. Fouassier, J. Lalevée, Acridinediones: Effect of Substituents on Their Photoinitiating Abilities in Radical and Cationic Photopolymerization, Macromolecular Chemistry and Physics. 214 (2013) 2276–2282. https://doi.org/10.1002/macp.201300363.

[217] H. Mokbel, F. Dumur, J. Lalevée, On demand NIR activated photopolyaddition reactions, Polym. Chem. 11 (2020) 4250–4259. https://doi.org/10.1039/D0PY00639D.

[218] H. Mokbel, B. Graff, F. Dumur, J. Lalevée, NIR Sensitizer Operating under Long Wavelength (1064 nm) for Free Radical Photopolymerization Processes, Macromolecular Rapid Communications. 41 (2020) 2000289. https://doi.org/10.1002/marc.202000289.

[219] V. Launay, F. Dumur, D. Gigmes, J. Lalevée, Near-infrared light for polymer re-shaping and re-processing applications, Journal of Polymer Science. 59 (2021) 2193–2200. https://doi.org/10.1002/pol.20210450.

[220] A. Caron, G. Noirbent, D. Gigmes, F. Dumur, J. Lalevée, Near-Infrared PhotoInitiating Systems: Photothermal versus Triplet–Triplet Annihilation-Based Upconversion Polymerization, Macromolecular Rapid Communications. 42 (2021) 2100047. https://doi.org/10.1002/marc.202100047.

[221] A.-H. Bonardi, F. Bonardi, F. Morlet-Savary, C. Dietlin, G. Noirbent, T.M. Grant, J.-P. Fouassier, F. Dumur, B.H. Lessard, D. Gigmes, J. Lalevée, Photoinduced Thermal Polymerization Reactions, Macromolecules. 51 (2018) 8808–8820. https://doi.org/10.1021/acs.macromol.8b01741.

[222] H. Li, M. Fang, T. Xu, Y. Hou, R. Tang, J. Chen, L. Liu, H. Han, T. Peng, Q. Li, Z. Li, New anthracene-based organic dyes: the flexible position of the anthracene moiety bearing isolation groups in the conjugated bridge and the adjustable cell performance, Org. Chem. Front. 3 (2016) 233–242. https://doi.org/10.1039/C5QO00377F.

[223] S. Jhulki, A.K. Mishra, T.J. Chow, J.N. Moorthy, Carbo[5]helicene versus planar phenanthrene as a scaffold for organic materials in OLEDs: the electroluminescence of anthracene-functionalized emissive materials, New J. Chem. 41 (2017) 14730–14737. https://doi.org/10.1039/C7NJ02233F.

[224] K. Duraimurugan, M. Harikrishnan, J. Madhavan, A. Siva, S.J. Lee, J. Theerthagiri, M.Y. Choi, Anthracene-based fluorescent probe: Synthesis, characterization, aggregation-induced emission, mechanochromism, and sensing of nitroaromatics in aqueous media, Environmental Research. 194 (2021) 110741. https://doi.org/10.1016/j.envres.2021.110741.

[225] L. Xu, L. Ni, F. Zeng, S. Wu, Tetranitrile-anthracene as a probe for fluorescence detection of viscosity in fluid drinks via aggregation-induced emission, Analyst. 145 (2020) 844–850. https://doi.org/10.1039/C9AN02157D.

[226] H. Li, Y. Yang, Y. Hou, R. Tang, T. Duan, J. Chen, H. Wang, H. Han, T. Peng, X. Chen, Q. Li, Z. Li, Organic Sensitizers Featuring 9,10-Diaryl-Substituted Anthracene Unit, ACS Sustainable Chem. Eng. 2 (2014) 1776–1784. https://doi.org/10.1021/sc500234a.

[227] Y. Toba, M. Saito, Anthracene-Sensitized Photolysis of Onium Tetrakis(Pentafluorophenyl) Borate Cationic Photoinitiators, Journal of Photoscience. 5 (1998) 111–120.

[228] Y. Toba, Anthracene-sensitized polymerization of vinyl ethers by onium tetrakis(pentafluorophenyl)borate initiators, Journal of Polymer Science Part A: Polymer Chemistry. 38 (2000) 982–987. https://doi.org/10.1002/(SICI)1099-0518(20000315)38:6<982::AID-POLA7>3.0.CO;2-H.

[229] Y. Toba, M. Saito, Y. Usui, Cationic Photopolymerization of Epoxides by Direct and Sensitized Photolysis of Onium Tetrakis(pentafluorophenyl)borate Initiators, Macromolecules. 32 (1999) 3209–3215. https://doi.org/10.1021/ma981860r.

[230] K. Tanaka, Y. Takahashi, T. Isobe, T. Satoh, R. Akimoto, T. Igarashi, T. Sakurai, Bond-cleavage mode of O-acyl anthracene-9-methanol derivatives in the singlet excited state and their abilities to initiate radical and cationic photopolymerizations, Journal of Photochemistry and Photobiology A: Chemistry. 174 (2005) 130–137. https://doi.org/10.1016/j.jphotochem.2005.02.018.

[231] J.V. Crivello, M. Jang, Anthracene electron-transfer photosensitizers for onium salt induced cationic photopolymerizations, Journal of Photochemistry and Photobiology A: Chemistry. 159 (2003) 173–188. https://doi.org/10.1016/S1010-6030(03)00182-5.

[232] J.-D. Cho, H.-K. Kim, Y.-S. Kim, J.-W. Hong, Dual curing of cationic UV-curable clear and pigmented coating systems photosensitized by thioxanthone and anthracene, Polymer Testing. 22 (2003) 633–645. https://doi.org/10.1016/S0142-9418(02)00169-1.

[233] J.-D. Cho, E.-O. Kim, H.-K. Kim, J.-W. Hong, An investigation of the surface properties and curing behavior of photocurable cationic films photosensitized by anthracene, Polymer Testing. 21 (2002) 781–791. https://doi.org/10.1016/S0142-9418(02)00012-0.

[234] Y. Hua, F. Jiang, J.V. Crivello, Photosensitized Onium-Salt-Induced Cationic Polymerization with Hydroxymethylated Polynuclear Aromatic Hydrocarbons, Chem. Mater. 14 (2002) 2369–2377. https://doi.org/10.1021/cm011703y.

[235] S.P. Pappas, Photoinitiation of cationic and concurrent radicalcationic polymerization. Part V11For Part IV, see ref. 39., Progress in Organic Coatings. 13 (1985) 35–64. https://doi.org/10.1016/0033-0655(85)80002-9.

[236] H. Kura, K. Fujihara, A. Kimura, T. Ohno, M. Matsumura, Y. Hirata, T. Okada, Initial step of anthracene-sensitized photoacid generation from diphenyliodonium hexafluorophosphate in an epoxy matrix studied by steady-state and laser-flash photolyses, Journal of Polymer Science Part B: Polymer Physics. 39 (2001) 2937–2946. https://doi.org/10.1002/polb.10051.

[237] M. Höfer, N. Moszner, R. Liska, Oxygen scavengers and sensitizers for reduced oxygen inhibition in radical photopolymerization, Journal of Polymer Science Part A: Polymer Chemistry. 46 (2008) 6916–6927. https://doi.org/10.1002/pola.23001.

[238] A. Allushi, S. Jockusch, G. Yilmaz, Y. Yagci, Photoinitiated Metal-Free Controlled/Living Radical Polymerization Using Polynuclear Aromatic Hydrocarbons, Macromolecules. 49 (2016) 7785–7792. https://doi.org/10.1021/acs.macromol.6b01752.

[239] Y. Liu, D. Chen, X. Li, Z. Yu, Q. Xia, D. Liang, H. Xing, Visible-light-induced controlled radical polymerization of methacrylates mediated by a pillared-layer metal–organic framework, Green Chem. 18 (2016) 1475–1481. https://doi.org/10.1039/C5GC02620B.

[240] M. Danko, Š. Chmela, P. Hrdlovič, Photochemical stability and photostabilizing efficiency of anthracene/hindered amine stabilizers in polymer matrices, Polymer Degradation and Stability. 79 (2003) 333–343. https://doi.org/10.1016/S0141-3910(02)00297-5.

[241] T. Ubukata, M. Nakayama, T. Sonoda, Y. Yokoyama, H. Kihara, Highly Sensitive Formation of Stable Surface Relief Structures in Bisanthracene Films with Spatially Patterned Photopolymerization, ACS Appl. Mater. Interfaces. 8 (2016) 21974–21978. https://doi.org/10.1021/acsami.6b07943.

[242] L. Grossmann, B.T. King, S. Reichlmaier, N. Hartmann, J. Rosen, W.M. Heckl, J. Björk, M. Lackinger, On-surface photopolymerization of two-dimensional polymers ordered on the mesoscale, Nature Chemistry. 13 (2021) 730–736. https://doi.org/10.1038/s41557-021-00709-y.

[243] X. Gao, J. Li, T. Li, Z. Su, X. Ma, J. Yin, X. Jiang, Photo-Polymerization Induced Hierarchical Pattern via Self-Wrinkling, Advanced Functional Materials. 31 (2021) 2106754. https://doi.org/10.1002/adfm.202106754.

[244] Q. Tang, Z. Zhang, J. Gong, Q. Zhao, UV-induced room temperature synthesis of microporous ladder polymers with efficient photosensitization, Reactive and Functional Polymers. 144 (2019) 104362. https://doi.org/10.1016/j.reactfunctpolym.2019.104362.

[245] Y. Morita, K. Takagi, M. Fukuchi-Mizutani, K. Ishiguro, Y. Tanaka, E. Nitasaka, M. Nakayama, N. Saito, T. Kagami, A. Hoshino, S. Iida, A chalcone isomerase-like protein enhances flavonoid production and flower pigmentation, The Plant Journal. 78 (2014) 294–304. https://doi.org/10.1111/tpj.12469.

[246] Ramya Kuber Banoth, A. Thatikonda, A Review on Natural Chalcones : An Update, International Journal Of Pharmaceutical Sciences And Research. 11 (2020) 546–555.

[247] Z. Rozmer, P. Perjési, Naturally occurring chalcones and their biological activities, Phytochem Rev. 15 (2016) 87–120. https://doi.org/10.1007/s11101-014-9387-8.

[248] H. Ghouila, N. Meksi, W. Haddar, M.F. Mhenni, H.B. Jannet, Extraction, identification and dyeing studies of Isosalipurposide, a natural chalcone dye from Acacia cyanophylla flowers on wool, Industrial Crops and Products. 35 (2012) 31–36. https://doi.org/10.1016/j.indcrop.2011.05.026.

[249] H.R. Allcock, C.G. Cameron, Synthesis of Photo-Cross-Linkable Chalcone-Bearing Polyphosphazenes, Macromolecules. 27 (1994) 3131–3135. https://doi.org/10.1021/ma00090a003.

[250] J.P. Fouassier, J. Lalevée, Three-component photoinitiating systems: towards innovative tailor made high performance combinations, RSC Adv. 2 (2012) 2621–2629. https://doi.org/10.1039/C2RA00892K.

[251] A. Ibrahim, B.E. Fouhaili, A.C. Yong, C. Ley, X. Allonas, C. Carré, Optimization of a Safranine O three-component photoinitiating system for use in holographic recording, Can. J. Chem. 93 (2015) 1345–1353. https://doi.org/10.1139/cjc-2014-0606.

[252] A. Balcerak, D. Kwiatkowska, K. Iwińska, J. Kabatc, Highly efficient UV-Vis light activated three-component photoinitiators composed of tris(trimethylsilyl)silane for polymerization of acrylates, Polym. Chem. 11 (2020) 5500–5511. https://doi.org/10.1039/D0PY00763C.

[253] S. Chen, C. Qin, M. Jin, H. Pan, D. Wan, Novel chalcone derivatives with large conjugation structures as photosensitizers for versatile photopolymerization, Journal of Polymer Science. 59 (2021) 578–593. https://doi.org/10.1002/pol.20210024.

[254] N. Srividya, P. Ramamurthy, V.T. Ramakrishnan, Photophysical studies of acridine(1,8)dione dyes: a new class of laser dyes, Spectrochimica Acta Part A: Molecular and Biomolecular Spectroscopy. 54 (1998) 245–253. https://doi.org/10.1016/S1386-1425(97)00211-4.

[255] H.-J. Timpe, A.G. Rajendran, Light-induced polymer and polymerization reactions—42. A kinetic study of cationic photopolymerization with (benzoin derivative)/(onium salt) systems, European Polymer Journal. 27 (1991) 77–83. https://doi.org/10.1016/0014-3057(91)90129-C.

[256] H.-J. Timpe, S. Ulrich, J.-P. Fouassier, Photochemistry and use of decahydroacridine-1,8-diones as photosensitizers for onium salt decomposition, Journal of Photochemistry and Photobiology A: Chemistry. 73 (1993) 139–150. https://doi.org/10.1016/1010-6030(93)80043-9.

[257] S. Ulrich, H.-J. Timpe, J.-P. Fouassier, F. Morlet-Savary, Photoreduction of decahydroacridine-1,8-diones by amines, Journal of Photochemistry and Photobiology A: Chemistry. 74 (1993) 165–170. https://doi.org/10.1016/1010-6030(93)80113-N.

[258] D. Kolosov, V. Adamovich, P. Djurovich, M.E. Thompson, C. Adachi, 1,8-Naphthalimides in Phosphorescent Organic LEDs: The Interplay between Dopant, Exciplex, and Host Emission, J. Am. Chem. Soc. 124 (2002) 9945–9954. https://doi.org/10.1021/ja0263588.

[259] G. Sivakumar, A.H. Bertoni, H.-S. Kim, P.E. Marchezi, D.R. Bernardo, A. Hagfeldt, M. Grätzel, S.M. Zakeeruddin, A.F. Nogueira, Design, synthesis and characterization of 1,8-naphthalimide based fullerene derivative as electron transport material for inverted perovskite solar cells, Synthetic Metals. 249 (2019) 25–30. https://doi.org/10.1016/j.synthmet.2019.01.014.

[260] J. Zhang, H. Xiao, X. Zhang, Y. Wu, G. Li, C. Li, X. Chen, W. Ma, Z. Bo, 1,8-Naphthalimide-based nonfullerene acceptors for wide optical band gap polymer solar cells with an ultrathin active layer thickness of 35 nm, J. Mater. Chem. C. 4 (2016) 5656–5663. https://doi.org/10.1039/C6TC01438K.

[261] X. Li, J. Hou, C. Peng, L. Chen, W. Liu, Y. Liu, A 1,8-naphthalimide-based fluorescent probe for selective and sensitive detection of peroxynitrite and its applications in living cell imaging, RSC Adv. 7 (2017) 34287–34292. https://doi.org/10.1039/C7RA04317A.

[262] G. Saito, D. Velluto, M. Resmini, Synthesis of 1,8-naphthalimide-based probes with fluorescent switch triggered by flufenamic acid, Royal Society Open Science. 5 (n.d.) 172137. https://doi.org/10.1098/rsos.172137.

[263] J. Cao, J. Gong, N. Fu, A 1,8-naphthalimide based fluorescent probe for sensing tyrosinase in zebrafish, Microchemical Journal. 173 (2022) 107007. https://doi.org/10.1016/j.microc.2021.107007.

[264] C. Geraghty, C. Wynne, R.B.P. Elmes, 1,8-Naphthalimide based fluorescent sensors for enzymes, Coordination Chemistry Reviews. 437 (2021) 213713. https://doi.org/10.1016/j.ccr.2020.213713.

[265] S.M. Sami, R.T. Dorr, D.S. Alberts, A.M. Sólyom, W.A. Remers, Analogues of Amonafide and Azonafide with Novel Ring Systems, J. Med. Chem. 43 (2000) 3067–3073. https://doi.org/10.1021/jm9905817.

[266] H. Lai, M. Lu, F. Chen, J. Lalevée, M.H. Stenzel, P. Xiao, Amphiphilic polymer coated nanodiamonds: a promising platform to deliver azonafide, Polym. Chem. 10 (2019) 1904–1911. https://doi.org/10.1039/C9PY00055K.

[267] V.J. Stella, Q. He, Cyclodextrins, Toxicol Pathol. 36 (2008) 30–42. https://doi.org/10.1177/0192623307310945.

[268] G.J. Chae, S.-H. Jeong, J.H. Baek, B. Walker, C.K. Song, J.H. Seo, Improved performance in TIPS-pentacene field effect transistors using solvent additives, J. Mater. Chem. C. 1 (2013) 4216–4221. https://doi.org/10.1039/C3TC30506F.

[269] H. Yoo, H.H. Choi, T.J. Shin, T. Rim, K. Cho, S. Jung, J.-J. Kim, Self-Assembled, Millimeter-Sized TIPS-Pentacene Spherulites Grown on Partially Crosslinked Polymer Gate Dielectric, Advanced Functional Materials. 25 (2015) 3658–3665. https://doi.org/10.1002/adfm.201501381.

[270] M.-A. Tehfe, J. Lalevée, F. Morlet-Savary, B. Graff, N. Blanchard, J.-P. Fouassier, Organic Photocatalyst for Polymerization Reactions: 9,10-Bis[(triisopropylsilyl)ethynyl]anthracene, ACS Macro Lett. 1 (2012) 198–203. https://doi.org/10.1021/mz200140y.

[271] S. Okazaki, M. Oyarna, S. Nomura, Correlation between the redox potentials of 9-substituted anthracenes and the results of PM3 calculation, Electroanalysis. 9 (1997) 1242–1246. https://doi.org/10.1002/elan.1140091605.

[272] J. Lalevée, X. Allonas, S. Jradi, J.-P. Fouassier, Role of the Medium on the Reactivity of Cleavable Photoinitiators in Photopolymerization Reactions, Macromolecules. 39 (2006) 1872–1879. https://doi.org/10.1021/ma052173k.

[273] J. Lalevée, L. Zadoina, X. Allonas, J.P. Fouassier, New sulfur-centered radicals as photopolymerization initiating species, Journal of Polymer Science Part A: Polymer Chemistry. 45 (2007) 2494–2502. https://doi.org/10.1002/pola.22012.

[274] J.P. Fouassier, X. Allonas, J. Lalevee, M. Visconti, Radical polymerization activity and mechanistic approach in a new three-component photoinitiating system, Journal of Polymer Science Part A: Polymer Chemistry. 38 (2000) 4531–4541. https://doi.org/10.1002/1099-0518(20001215)38:24<4531::AID-POLA220>3.0.CO;2-U.

[275] J. Lalevée, M. El-Roz, X. Allonas, J. Pierre Fouassier, Free-radical-promoted cationic photopolymerization under visible light in aerated media: New and highly efficient silane-containing initiating systems, Journal of Polymer Science Part A: Polymer Chemistry. 46 (2008) 2008–2014. https://doi.org/10.1002/pola.22535.

[276] J. Lalevée, A. Dirani, M. El-Roz, X. Allonas, J.P. Fouassier, Germanes as efficient coinitiators in radical and cationic photopolymerizations, Journal of Polymer Science Part A: Polymer Chemistry. 46 (2008) 3042–3047. https://doi.org/10.1002/pola.22644.

[277] Y.Y. Durmaz, N. Moszner, Y. Yagci, Visible Light Initiated Free Radical Promoted Cationic Polymerization Using Acylgermane Based Photoinitiator in the Presence of Onium Salts, Macromolecules. 41 (2008) 6714–6718. https://doi.org/10.1021/ma801208n.

[278] M.-A. Tehfe, J. Lalevée, D. Gigmes, J.P. Fouassier, Green Chemistry: Sunlight-Induced Cationic Polymerization of Renewable Epoxy Monomers Under Air, Macromolecules. 43 (2010) 1364–1370. https://doi.org/10.1021/ma9025702.

[279] M.-A. Tehfe, J. Lalevée, D. Gigmes, J.P. Fouassier, Combination of transition metal carbonyls and silanes: New photoinitiating systems, Journal of Polymer Science Part A: Polymer Chemistry. 48 (2010) 1830–1837. https://doi.org/10.1002/pola.23956.

[280] J. Iwaki, S. Suzuki, C. Park, N. Miyagawa, S. Takahara, T. Yamaoka, Sensitization Mechanism of the Anthracene Derivatives/Photoacid Generator Photoinitiating System,

Journal of Photopolymer Science and Technology. 17 (2004) 123–124. https://doi.org/10.2494/photopolymer.17.123.

[281] S. Dadashi-Silab, S. Doran, Y. Yagci, Photoinduced Electron Transfer Reactions for Macromolecular Syntheses, Chem. Rev. 116 (2016) 10212–10275. https://doi.org/10.1021/acs.chemrev.5b00586.

[282] J. Christmann, X. Allonas, C. Ley, A. Ibrahim, C. Croutxé-Barghorn, Triazine-Based Type-II Photoinitiating System for Free Radical Photopolymerization: Mechanism, Efficiency, and Modeling, Macromolecular Chemistry and Physics. 218 (2017) 1600597. https://doi.org/10.1002/macp.201600597.

[283] C. Kütahya, Y. Zhai, S. Li, S. Liu, J. Li, V. Strehmel, Z. Chen, B. Strehmel, Distinct Sustainable Carbon Nanodots Enable Free Radical Photopolymerization, Photo-ATRP and Photo-CuAAC Chemistry, Angewandte Chemie International Edition. 60 (2021) 10983–10991. https://doi.org/10.1002/anie.202015677.

[284] T. Xue, D. Zhao, T. Hao, X. Li, T. Wang, J. Nie, Synthesis, one/two-photon optical and electrochemical properties and the photopolymerization-sensitizing effect of anthracene-based dyes: influence of the donor groups, New J. Chem. 43 (2019) 6737–6745. https://doi.org/10.1039/C8NJ06520A.

[285] D. Zhao, J. You, H. Fu, T. Xue, T. Hao, X. Wang, T. Wang, Photopolymerization with AIE dyes for solid-state luminophores, Polym. Chem. 11 (2020) 1589–1596. https://doi.org/10.1039/C9PY01671F.

[286] J. Lalevée, X. Allonas, S. Genet, J.-P. Fouassier, Role of Charge-Transfer Configurations on the Addition Reaction of Aminoalkyl Radicals onto Acrylate Double Bonds, J. Am. Chem. Soc. 125 (2003) 9377–9380. https://doi.org/10.1021/ja034750v.

[287] F. Bureš, Fundamental aspects of property tuning in push–pull molecules, RSC Adv. 4 (2014) 58826–58851. https://doi.org/10.1039/C4RA11264D.

[288] T. Xue, T. Wang, J. Nie, Unveiling the electronic effect of substituent on sensitized photopolymerization: An experimental and theoretical investigation, Journal of Photochemistry and Photobiology A: Chemistry. 397 (2020) 112551. https://doi.org/10.1016/j.jphotochem.2020.112551.

[289] Y. Shi, B. Wang, X. Jiang, J. Yin, M. Kaji, H. Yori, Photoinitiation properties of heterocyclic hexaarylbiimidazoles with high UV-vis absorbance, Journal of Applied Polymer Science. 105 (2007) 2027–2035. https://doi.org/10.1002/app.26301.

[290] Y. Shi, J. Yin, M. Kaji, H. Yori, Photopolymerization of acrylate derivatives initiated by hexaarylbiimidazole with ether groups, Polymer International. 55 (2006) 330–339. https://doi.org/10.1002/pi.1968.

[291] A.D. Liu, A.D. Trifunac, V.V. Krongauz, Photodissociation of hexaarylbiimidazole. 2. Direct and sensitized dissociation, J. Phys. Chem. 96 (1992) 207–211. https://doi.org/10.1021/j100180a040.

[292] D. Ahn, S.R. Zavada, T.F. Scott, Rapid, Photomediated Healing of Hexaarylbiimidazole-Based Covalently Cross-Linked Gels, Chem. Mater. 29 (2017) 7023–7031. https://doi.org/10.1021/acs.chemmater.7b02640.

[293] J. Lei, T. Akitoshi, S. Katou, Y. Murakami, J. Yin, X. Jiang, 9,10-Dithio/oxo-Anthracene as a Novel Photosensitizer for Photoinitiator Systems in Photoresists, Macromolecular Chemistry and Physics. 220 (2019) 1900152. https://doi.org/10.1002/macp.201900152.

[294] T. Zhou, Y. Du, A. Borgna, J. Hong, Y. Wang, J. Han, W. Zhang, R. Xu, Post-synthesis modification of a metal–organic framework to construct a bifunctional photocatalyst for

hydrogen production, Energy Environ. Sci. 6 (2013) 3229–3234. https://doi.org/10.1039/C3EE41548A.

[295] T. Zhang, W. Lin, Metal–organic frameworks for artificial photosynthesis and photocatalysis, Chem. Soc. Rev. 43 (2014) 5982–5993. https://doi.org/10.1039/C4CS00103F.

[296] J.-L. Wang, C. Wang, W. Lin, Metal–Organic Frameworks for Light Harvesting and Photocatalysis, ACS Catal. 2 (2012) 2630–2640. https://doi.org/10.1021/cs3005874.

[297] R. Liang, L. Shen, F. Jing, W. Wu, N. Qin, R. Lin, L. Wu, NH2-mediated indium metal– organic framework as a novel visible-light-driven photocatalyst for reduction of the aqueous Cr(VI), Applied Catalysis B: Environmental. 162 (2015) 245–251. https://doi.org/10.1016/j.apcatb.2014.06.049.

[298] P. Wu, C. He, J. Wang, X. Peng, X. Li, Y. An, C. Duan, Photoactive Chiral Metal–Organic Frameworks for Light-Driven Asymmetric α-Alkylation of Aldehydes, J. Am. Chem. Soc. 134 (2012) 14991–14999. https://doi.org/10.1021/ja305367j.

[299] K.G.M. Laurier, F. Vermoortele, R. Ameloot, D.E. De Vos, J. Hofkens, M.B.J. Roeffaers, Iron(III)-Based Metal–Organic Frameworks As Visible Light Photocatalysts, J. Am. Chem. Soc. 135 (2013) 14488–14491. https://doi.org/10.1021/ja405086e.

[300] A. Ohtsuki, L. Lei, M. Tanishima, A. Goto, H. Kaji, Photocontrolled Organocatalyzed Living Radical Polymerization Feasible over a Wide Range of Wavelengths, J. Am. Chem. Soc. 137 (2015) 5610–5617. https://doi.org/10.1021/jacs.5b02617.

[301] X. Pan, M. Lamson, J. Yan, K. Matyjaszewski, Photoinduced Metal-Free Atom Transfer Radical Polymerization of Acrylonitrile, ACS Macro Lett. 4 (2015) 192–196. https://doi.org/10.1021/mz500834g.

[302] M. Kato, M. Kamigaito, M. Sawamoto, T. Higashimura, Polymerization of Methyl Methacrylate with the Carbon Tetrachloride/Dichlorotris-(triphenylphosphine)ruthenium(II)/Methylaluminum Bis(2,6-di-tert-butylphenoxide) Initiating System: Possibility of Living Radical Polymerization, Macromolecules. 28 (1995) 1721–1723. https://doi.org/10.1021/ma00109a056.

[303] K. Matyjaszewski, Atom Transfer Radical Polymerization (ATRP): Current Status and Future Perspectives, Macromolecules. 45 (2012) 4015–4039. https://doi.org/10.1021/ma3001719.

[304] K. Matyjaszewski, N.V. Tsarevsky, Macromolecular Engineering by Atom Transfer Radical Polymerization, J. Am. Chem. Soc. 136 (2014) 6513–6533. https://doi.org/10.1021/ja408069v.

[305] K. Matyjaszewski, J. Xia, Atom Transfer Radical Polymerization, Chem. Rev. 101 (2001) 2921–2990. https://doi.org/10.1021/cr940534g.

[306] D. Konkolewicz, K. Schröder, J. Buback, S. Bernhard, K. Matyjaszewski, Visible Light and Sunlight Photoinduced ATRP with ppm of Cu Catalyst, ACS Macro Lett. 1 (2012) 1219–1223. https://doi.org/10.1021/mz300457e.

[307] M.A. Tasdelen, Y. Yagci, Light-induced copper(I)-catalyzed click chemistry, Tetrahedron Letters. 51 (2010) 6945–6947. https://doi.org/10.1016/j.tetlet.2010.10.166.

[308] N.J. Treat, B.P. Fors, J.W. Kramer, M. Christianson, C.-Y. Chiu, J. Read de Alaniz, C.J. Hawker, Controlled Radical Polymerization of Acrylates Regulated by Visible Light, ACS Macro Lett. 3 (2014) 580–584. https://doi.org/10.1021/mz500242a.

[309] M.A. Tasdelen, Y. Yagci, Light-Induced Click Reactions, Angewandte Chemie International Edition. 52 (2013) 5930–5938. https://doi.org/10.1002/anie.201208741.

[310] M.A. Tasdelen, G. Yilmaz, B. Iskin, Y. Yagci, Photoinduced Free Radical Promoted Copper(I)-Catalyzed Click Chemistry for Macromolecular Syntheses, Macromolecules. 45 (2012) 56–61. https://doi.org/10.1021/ma202438w.

[311] X. Li, D. Chen, Y. Liu, Z. Yu, Q. Xia, H. Xing, W. Sun, Anthracene-based indium metal–organic framework as a promising photosensitizer for visible-light-induced atom transfer radical polymerization, CrystEngComm. 18 (2016) 3696–3702. https://doi.org/10.1039/C6CE00465B.

[312] C.E. Tait, P. Neuhaus, H.L. Anderson, C.R. Timmel, Triplet State Delocalization in a Conjugated Porphyrin Dimer Probed by Transient Electron Paramagnetic Resonance Techniques, J. Am. Chem. Soc. 137 (2015) 6670–6679. https://doi.org/10.1021/jacs.5b03249.

[313] T. Lee, Z.X. Liu, H.L. Lee, A Biomimetic Nose by Microcrystals and Oriented Films of Luminescent Porous Metal–Organic Frameworks, Crystal Growth & Design. 11 (2011) 4146–4154. https://doi.org/10.1021/cg200710p.

[314] D.K. Balta, N. Arsu, Y. Yagci, S. Jockusch, N.J. Turro, Thioxanthone−Anthracene: A New Photoinitiator for Free Radical Polymerization in the Presence of Oxygen, Macromolecules. 40 (2007) 4138–4141. https://doi.org/10.1021/ma0628735.

[315] L. Cokbaglan, N. Arsu, Y. Yagci, S. Jockusch, N.J. Turro, 2-Mercaptothioxanthone as a Novel Photoinitiator for Free Radical Polymerization, Macromolecules. 36 (2003) 2649–2653. https://doi.org/10.1021/ma0214613.

[316] M. Aydin, N. Arsu, Y. Yagci, One-Component Bimolecular Photoinitiating Systems, 2, Macromolecular Rapid Communications. 24 (2003) 718–723. https://doi.org/10.1002/marc.200300019.

[317] F. Catalina, J.M. Tercero, C. Peinado, R. Sastre, J.L. Mateo, N.S. Allen, Photochemistry and photopolymerization study on 2-acetoxy and methyl-2-acetoxy derivatives of thioxanthone as photoinitiators, Journal of Photochemistry and Photobiology A: Chemistry. 50 (1989) 249–258. https://doi.org/10.1016/1010-6030(89)85019-1.

[318] D.K. Balta, N. Arsu, Y. Yagci, A.K. Sundaresan, S. Jockusch, N.J. Turro, Mechanism of Photoinitiated Free Radical Polymerization by Thioxanthone−Anthracene in the Presence of Air, Macromolecules. 44 (2011) 2531–2535. https://doi.org/10.1021/ma200147f.

[319] D. Tunc, B. Gacal, Y. Yagci, An amphipathic thioxanthone-anthracene photoinitiator for free-radical polymerization, Turkish Journal of Chemistry. 37 (2013) 525–537.

[320] D.K. Balta, N. Arsu, Thioxanthone-ethyl anthracene, Journal of Photochemistry and Photobiology A: Chemistry. 257 (2013) 54–59. https://doi.org/10.1016/j.jphotochem.2013.02.014.

[321] S. Mutlu, K. Watanabe, S. Takahara, N. Arsu, Thioxanthone–anthracene-9-carboxylic acid as radical photoinitiator in the presence of atmospheric air, Journal of Polymer Science Part A: Polymer Chemistry. 56 (2018) 1878–1883. https://doi.org/10.1002/pola.29072.

[322] D.K. Balta, N. Arsu, Photodimerization of thioxanthone–anthracene: formation of monochromophoric Type II initiator, Null. 19 (2016) 222–226. https://doi.org/10.1080/15685551.2015.1136528.